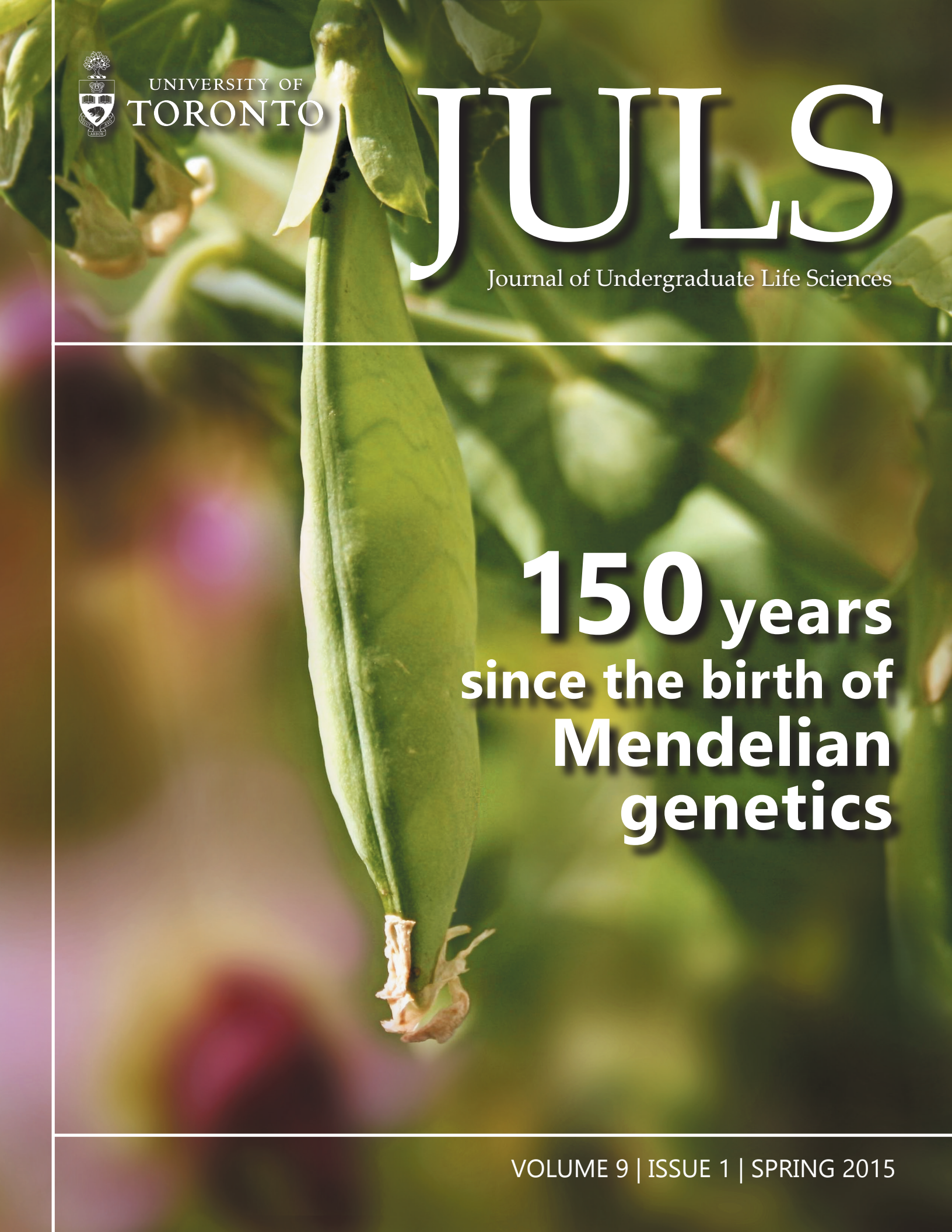

UNIVERSITY OF TORONTO

# JULS

Journal of Undergraduate Life Sciences

## 150 years since the birth of Mendelian genetics

VOLUME 9 | ISSUE 1 | SPRING 2015

# *On the Cover*

*Imindu Liyanage*

***Celebrating Gregor Mendel***

*In 1854, an unassuming Augustinian priest and a recent student of physics began a series of botanical experiments, initially to understand why peas had varying seed shapes. Having gotten permission from the Monastery abbot to borrow the gardens, he began planting, crossing and cataloguing the growth and characteristics of his peas.*

*Over time, he would learn of the ability of some traits to overpower or dominate others, and with little more than a series of numerical ratios, he crafted a model of inheritance which remains a fundament of modern genetics. We therefore dedicate this issue to the work of Gregor Mendel, and his discovery of genetic inheritance - 150 years after its first publication.*

# Sponsors

*The Journal of Undergraduate Life Sciences would like to thank the following sponsors for supporting the production of this year's issue.*


UNIVERSITY OF TORONTO
FACULTY OF MEDICINE


Human Biology
UNIVERSITY OF TORONTO


Molecular Genetics
UNIVERSITY OF TORONTO


Immunology
UNIVERSITY OF TORONTO


TRINITY COLLEGE
IN THE UNIVERSITY OF TORONTO


Laboratory Medicine & Pathobiology
UNIVERSITY OF TORONTO


Department of Psychology
UNIVERSITY OF TORONTO

**ISSN 1911-8899** | University of Toronto Journal of Undergraduate Life Sciences (Print)
juls.sa.utoronto.ca
jps.library.utoronto.ca/index.php/juls

VOLUME 9 • ISSUE 1 • SPRING 2015

# Table of Contents

## About Us



## News



## Research



## Reviews



## Interviews

JULS
Journal of Undergraduate Life Sciences
University of Toronto

## Staff List

### Editors-in-Chief


Maya Deeb


Asha Sardar

### Senior Editors


Claudia Dziegielewski


D'Arcy Prendergast


Kristiana Xhima


Alena Zelinka

### External Affairs


Aditya Chawla


Chloe Gui

### News Managers


Andrea Macikunas

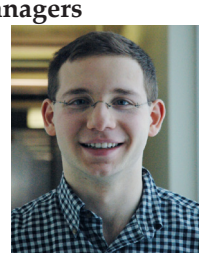
Aryeh Price

### Layout

*Managers*

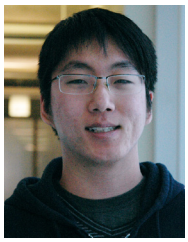
Alan Yu


Priscilla Yung

*Associates*
Grace Gao
Lisa Qiu
Kenneth Ting
Lael Jung
Tianyu Wang
Joshua Efe

*Cover Design*
Priscilla Yung

### Review Board

*Managers*

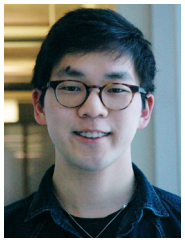
Charles Lee


Imindu Liyanage

*Members*
Samin Alikhanzadeh
Samuel Chan
Michael Dao
Osman Mahamud
Albert Nguyen
Farzan Pavri
Brandon Sit
Caroline Wang
Ashley Zhang

*Faculty*
Dr. Alistair Dias
Dr. Michelle French
Dr. William Ju
Dr. Thierry Mallevaey
Dr. Barbara Morra
Dr. Douglas Templeton

JULS
Journal of Undergraduate Life Sciences
University of Toronto

# Letter *from the* Editors

DEAR READER,

As our term as Editors-in-Chief of the Journal of Undergraduate Life Sciences (JULS) comes to an end, we reflect upon our efforts over the last year in the creation and long-awaited publication of this very volume of JULS.

After countless hours of revision and preparation, we are proud to present you with the journal's 9th volume, on behalf of the entire JULS team. As the only peer-reviewed undergraduate life sciences journal at the University of Toronto, JULS serves to fill the disproportionate gap between the high prospect of student research versus available opportunity for publication. This end could not have been fulfilled without the expertise, dedication, and support of our executive and associate members, and faculty advisors; as well as the perseverance and patience of our contributing student authors. We thank each of them for their invaluable insights and efforts, and applaud them for their achievements and role in helping JULS showcase the great potential that exists within undergraduate research.

This 2015 publication of JULS celebrates the momentous work of Gregor Mendel. One hundred and fifty years ago, this Augustinian friar and scientist employed the scientific method to establish laws of inheritance. Such laws had been unknowingly used for centuries by farmers who used cross-breeding to yield desirable traits in their livestock. Despite the profound and lasting impact that Mendel's simple pea-based experiments have since had in biology, his work was largely rejected and ignored by the greater scientific community during his lifetime. Mendel's work would not resurface until almost three decades later, as the pursuit of laws of inheritance aimed at uncovering an explanation that paralleled Darwin's theory of natural selection. Though initially discounted, the results of his initial experiments would become fundamental to the understanding of genetics. This issue of JULS hopes to commemorate impactful science that can often go unrecognized by bringing you a variety of undergraduate works that may not have even been possible without Mendel's contribution to genetics, which itself has far-reaching interdisciplinary implications.

In this issue, you will find articles that address a variety of scientific domains, ranging from bioinformatics to immunology. Not only does this diversity speak to the strength of JULS' multidisciplinarity, but it also gives readers a glimpse into the many research opportunities that the University of Toronto has to offer. As Editors-in-Chief of JULS, and sound supporters of undergraduate research and publication, we encourage our readers to embark upon their own journeys of scientific discovery and to one day consider JULS as a platform through which they may display and empower their works.

Thank you for reading JULS. We hope you enjoy the issue.

Sincerely,

Maya Deeb & Asha Sardar
Editors-in-Chief, 2014-2015

# Multimodal Imaging of the Savant Brain: How Biochemical and Structural Differences Support the Role of Right Hemisphere Dominance in Behaviour

Nicole Fogel

Previous studies have demonstrated that the brains of those with savant syndrome possess different structural and biochemical properties when compared to healthy individuals. In this study, the authors aimed to characterize the neurophysiological changes underlying the unique skills exhibited by savants, such as exceptional memory. Experimental findings validated some previous observations showing an increase in right hemisphere and hippocampal volumes in savant brains compared to non-savant brains. However, using newer imaging modalities, the authors observed a great increase in total cerebral volume and cerebral spinal fluid (CSF). Caudate, amygdala, corpus callosum, and occipital lobe volumes were not consistent with previously reported values; further, decreases in GABA and glutamate were detected in the parietal lobe. These differences may influence regulation of learning and memory.

Savant syndrome is typically associated with having abnormal skills, such as exceptional memory or prodigious talent in a particular area like music or math [1-3]. Age of onset varies depending on whether the condition is congenital, or acquired in response to injury or as a consequence of other developmental disabilities [1-5]. Affected individuals can have a low or superior IQ score; they practice their skill often. Although the disorder is not detrimental to health, there are social and emotional challenges with which the savant is faced [2, 5, 6]. In other words, having exceptional memory or abnormal abilities in a particular area might foster social isolation and an inability to cope independently. Affected individuals might hide their abilities, for fear of being exploited, or for fear of being put in a special class different from those of their peers [2]. In order to help regulate their talent by providing proper help, treatment, and resources, it is necessary to better understand the disorder. Questions remain regarding how the disorder should be defined, how it may be differentiated from autism spectrum disorder (ASD) [6, 7], and which hypothetical model should be accepted as the cause of the disorder. The neurophysiological mechanisms as well as the structural and biochemical abnormalities of savant brains have yet to be fully understood.

To expand on the limited knowledge and number of studies on savant syndrome, the authors wanted to use newer imaging techniques other than commonly used functional imaging to examine the neuroanatomy, regional brain connectivity, and neurochemistry of savant versus non-savant brains [1]. Since savant skills are manifested differently in different individuals, the authors studied changes in the brain of a 63-year-old male savant with autism and artistic talent, a different type of savant skill not normally studied [1, 2]. During a single scanning session, the authors were able to acquire data using methods that will be described: high-resolution magnetic resonance (MR) imaging, 2-dimensional J-resolved MR spectroscopy, and diffusion tensor imaging [1]. These findings demonstrate that newer imaging techniques could provide greater understanding of the characterization of unique savant brain features, connecting the cause of the disorder to its behavioural dispositions.

## Structural Imaging to Examine Differences in Brain Morphology

Corrigan *et al.* used magnetic resonance (MR) imaging to better understand the cyto-architecture underlying the exceptional intelligence displayed by savants [1]. Results from MR scanning revealed that all regional and compartmental brain structures were intact, contrary to a previously documented case with severe anatomical brain abnormalities [8]. These findings suggest that atypical gross anatomical brain structure may not entirely account for prodigious savant skills.

Upon volumetric assessment of brain morphology using an imaging-specific analysis program called MEASURE, cerebral volume in the savant case (1362 mL) was shown to exceed control subjects by a statistically significant amount (**Figure 1**) [1]. Hemispheric asymmetry was observed upon regional brain analysis, revealing an enlarged right side amygdala (24%) and caudate nucleus (9.9%), in addition to a larger left side putamen (8.3%) (**Table 1**). These right side enlargements may provide an explanation for the different types of prodigious savant skills, which are generally correlated with right side cerebral hemisphere function [1, 2]. Furthermore, the caudate and amygdala have

been associated with implicit and explicit memory integration, which may play a role in the savant's exceptional memory.

Segmentation analysis was used to differentiate the compartmental volumes of white matter, gray matter, and CSF to identify potential differences in cumulative patterns of abnormal physiological brain development [1]. Although there were no differences in gray or white matter in the savant case compared to normal values, CSF volume was increased by 2.5 standard deviations (SD).

## Diffusion Tensor Imaging (DTI) to Evaluate Brain Connectivity

By measuring the speed and direction of water diffusion in axons, DTI provides information about white matter tract health and connectivity, which may give insight into savant cognitive task performance [1]. The right hemisphere of the savant subject had larger fractional anisotropy measurements in all regions except in the occipital lobe. This suggests increased right hemisphere connectivity, since fractional anisotropy is a measure of myelination, directionality and organization of white matter tracts [1]. Previous studies have also shown right hemisphere enlargements in savant brains; thus, these findings provide converging evidence that savant subjects tend to have right-sided functional dominance [1, 3].

Increased axial, radial, and mean diffusivity indicates decreased myelination as well as axonal damage [1, 2]. Both the left and right hippocampi had greater axial and mean diffusivity measurements compared to control (>8 SD and >3 SD, respectively) [1]. Furthermore, the corpus callosum and left amygdala had increased axial, radial, and mean diffusivity (>3 SD). Overall, DTI analysis revealed reduced circuitry and connectivity in these structures in the savant [1]. Again, lack of current research made it difficult to fully explain these findings.

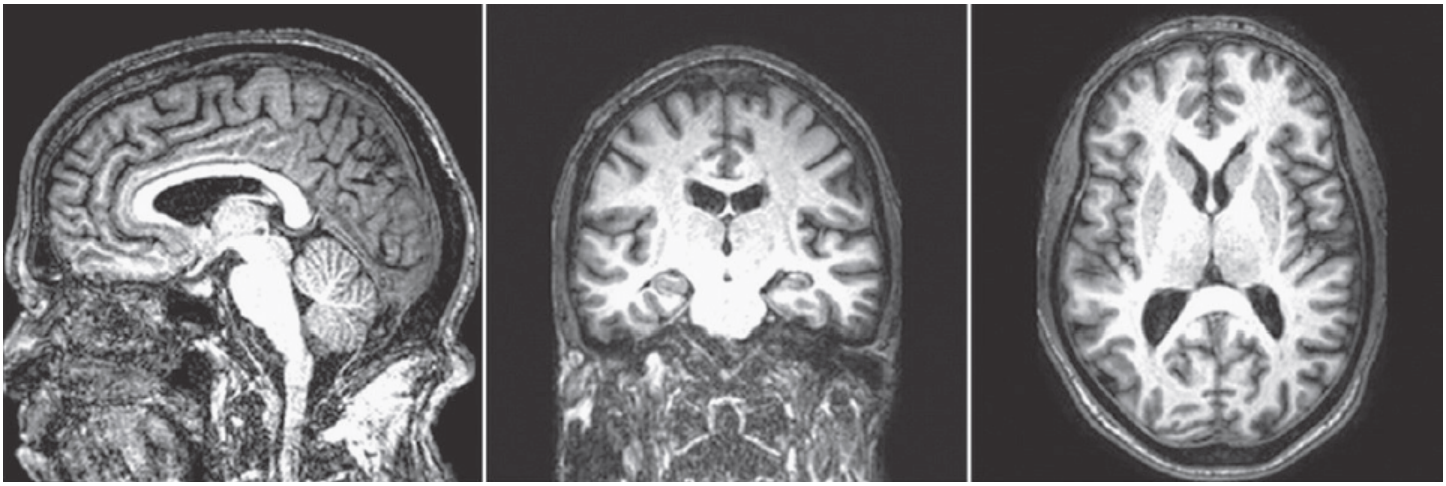

**Figure 1.** Midsectional MRI of the savant artistic brain. Total cerebral volume exceeded normative literature values. Larger structures, such as the amygdala and caudate, are visually represented [1].

**Table 1.** Regional brain volumes of the savant case. A symmetry index was used to calculate differences between the right (R) and left (L) hemispheric volumes. This was found using the following formula: 2(R-L)/(R+L)*100 [1].

| | Left hemisphere (mL) | Right hemishpere (mL) | Total volume (mL) | Symmetry index |
|---|---|---|---|---|
| ***Cerebrum** | *674.3 | *687.4 | *1361.7 | *1.93 |
| ***Amygdala** | *2.1 | *2.7 | *4.8 | *23.97 |
| **Hippocampus** | 3.9 | 4.0 | 7.9 | 0.76 |
| ***Caudate** | *5.7 | *6.3 | *12.1 | *9.93 |
| ***Putamen** | *5.9 | *5.5 | *11.4 | *-8.27 |
| **Thalamus** | 7.8 | 7.8 | 15.6 | -0.64 |
| **Frontal Lobe** | 231.0 | 227.9 | 458.9 | -1.36 |
| **Occipital Lobe** | 94.9 | 97.1 | 191.9 | 2.33 |
| **Cerebellum** | 86.5 | 91.6 | 178.1 | 5.78 |

## Magnetic Resonance Spectroscopy (MRS) to Measure Biochemical Concentration

Using 2D J-resolved spectroscopy, investigators found that the savant subject had lower concentrations of brain metabolites, with considerable reductions in GABA and glutamate (>2 SD), among other neurotransmitters studied, compared to control subjects (**Table 2**) [1, 9]. These neurotransmitters play important roles in learning and memory. However, the investigators were unable to make specific conclusions about the effects of these deficits. It is undetermined whether these findings are unique to this participant or common amongst savants as evidence supports reduced GABA levels in autistic patients [10]. Thus, these lowered levels may be common amongst autistic savants, limiting the generalizability of this study [10].

**Table 2.** Brain chemical concentrations measured though MRS. All concentrations of chemicals were found to be lower in the savant brain versus the control group. Glu and GABA had lower concentrations in the savant by more than 2 SDs. Data presented in millimoles per liter, with mean (SD) in the controls. NAA = N-acetyl aspartate; Cho = Choline; Cre = Creatine; Glu = Glutamate; GABA = γ-aminobutyric acid [1].

| | Savant | Comparison group mean (SD) |
|---|---|---|
| **NAA** | 9.28 | 10.69 (1.38) |
| **Cho** | 2.00 | 2.16 (0.37) |
| **Cre** | 6.34 | 6.66 (0.87) |
| ***Glu** | *7.27 | *11.48 (1.98) |
| ***GABA** | *0.66 | *0.99 (0.15) |

Corrigan *et al.* used imaging methodologies to support the hypothesis that there are neurophysiological differences in the savant brain compared to the non-savant brain [1]. Even though the authors used many imaging techniques, their broad focus and interpretations of the data could not precisely account for their findings nor provide a causal link between savant brain changes and behaviour. However, their experiments demonstrated a right-over-left preponderance, as well as significant enlargements in the right hemispherical amygdala and caudate nucleus. Since these structures are involved in learning and memory circuits [2], focusing on the right hemisphere in future studies could potentially elucidate savant prodigious function [11]. One way to do this could be to suppress left hemisphere function.

It is important to note that the imaging performed in this study was conducted on a single savant of one type of skill [1], which limits the extension of these findings in explaining other types of savant biochemical and structural changes. Additionally, results across the literature are hard to compare since each imaging technique results in a different interpretation of results, questioning the reliability of this study's data.

Therefore, future experiments should seek to elucidate underlying differences in the savant brain based on a standardized methodology. This would permit data comparison between all types of savants (e.g., congenital versus acquired) in all modalities so that findings can eventually be generalized for the broader savant population. Some researchers postulate that savant function is a result of unique utilization of neuronal networks in particular regions [11, 12]. Thus, whether a unique utilization is shared across all savants or just savants within a particular skill modality warrants further research.

Additionally, it would be beneficial to investigate how modulating GABA and glutamate activity within structurally altered regions affects specific savant skills and regulation of learning and memory [1]. Significantly, multimodal imaging techniques used in this study could be applied to future neuroscience studies to aid in understanding ASD, as well as the brain in general, regarding its potential and role in learning and memory. The future studies suggested above would contribute to a deeper understanding of the causes and associated behaviours of savant syndrome resulting from structural and biochemical differences, and ultimately, influence how the savant individual can find their place in society.

## References

1. Corrigan NM, Richards TL, Treffert DA, Dager SR. Toward a better understanding of the savant brain. Comp Psych 2012;53(6):706–17.
2. Treffert DA. The savant syndrome: an extraordinary condition. A synopsis: past, present, future. Phil Trans R Soc B 2009;364:1351-7.
3. Treffert DA. Savant syndrome: realities, myths, and misconceptions. J Autism Dev Disord. 2014;44(3):564-71.
4. Treffert DA. The "acquired" savant: could such dormant potential exist within us all? Wisconsin Medical Society [Internet]. 1841 [cited 2014]. Available from: https://www.wisconsinmedicalsociety.org
5. Wisconsin medical Society. Savant syndrome: frequently asked questions. Wisconsin Medical Society [Internet]. 1841 [cited 2014]. Available from: https://www.wisconsinmedicalsociety.org/professional/savant-syndrome/faqs/
6. Rohan S. What is savantism? Wikispaces [Internet]. 2012 [cited 2014]. Available from: http://autismsummer2010.providence.wikispaces.net/file/view/Savantism%20Project%20EDU%20599.pdf/148611937/Savantism%20Project%20EDU%20599.pdf
7. Shah S. Autism and savant syndrome. Bryn Mawr College [Internet]. 1994 [cited 2014]. Available from: http://serendip.brynmawr.edu/exchange/node/1805
8. Treffert DA, Christensen DD. Inside the mind of a savant. Sci Am 2005;293:108-13.
9. Gujar SK, Maheshwari S, Björkman-Burtscher I, Sundgren PC. Magnetic resonance spectroscopy. J Neuroophthalmol 2005;25:217-26.
10. Harada M, Taki MM, Nose A, Kubo H, Mori K, Nishitani H, Matsuda T. Non-invasive evaluation of the GABAergic/glutamatergic system in autistic patients observed by MEGA-editing proton MR spectroscopy using a clinical 3 tesla instrument. J Autism Dev Disord 2011;41(4):447-54.
11. Packard MG, Knowlton BJ. Learning and memory functions of the basal ganglia. Annu Rev Neurosci 2002;25:563-93.
12. Takahata K, Kato M. Neural mechanism underlying autistic savant and acquired savant syndrome. Brain Nerve 2008;60(7):861-69.

# Fabricating Organs: From Fiction to Reality

Imindu Lian

To fabricate a functioning human organ seems as outlandish an idea as any science fiction author could conceive. Yet, the promise of an unending supply of viable organs, effectively terminating the infamous waitlists for transplantation, as well as providing a cure for countless end-stage organ diseases, is a prospect too enticing to dismiss. It is for this reason that much effort in regenerative medicine is being increasingly diverted to the field of *whole organ fabrication* (also referred to as *whole organ bioengineering*). Currently there are several, quite distinct strategies working towards this objective.

The simplest stratagem forgoes the idea of 'fabricating' altogether and instead attempts to create a viable human organ from a previously viable animal organ [1, 2]. To achieve this, a freshly acquired animal organ is perfused with a variety of detergents to *decellularize* the organ [2]. The resulting white, almost amorphic mass is the organ's extracellular matrix, and it is the structural framework upon which a new organ can be built [2]. The next steps are a matter of some debate, but generally involve seeding the new matrix with a complex mix of growth factors and ligands that will allow for the recolonization of the matrix with new cells. Finally, human cells – typically some type of pluripotent cell – are introduced to the matrix and allowed to *recellularize* the structure and create what is hoped to be a viable human organ [1]. However xenogeneic (or interspecies) transplant has been associated with significant immunological complications upon transplantation. Furthermore, recellularization is still a tenuous endeavour at best, and though experiments have created beating hearts and functioning livers, they are typically of insufficient quality [1, 2].

The alternative stratagem attempts to truly fabricate an organ from simple, cellular precursors. However, this field is fundamentally challenged by the extracellular matrix, for an organ cannot be built without this framework, and a handful of replicating stem cells cannot simply create a matrix. This problem has been particularly confounding for the regeneration of the heart, which relies on a highly organized matrix to both function and remain viable [3]. One solution here is to employ epicardial cells, which are known to support cardiomyoctye proliferation in early organ development [3-5]. These cells, among many supporting functions, yield fibroblasts, which secrete several *fibrous* proteins crucial to fabricating the extracellular matrix [3, 5]. Furthermore, epicardial cells have demonstrated important roles in cardiac remodelling, making them a vital consideration for any regeneration attempt of the heart [3]. However, previously there was no effective means to generate these cells from pluripotent precursors, and therefore they were largely precluded from having any meaningful role in the regeneration process [3].

Yet, in a landmark investigation conducted at the University of Toronto, in partnership with the McEwen Centre for Regenerative Medicine, an epicardial cell lineage was successfully derived from pluripotent stem cells [3]. The protocol relied on stage-specific activation of the *BMP* and *WNT* signalling pathways, and it resulted in cells displaying both morphological and biochemical characteristics of the desired epicardial cells [3]. Furthermore, with additional induction, the cells differentiated into fibroblast and smooth muscle lineages – the essential engineers of the extracellular matrix [3].

This work lays the foundation for future studies examining cardiac regeneration, and may contribute to the fabrication of transplantable human organs - perhaps not such an outlandish idea after all…

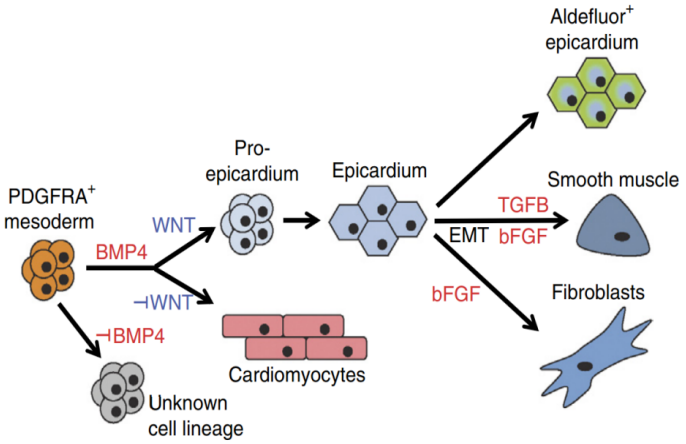


**Figure 1.** The development schema of the epicardial cells from a mesodermal pluripotent progenitor. [Image modified from publication by Keller et al.]

## References

1. Arenas-Herrera JE, Ko IK, Atala A, Yoo JJ. Decellularization for whole organ bioengineering. Biomed Mater 2013;8(1):014106.
2. Gilbert TW, Sellaro TL, Badylak SF. Decellularization of tissues and organs. Biomaterials 2006;27(19):3675-83.
3. Witty A, Mihic A, Tam R, Fisher S, Mikryukov A, Schoichet M, Li R, Kattman S, Keller G. Generation of the epicardial lineage from human pluripotent stem cells. Nat Biotechno 2014;32(10):1026.
4. Hamdi H, Planat-Bénard V, Bel A, Neametalla H, Saccenti L, Calderón D, Bellamy V, Bon M, Perrier MC, Mandet C, Bruneval P, Casteilla L, Hagège AA, Pucéat M, Agbulut O, Menasché P. Long term functional benefits of epicardial patches as cell carriers. Cell Transplant 2012;23:87-96.
5. Schlueter J, Brand T. Epicardial progenitor cells in cardiac development and regeneration. J Cardiovasc Transl Res 2012;5(5):641-53.

# Healing and the Heart: Conference on Cardiovascular Regenerative Medicine

Aditya Chawla


**Laboratory Medicine and Pathbiology Student Union (LMPSU) executive team members.** Top row (L-R): Michael Nguyen, Sudarshan Bala, Charles Lee, Maya Deeb, Alena Zelinka, Amber Cintosun, Stephanie Poon, and Jelena Tanic. Bottom row (L-R): Lisa Qiu, Ashley Zhang, and Andrew Rajkumar.

**Guest Speakers take questions from the audience at the panel discussion section of the conference.** Panel (L to R): Dr. Gordon Keller, Dr. Ian Scott, Dr. Jason Fish, Dr. Paul Olguin Delgado, Dr. Richard Weisel and Dr. Phyllis Billia.

On Saturday, January 17th, 2015, over 200 members of the community came to the University of Toronto for Healing and the Heart, an undergraduate-led conference on cardiovascular regenerative medicine. Organized by the Laboratory Medicine and Pathobiology Student Union (LMPSU), the conference focused on how research in regenerative medicine can transform the clinical management of cardiovascular disease.

The LMPSU co-presidents, Alena Zelinka and Maya Deeb, shared their motivation for planning the conference.

"We were both inspired to look at cardiovascular disease because both of our families have been impacted by it," said Deeb during the opening remarks of the conference.

The conference began with a presentation by Dr. Gordon Keller on modeling the development of cardiovascular disease with pluripotent stem cells. Dr. Keller's goal is to make a complete model of the human heart in a petri dish to replace damaged cells in a heart attack. "This is not just an idea, it is happening now," said Dr. Keller at the end of his presentation.

Following Dr. Keller, Dr. Ian Scott presented his research investigating signaling molecules and factors that may allow the heart to regenerate itself after a myocardial infarction (heart attack). One implication of his research is the possibility of a drug that can re-activate the regenerative mechanism of the heart following a heart attack.

The second half of the conference was based on research by Drs. Richard Weisel, Vivek Rao, Milica Radisic, and Phyllis Billia, who discussed how bone marrow is utilized for heart regeneration, how the extracellular matrix is important in regeneration, and how gene therapy could be utilized in clinical practice.

In particular, Dr. Weisel took some time for interview regarding his research and motivations. (**AC** – Aditya Chawla; **RW** – Dr. R. Weisel)

**AC:** Could you describe your journey as a scientist?

**RW:** I started my interest in cardiac surgery at age 6, and I started going to the operating room when I was 14. I knew early on what I wanted to do, so I planned my undergraduate, graduate and medical school graduate studies very carefully to go into cardiac medicine. That took about 30 years or so. However, I decided when I went to Yale University that I would take philosophy and

Aditya Chawla (right) interviews Dr. Richard Weisel (left).

Dr. Milica Radisic addresses the audience on human cardiac biowires and injectable tissues.

religion, knowing I would do science for the rest of my life. I don't regret that decision.

**AC:** What were some of your biggest challenges?

**RW:** The first challenge was to get into medical school – that was difficult. Then, it was to decide where you were going to do your residency. So you sort of have to set your working environment so that you can do research, but that's difficult in a very competitive marketplace.

**AC:** What advice would you give to aspiring researchers?

**RW:** If it's possible, decide where you want to go, and what you want to do. You'll be at a much greater advantage. A lot of students don't decide, and end up passively following a career choice they're not happy with. That's why I've been trying to get undergraduate students in our laboratories and operating rooms over the years.

**AC:** What advances do you predict in your field within the next 20 years?

**RW:** We've learned a lot about cell therapy, and I've worked with Dr. Keller to try to modify the cellular mechanisms, and we would probably be able to accomplish it in the next few years. Over time, we'll build our programs, and find alternatives that will work. It takes a lot of effort and patients to find therapies for patient care, but we've been doing that for the past 20 years and we'll continue to do that.

In a slightly different theme to the concept of developmental biology discussed in the first half, Dr. Milica Radisic offered a unique engineering approach with her human cardiac biowires. Dr. Radisic also spoke with us about her life and research. (**AC** – Aditya Chawla; **MR** – Dr. M. Radisic)

**AC:** Could you describe your journey as a scientist?

**MR:** In my undergrad, I studied chemical engineering, and at that time biology wasn't really integrated. So I didn't have any biology until I went to grad school. When I came to MIT, I started taking biology courses and it was really hard initially. For a student who was always on top, getting 50s was really hard.

**AC:** What advice would you give to aspiring researchers?

**MR:** It's a very long journey, so you absolutely have to choose what you like. You really have to pick a topic that keeps you awake at night; it's not a job, it's a lifestyle. So, if you think you can succeed in science, you really need to focus your efforts on a topic that you like.

**AC:** What advances do you predict in your field within the next 20 years?

**MR:** Right now, what is reaching practical use is the use of artificial tissues as drug tissues. So, I envision developments in that arena, where we can study really important drug interactions with multiple cell types. There also needs to be a clinical trial that looks at these cells. We already have platforms to simulate an entire human on a chip, and it could happen within the next few years.

The pace of cardiovascular research is astounding, and will only continue to increase in the future. This conference was planned at an integral period in the cardiovascular research field. Recently, the University of Toronto announced a partnership with the Hospital for Sick Children (SickKids) and University Health Network to create the new Ted Rogers Center for Heart Research, representing an unprecedented $130 million donation. Clearly, in these exciting times, conferences like these will only serve to inspire the next generation of scientists.

JULS RESEARCH

# Ab Initio Study on the Possible Mechanisms of Alkene Hydration and its Potential as a Step towards Finding a Treatment for Fumarase Deficiency

Dhia Azzouz[1P], Nidaa Rasheed[1S], Peiqi Yu[1S], Cheng Min Sung[1S], Lie Yun Kok[1S], Saad Khan[1T], Sudarshan Bala[1T], Rachel Chen[1T], Vivian Xie[1T], Skye Marie Daley[1T], David Kim[1T], Natalie J Galant[T], Bela Viskolcz[3T], and Imre G Csizmadia[1,2T]

[P]Primary Author, [S]Second Authors, [T]Third Authors
[1]Department of Chemistry, University of Toronto, ON, Canada
[2]Department of Medical Biophysics, University of Toronto, ON, Canada
[3]Department of Chemical Informatics, University of Szeged, Szeged, Hungary

## Abstract

**In patients with fumarase deficiency, the lack of fumarase-facilitated hydration of fumarate to malate triggers complications such as encephalopathy, seizures, leukopenia, and pancreatitis. The disease results from a malfunction in the citric acid cycle, a cycle that takes place continuously in the mitochondria and is essential to cellular respiration. Quantum chemical computations were carried out at the B3LYP/6-31G(d) level of theory to calculate the energetics of plausible alkene hydration reaction mechanisms. These methods were used to mimic the hydration of fumarate to malate in the citric acid cycle in the absence of an enzyme, as is the case in patients with fumarase deficiency. The two most plausible mechanisms for the hydration of alkenes were examined: the concerted uncatalyzed mechanism and the stepwise acid-catalyzed mechanism. Thermodynamic results revealed that a single large energy barrier (237.96 kJ/mol) must be overcome during a concerted uncatalyzed reaction. In contrast, it was found that multiple smaller energy barriers (84.75 kJ/mol and 73.77 kJ/mol) must be overcome to undergo the stepwise acid-catalyzed mechanism reaction. Therefore, the latter mechanism was found to be a more energetically favourable pathway for the alkene hydration reactions, which may shed light on the future treatment of fumarase-deficient patients.**

## Introduction

The citric acid cycle (also referred to as the Krebs cycle) is a metabolic pathway that involves the reduction of $NAD^+$ and FAD molecules to NADH and $FADH_2$, respectively, eventually leading to the synthesis of ATP – the primary energy conduit of the body [1, 2]. Thus, the malfunction or deficiency of enzymes involved in any process of the citric acid cycle may profoundly impact the human body. Diseases involving the disruption of the Krebs cycle include pyruvate dehydrogenase complex (PDC) deficiency, fumarase deficiency, aconitase deficiency, and succinate dehydrogenase deficiency [3].

Fumarase, or fumarate hydratase, is the enzyme responsible for converting fumarate to malate and is a tumour suppressor [4]. Inactivation of fumarase causes fumarate to accumulate in the cells, which may lead to renal cancer [5]. Loss of fumarase activity was shown to permit accumulation of hypoxia-inducible factors (HIF), which are highly expressed in tumours and cancer cell lines [5]. HIF prolyl hydroxylase, the enzyme that regulates the hydroxylation and deactivation of HIF, is inhibited by fumarate; therefore, fumarate causes up-regulation of HIF [5].

In addition, studies have found that fumarase deficiency has an impact on the central nervous systems. Patients with fumarase deficiency show symptoms such as microcephaly, hypotonia, infantile spasms, and psychomotor retardation, which may lead to death during infancy [6, 7]. The accumulation of fumarate has also been found to inhibit adenylosuccinate lyase (ASL), the catalyst essential for purine nucleotide synthesis [7, 8]. The inhibition of ASL was suggested to be involved in neurological impairment in patients with fumarase deficiency [6].

There are two reactions in the citric acid cycle that involve the hydration of alkenes: the conversion of *cis*-aconitate to *iso*-

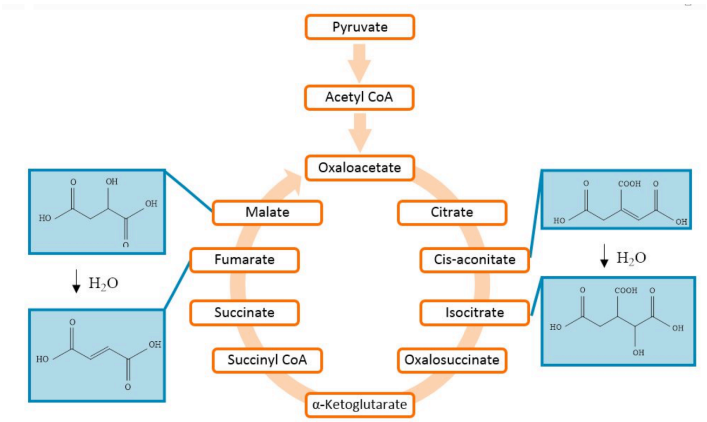


**Figure 1.** A schematic illustration of the major molecules involved in the citric acid cycle. Molecules enclosed in blue rectangles make up the alkene hydration reactions. Fumarate-mimic ethylene was used in the study.

citrate catalyzed by aconitase and the conversion of fumarate to malate catalyzed by fumarase (**Figure 1**) [11, 12]. A previous study conducted by Fisher *et al.* demonstrated that the hydration of fumarate to malate was stereospecific. However, the study failed to observe/report whether the addition of water was in a *cis-* or *trans-* manner [13]. This was later shown in a different study done by Farrar *et al.* [14], which demonstrated that the hydration of fumarate by water occurred in a *cis*-manner when catalyzed by the enzyme fumarase. The knowledge obtained from these studies on the stereospecificity gave an insight into the mechanism of the reaction. However, since the studies were done experimentally in the presence of an enzyme rather than computationally, there were no thermodynamic values obtained for the reactions, which would provide insight into the energetics of the reaction. The concerted uncatalyzed mechanism (**Figure 2a**) [15] and the stepwise acid-catalyzed mechanism (**Figure 2b**) [16] were proposed to mimic the hydration of fumarate in the citric acid cycle in the absence of fumarase, as is the case in patients with fumarase deficiency. The two reactions were studied in order to determine the most probable mechanism of fumarate hydration in patients with fumarase deficiency, assuming the reaction takes place at a slow rate. The results were obtained using Gaussian 09 software [17].

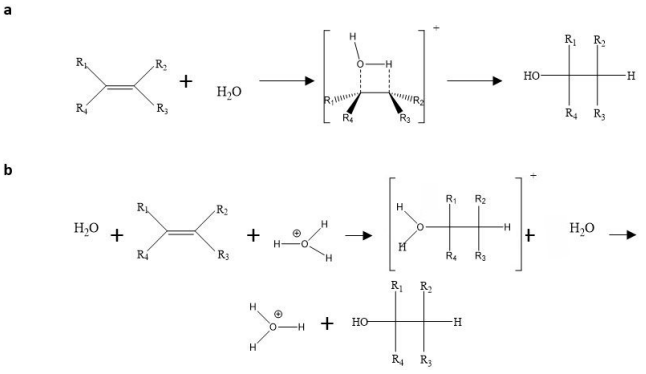


**Figure 2.** Schematic illustrations of (a) the concerted uncatalyzed mechanism of alkene hydration and (b) the stepwise acid catalyzed mechanism of alkene hydration. R groups can be any atoms.

Due to the absence of any complex functional groups and hindrance near the carbon-carbon double bond of fumarate (**Figure 3**), calculations were performed on the preliminary model of ethylene hydration (**Figure 4**).

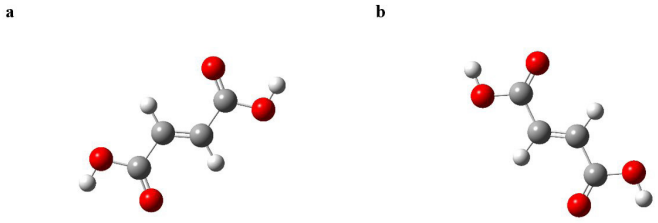


**Figure 3.** (a) front view of fumarate, (b) back view of fumarate. Models generated in Gaussview 5.0 software.

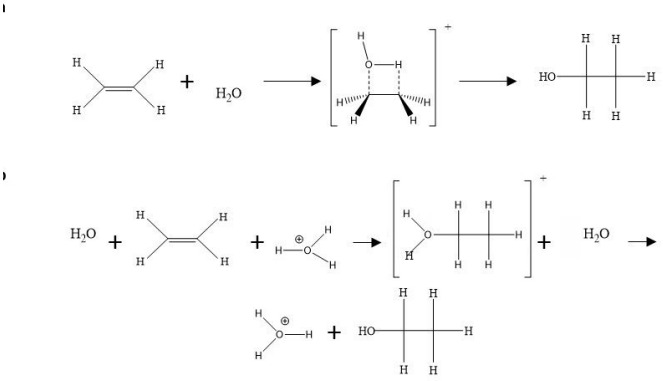


**Figure 4.** Schematic illustrations of (a) the concerted uncatalyzed mechanism of alkene hydration and (b) the stepwise acid-catalyzed mechanism of ethylene hydration.

## Methods

The reactants, intermediates, products, and transition states for both mechanisms were constructed in Gaussview 5.0 software and were studied in gaseous states at the B3LYP/6-31G(d) level of theory using the Gaussian 09 software [17, 18]. Each molecule was submitted for optimization in Gaussian 09 software using the B3LYP/6-31G(d) level of theory. Reactants and products were optimized to a minimum and the transition states were optimized to obtain a maximum. To verify that the chosen transition state structure was correct, Intrinsic Reaction Coordinates (IRC) graphs were obtained. A maximum on an IRC curve enforced the notion that the structure was a transition state [19]. The total energy values at 0K and 298K, enthalpy change ($\Delta H°$), and change in Gibbs free energy ($\Delta G°$), were obtained and activation energies were compared for the concerted uncatalyzed mechanism and the stepwise acid-catalyzed mechanism of alkene hydration.

## Results

Moving forward, the names in **Figure 5** and **Figure 6** will be used to distinguish between the different molecules.

Thermodynamic results for the two model reactions indicated key distinctions between the concerted uncatalyzed mechanism and the stepwise acid-catalyzed mechanism. It was found that a single large energy barrier of approximately 237.96 kJ/mol must be overcome in order for the concerted uncatalyzed reaction mechanism to take place (**Table 1**, **Figure 7**). On the other hand, it was

found that two smaller energy barriers (84.75 kJ/mol and 73.77 kJ/mol) must be overcome in order for the stepwise acid-catalyzed reaction mechanism to take place (**Table 2**, **Figure 8**).

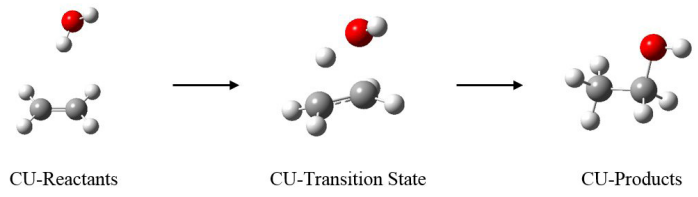


**Figure 5.** Ball and bond illustrations of molecules involved in concerted uncatalyzed reaction mechanism for the hydration of ethylene. Grey orbs = carbon; red orbs = oxygen; white orbs = hydrogen; dashed single bonds = hydrogen bonds. Models generated in Gaussview 5.0 software.

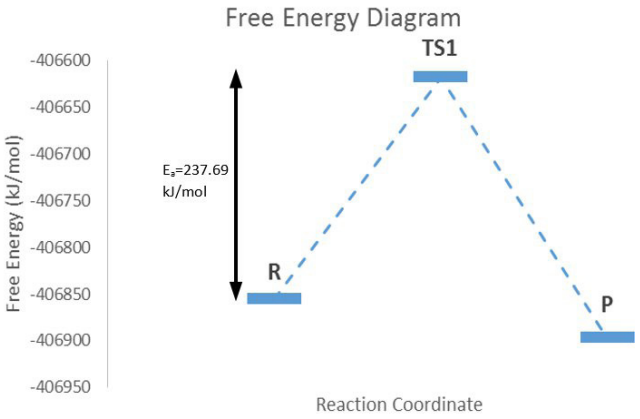


**Figure 7.** ΔG° energy curve for the concerted uncatalysed reaction mechanism for the hydration of alkenes. R = CU-Reactants; TS1 = CU-Transition State; P = CU-Products.

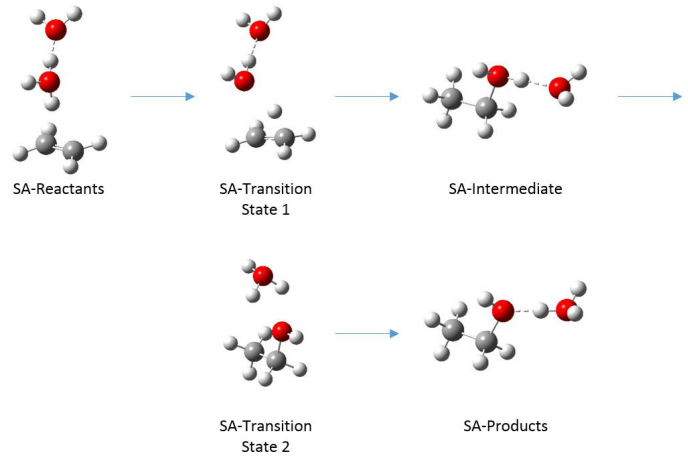


**Figure 6.** Ball and bond illustrations of molecules involved in stepwise acid catalyzed reaction mechanism for the hydration of ethylene. Grey orbs = carbon; red orbs = oxygen; white orbs = hydrogen; dashed single bonds = hydrogen bonds.

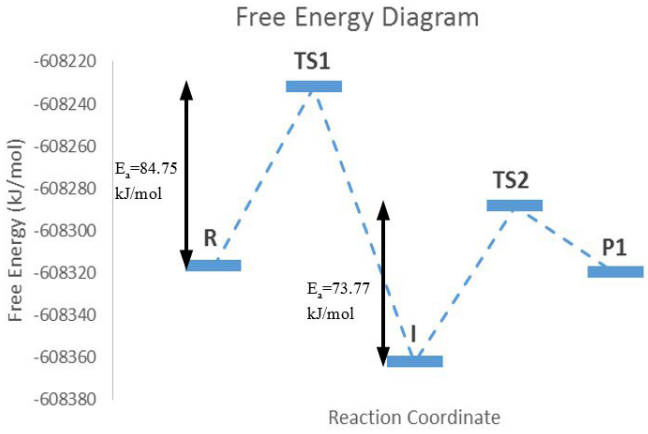


**Figure 8.** ΔG° energy curve for the stepwise acid catalyzed reaction mechanism for the hydration of alkenes. R = SA-Reactants; TS1 = SA-Transition State 1; I = SA-Intermediate; TS2 = SA-Transition State 2; P1 = SA-Products.

**Table 1.** Thermodynamic values for the concerted uncatalysed reaction mechanism for the hydration of ethylene.

| Molecules | Zero-point Energies (kJ/mol) | Thermal Energies (kJ/mol) | Thermal Enthalpies (kJ/mol) | Thermal Free Energies (kJ/mol) | Activation Energy (kJ/mol) |
|---|---|---|---|---|---|
| CU-Reactants | -406753 | -406738 | -406733 | -406856 | |
| CU-Transition State | -406552 | -406541 | -406538 | -406618 | 237.962169 |
| CU-Products | -406830 | -406819 | -406817 | -406897 | |

**Table 2.** Thermodynamic values obtained for the stepwise acid catalyzed reaction mechanism for the hydration of ethylene. Values obtained from calculations conducted in Gaussian 09 software.

| Molecules | Zero-point Energies (kJ/mol) | Thermal Energies (kJ/mol) | Thermal Enthalpies (kJ/mol) | Thermal Free Energies (kJ/mol) | Activation Energy (kJ/mol) |
|---|---|---|---|---|---|
| SA-Reactants | -608229 | -608206 | -608204 | -608317 | |
| SA-Transition State 1 | -608147 | -608125 | -608123 | -608232 | 84.745880 |
| SA-Intermediate | -608284 | -608266 | -608263 | -608362 | |
| SA-Transition State 2 | -608210 | -608192 | -608190 | -608288 | 73.771291 |
| SA-Products | -608243 | -608227 | -608225 | -608320 | |

## Discussion

Transition states are often difficult to obtain and in many cases IRC scan curves are obtained by modifying the supposed transition state structure towards the conformation of the products and/or the reactants (scans were conducted in both directions in the present study) and the energies of the new conformations are plotted. As seen in our figures (**Figure 9**, **Figure 10**, and **Figure 11**), if the highest energy value is observed when at the reaction coordinate which corresponds to the proposed transition state, the IRC scan curve supports the claim that the proposed structure represents the transition state of the reaction step.

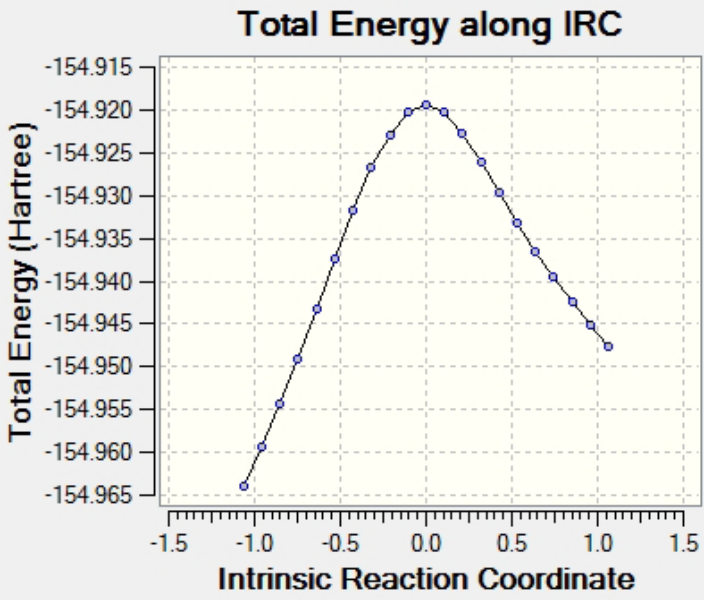


**Figure 9.** IRC curve supporting the obtained structure for the transition state of the concerted uncatalysed reaction mechanism for the hydration of ethylene.

Thermodynamic analysis of these reactions was of significant biological relevance as results showed that the concerted uncatalyzed mechanism took place at a slower rate as determined by the activation energy (237.96 kJ/mol) when compared to the stepwise acid-catalyzed reaction mechanism, which had two smaller energy barriers (84.75 kJ/mol and 73.77 kJ/mol). This suggests that numerous small energy barriers were kinetically favoured over a single large energy barrier. Therefore, in a biological context, the stepwise acid-catalyzed mechanism would be energetically preferred due to the relatively faster reaction rate as determined by theoretical computational analyses and would be more prominent in the body than the uncatalyzed mechanism, which would have minimal significance.

Given this prediction, further computational studies are required to confirm the thermodynamically favourable reaction given biologically accurate conditions such as pH, solution composition, and temperature. Furthermore, using ethylene in the place of fumarate in the calculations eliminated the effect of steric hindrance, which might play a role in which mechanism is biologically favoured. Future studies would involve accounting for such factors when setting up calculations for both the stepwise acid-catalyzed mechanism and the concerted uncatalyzed mechanism.

The results obtained from this and future computational studies could promote further research regarding the treatment of fumarase deficiency and inform the creation of a clinically useful mechanism by which fumarate can be hydrated to malate, thereby reducing the biological harm induced by fumarate accumulation.

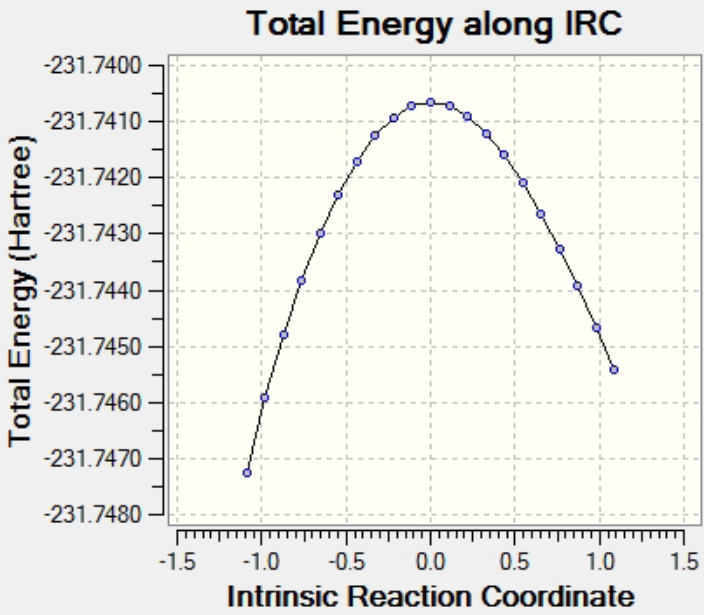


**Figure 10.** IRC curve supporting the obtained structure for the first transition state of the stepwise acid-catalyzed reaction mechanism for the hydration of ethylene.

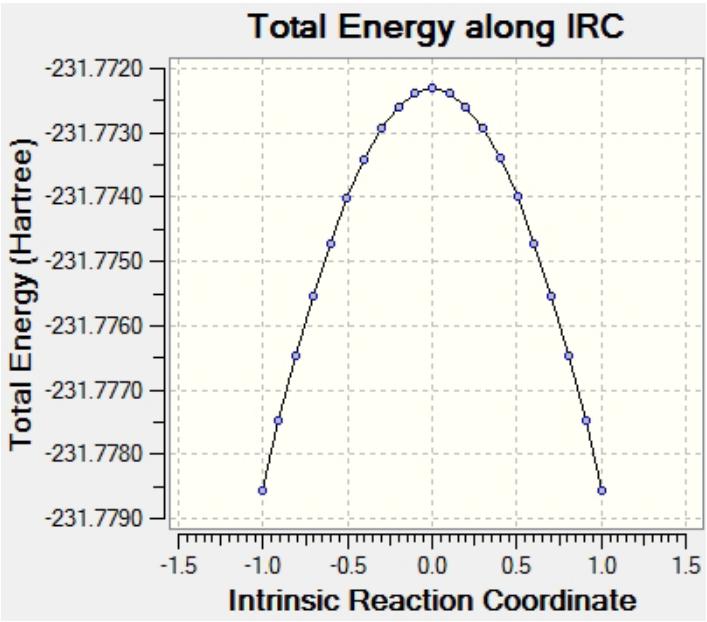


**Figure 11.** IRC curve supporting the obtained structure for the second transition state of the stepwise acid-catalyzed reaction mechanism for the hydration of ethylene.

## Conclusions

Having modelled both of the plausible reaction mechanisms, results indicated that compared to the concerted uncatalyzed mechanism, the stepwise acid-catalyzed alkene mechanism was more favourable and therefore more likely to take place. The conclusions regarding the hydration of fumarate occurring in the citric acid cycle are a direct consequence only of the activation energies and other thermodynamic properties obtained through the preliminary model systems.

## References

1. Nazaret C, Heiske M, Thurley K, Mazat JP. Mitochondrial energetic metabolism: a simplified model of TCA cycle with ATP production. J Theor Biol 2009;258(3):455-64.
2. Korla K, Mitra CK. Modelling the Krebs cycle and oxidative phosphorylation. J Biomol Struct Dyn 2014;32(2):242.
3. Lloyd SJ, Lauble H, Prasad GS, Stout CD. The mechanism of aconitase: 1.8 Å resolution crystal structure of the S642A: citrate complex. Protein Sci 1999;8(12):2655-62.
4. King A, Selak MA, Gottlieb E. Succinate dehydrogenase and fumarate hydratase: linking mitochondrial dysfunction and cancer. Oncogene 2006;25(34):4675-82.
5. Isaacs JS, Jung YJ, Mole DR, Lee S, Torres-Cabala C, Chung YL, Merino M, Trepel J, Zbar B, Toro J, Ratcliffe PJ, Linehan WM, Neckers L. HIF overexpression correlates with biallelic loss of fumarate hydratase in renal cancer: novel role of fumarate in regulation of HIF stability. Cancer Cell 2005;8(2):143-53.
6. Zeman J, Krijt J, Stratilová L, Hansíková H, Wenchich L, Kmoch S, Chrastina P, Houstek J. Abnormalities in succinylpurines in fumarase deficiency : Possible role in pathogenesis of CNS impairment. J Inherit Metab Dis 2000;23(4):371-4.
7. Elpeleg ON, Amir N, Christensen E. Variability of clinical presentation in fumarate hydratase deficiency. J Pediatr 1992;121(5):752–4.
8. Barnes LB, Bishop SH. Adenylosuccinate lyase from human erythrocytes. Int J Biochem 1975;6(7):497-503.
9. Hall RE, Henriksson KG, Lewis SF, Haller RG, Kennaway NG. Mitochondrial myopathy with succinate dehydrogenase and aconitase deficiency: abnormalities of several iron-sulfur proteins. J Clin Invest 1993;92(6):2660–6.
10. Haller RG, Henriksson KG, Jorfeldt L, Hultman E, Wibom R, Sahlin K, Areskog NH, Gunder M, Ayyad K, Blomgvist CG. Deficiency of skeletal muscle succinate dehydrogenase and aconitase: pathophysiology of exercise in a novel human muscle oxidative defect. J Clin Invest 1991;88:1197-1206.
11. Rahman S, Blok RB, Dahl HH, Danks DM, Kirby DM, Chow CW, Christodoulou J, Thorburn DR. Leigh syndrome: clinical features and biochemical and DNA abnormalities. Ann Neurol 1996;39:343–51.
12. Robinson BH, MacKay N, Chun K, Ling M. Disorders of pyruvate carboxylase and the pyruvate dehydrogenase complex. J Inherit Metab Dis 1996;19:452–62.
13. Fisher HF, Frieden C, McKee JSM, Alberty RA. Concerning the stereospecificity of fumarase reaction and the demonstration of a new intermediate. J Am Chem 1955;77(16):4436.
14. Farrar TC, Gutowsky HS, Alberty RA, Miller WG. The mechanism of the stereospecific enzymatic hydration of fumarate to L-malate. J Am Chem Soc 1957;79(15):3978–80.
15. Lillford PJ, Satchell DPN. The kinetics and mechanism of the spontaneous and acid-catalysed reactions of dimethylketen with water and alcohols. J Chem Soc 1968;889-97.
16. Vinnik MI, Obraztsov PA. The mechanism of the dehydration of alcohols and the hydration of alkenes in acid solution. Russ Chem Rev 1990;59(1):106-31.
17. Gaussian 09, Revision A.02, Frisch MJ, Trucks GW, Schlegel HB, Scuseria GE, Robb MA, Cheeseman JR, *et al*. Gaussian, Inc., Wallingford CT, 2009.
18. GaussView, Version 5.0, Dennington R, Keith T, Millam John J. Semichem Inc., Shawnee Mission, KS, 2009.
19. Taketsugu T, Gordon MS. Dynamic reaction path analysis based on an intrinsic reaction coordinate. J Chem Phys 1995;103(23):10042-9.

JULS RESEARCH

# Addition of Rank-Sensitive Statistical Procedures into Enrichment Map App Increases miR Prediction Accuracy by Verifying the Differential Expression of Target Genes

Victor Kofia[1], Ruth Isserlin[1], Veronique Voisin[1], and Gary Bader [1]

[1]The Donnelly Centre, University of Toronto, 60 College Street, Toronto, Ontario, Canada, M5S 3E1

## Abstract

**DNA microarrays enable scientists to measure the change in the expression level of large numbers of genes. A microarray typically yields a gene list that contains the expression level change of each gene. Pathway enrichment analysis is a function-oriented analytical tool that is used to interpret large gene lists. Cytoscape is an open-source software platform for visualizing complex networks and the Enrichment Map app is a tool developed for Cytoscape that is capable of building intuitive visual representations of various enrichment results. The app also allows existing enrichment maps to be supplemented with additional annotation terms, such as micro-RNAs or miRs. A new statistical test that incorporates gene-ranks into the calculation of *p*-values was added to the app so that target gene expression level could be determined. This report examines how miR predictions have been affected by the new changes. The Mann-Whitney U test was implemented in the app to identify potentially significant miRs. Compared to the Hypergeometric test, the Mann-Whitney U test was more sensitive to target gene expression levels. However, use of the test led to the identification of spurious targets and its non-parametric nature meant that the direction of change in gene expression could not be determined. Increased accuracy of miR prediction by the app was detected using the Mann-Whitney U test. Both the Mann-Whitney U test and the Hypergeometric test will enable researchers to predict miRs likely to influence observable changes in gene expression. However, since each miR gene set only indicates potential targets, there is a risk of false positives. Furthermore, the Mann-Whitney U test performs best when the parameters of the gene-rank distributions are known. Future research will focus on adding support for one-sided Mann-Whitney U tests. Availability and implementation: http://baderlab.org/ControllerMoleculePathwayAnalysis/SupplementaryMaterial?action=AttachFile&do=view&target=final_data.zip**

## Introduction

Microarrays are tools that allow biologists to track changes in gene expression on a large scale. While getting the expression profiles of entire genomes is quite feasible, no easy or intuitive way of analyzing vast amounts of expression data is currently available. Early attempts focused on examining the expression of single genes, but these methods had inherent weaknesses as even the simplest of biological processes are described by the actions of more than one gene. In order to direct research towards a more gene-group oriented view rather than an individual-gene oriented view, various analytical methods have been developed over the years [1]. These methods typically examine the enrichment (expression level) of pathways and fall under three broad categories: (i) Singular Enrichment Analysis (SEA); (ii) Modular Enrichment Analysis (MEA); (iii) Gene Set Enrichment Analysis (GSEA) [1-5].

The Enrichment Map app, developed for Cytoscape, can be used in conjunction with currently available enrichment tools [6, 7]. At the moment, the Enrichment Map app is only compatible with 2-class experiments and supports the concurrent visualization of two enrichment maps. Experiments of the 2-class nature consist of gene expression profiles collected from two samples (e.g., drug resistant vs. drug sensitive). In typical enrichment maps, nodes represent the annotation terms or gene-sets being examined, edges represent the overlap between similar gene-sets, and clusters consist of biologically similar gene-sets. Colour variation is used to denote the extent and direction of enrichment change. Red, for example, denotes gene-sets that have undergone some degree of up-regulation and are tied to a particular phenotype, P1; while blue indicates that the examined gene-sets have been down-regulated and are tied to an alternate

phenotype, P2. Absence of colour (i.e., white) indicates no change in gene expression.

The Enrichment Map app provides a query set post-analysis feature that allows researchers to find out whether the changes in gene expression observed in an experiment can be explained by the presence of known miRs. This feature has been used extensively and various enhancements have been proposed. Currently, users must possess some prior knowledge of the likelihood of a particular miR influencing the observed changes in expression. However, it would be useful if the system could automatically list miRs that have the greatest likelihood of affecting observed changes in expression. This feature would enable users to quickly identify miRs that merit further investigation; these miRs could then be validated experimentally.

The most recent official release of the app contains an miR prediction system. To identify significant miRs from an entire collection of miR gene-sets, users can opt to do a first-pass check. The first-pass designation indicates that the check is performed only once. The check itself consists of a search for overlap between every miR gene-set and at least one enriched gene-set. The search terminates only when the list of enriched gene-sets has been exhausted or a significant overlap has been found between the miR gene-set and an enriched gene-set in the map. The most recent release of the app allows users to adjust the overlap percentage between enriched gene-sets and miR gene-sets. This overlap percentage is a threshold that enables users to determine if an miR influences a particular pathway, in which case it is represented by an enriched gene-set. The addition of more rigorous statistical measures like the Hypergeometric Test (implemented elsewhere on the app) and the Mann-Whitney U Test will be important elements of the new prediction system [8, 9].

Lechman and colleagues found that miR-126 regulated cell cycle progression for hematopoietic stem cells (HSCs) both *in vivo* and *in vitro* [10]. miR-126 was knocked out in one group of HSCs and overexpressed in another group using lentiviral vectors [10]. HSCs in which miR-126 was knocked out showed increased proliferation. Conversely, HSCs in which miR-126 was overexpressed had impaired cell cycle progression. Enrichment maps built using the Enrichment Map app were used to visualize miR-126's targets. These targets range from factors that regulate cell cycle progression and cell adhesion to genes critical in the early development of HSCs [10, 12]. The new miR prediction system was used to predict which miRs were most likely to have influenced the observed changes in gene expression. This report documents the results that were obtained from the new miR prediction system. It also discusses the implications of the results and provides suggestions for future improvements to the system.

## Materials and Methods

Micro-RNA prediction was performed using data from a study by Lechman *et al.*, where miR-126 was shown to regulate cell cycle progression in human stem cells [10]. Since the creation of the enrichment map presented in the study required a high level of human intervention, duplication was not the primary goal in the present study. However, in order to ensure some level of consistency, comparisons looking at correspondence at the level of general functional themes were performed. As a first step, the enrichment results used by Lechman *et al.* were used to construct an enrichment map. The Signature Discovery option in the post-analysis input panel was selected and miRs were directly loaded onto the enrichment map. The GMT file containing the miR gene-set data (targetscan_62_conservedmiRs.gmt) was specified and prediction was performed using both the Hypergeometric test and Mann-Whitney U test. Micro-RNA gene-sets with significant overlaps were displayed in the *Available Signature-Genesets* display box.

Assume that $n$ number of items have been drawn from a population of size $N$ with $M$ total successes. The Hypergeometric test is used to determine the likelihood of obtaining $k$ successes out of $n$ draws [9]. For the test to yield reliable $p$ values, certain conditions must be met. For example, replacement must not occur for the population being sampled. The Hypergeometric probability distribution, which serves as the basis of the test, only accurately describes the probability of drawing $n$ samples from populations with a fixed size of $N$. In such populations, every draw alters the probability of subsequent draws and the final distribution deviates from the expected binomial type. In the context of post-analysis, $N$ is the total number of genes in the enrichment map. The number of genes in the miR gene-set being considered is $n$. $M$, on the other hand, corresponds to the number of genes in the enriched gene-set. Finally, $k$ represents the number of genes that make up the overlap between the miR gene-set and the enriched gene-set.

The primary purpose of the Hypergeometric test in the Enrichment Map app is to determine whether a certain disease or miR target are of interest and warrant further examination. In a typical enrichment map, interesting targets typically yield unusually small $p$-values when the test is applied to them.

The Mann-Whitney U test is capable of assessing the relative expression levels of overlapping genes (i.e., through rank) by calculating a statistic based on this information [8]. When two distributions are non-equal, the Mann-Whitney U test can be used to determine whether one distribution is shifted upward or downward relative to another (one-sided test). However, it is only possible to conclude this if one or more parameters associated with both distributions are known. The Mann-Whitney U test by nature is non-parametric which was suitable as no assumptions were made about the distributions of the overlapping genes. However, conclusions derived from the test were less informative than they would have been had assumptions been made about the shape of the gene distributions. In the context of the gene-set data, this meant that it was only possible to conclude that a group of overlapping genes had been differentially expressed. It was not possible to determine whether the genes were up-regulated or down-regulated.

## Results

After miR prediction was performed using the Hypergeometric test (set at a $p$-value cut-off of 0.25), exactly 22 miR-126 target pathways were identified. Information on the specific genes that were affected is available in the Supplementary Materials section. Two target pathways, cell junction assembly (GO|GO:0034329) and cell junction organization (GO|GO:0034330), yielded low $p$-values. While miR-126 is known to affect cell adhesion [10], these pathways made up only 2 of the 22 targets that the test marked as being of interest. A number of pathways overlapped with genes that had registered no change in expression in the course of the experiment. Cell adhesion (GO|GO:0045785) is an example of a target pathway that was rife with genes of this type. The overlap of miR-126 with GO|GO:0045785 consisted of only two genes and no change in expression was detected for either. Since the overall gene-set or pathway was marked as being up-regulated by GSEA, any overlapping genes were expected to have undergone a similar

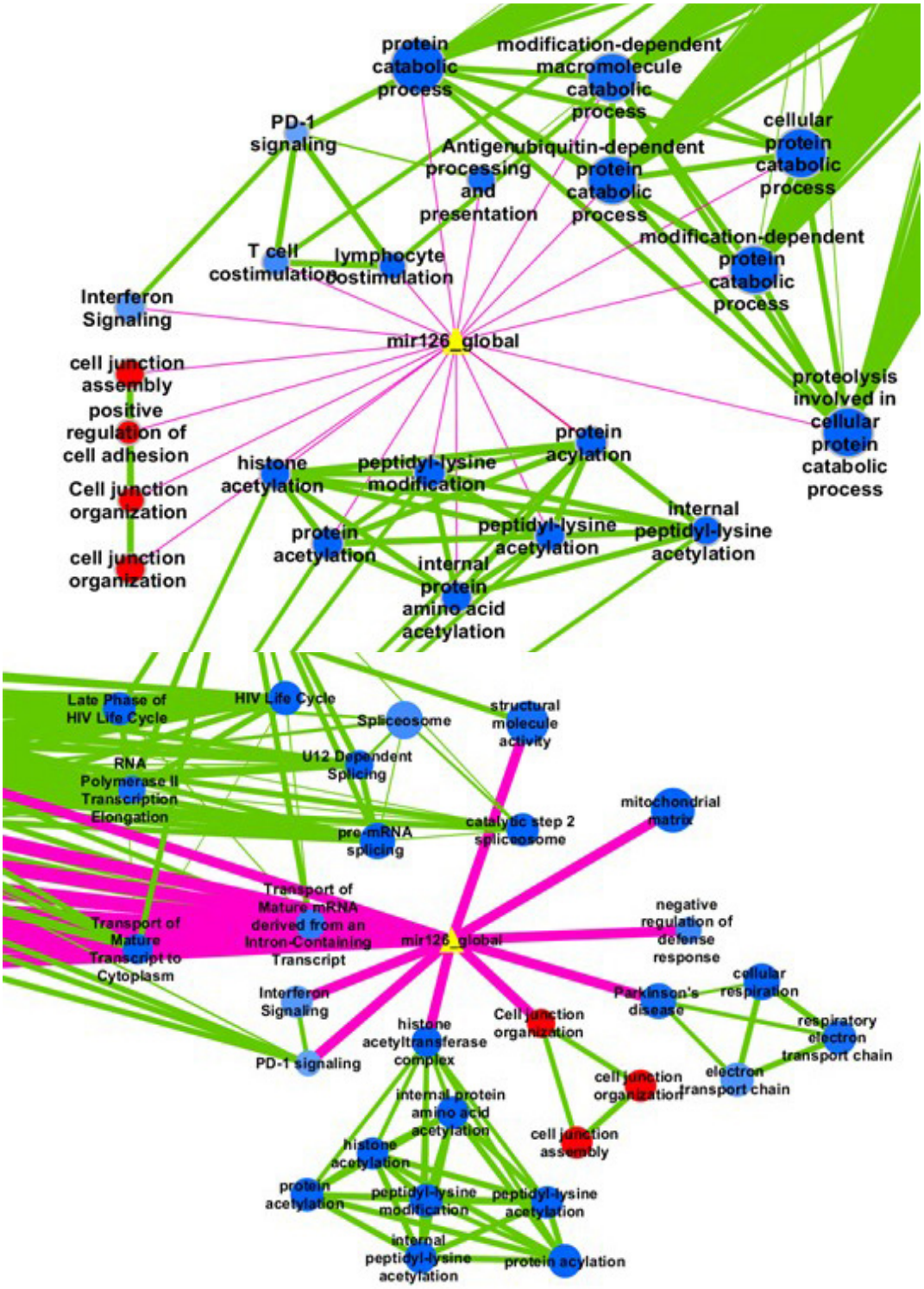


**Figure 1.** (A) Top. Predicted miR-126 targets with Hypergeometric test set at a *p*-value cutoff of 0.25. When a cut-off of 0.25 was used, exactly 22 miR-126 target pathways were identified. Two targets, Cell Junction Assembly (GO|GO:0034329) and Cell Junction Organization (GO|GO:0034330), yielded unusually low *p*-values. (B) Bottom. Predicted miR-126 targets with Mann-Whitney U test at a *p*-value cutoff of 0.25. Over 31 miR-126 targets were identified when a cut-off of 0.25 was used.

change in expression. Given that no change in expression was detected for the overlapping genes, it is clear that miR-126 had no effect on their expression.

Over 31 miR-126 targets were identified when miR prediction was performed using the Mann-Whitney U test (set at a *p*-value cut-off of 0.25). The list of targets included gene-sets that contained genes involved in cell adhesion and cell cycle regulation, as well as genes implicated in Parkinson's disease (KEGG|HSA05012). The latter association of miR-126 with Parkinson's disease was unsurprising. In a study by Kim *et al.*, over-expression of miR-126 was found to increase the susceptibility of neuronal cell systems to 6-OHDA, a neurotoxin [13]. The overlap of miR-126 with the Programmed Death Protein 1 (PD-1) signaling pathway, which induces apoptosis, (REACTOME|REACT_19324.1) consisted of one gene [14]. Since miR-126 has been shown to restrict cell cycle progression, the link between miR-126 and the PD-1 signaling pathway has much biological significance [10]. However, given that there is only one overlapping gene and PD-1 signaling involves 15 genes – most of which are down-regulated – whether this relationship warrants further investigation is unclear.

Exactly two enriched gene-sets were identified when miR prediction was performed with the Hypergeometric test set to a *p*-value cut-off of 0.05: (1) Cell Junction Assembly (GO|GO:0034329) and (2) Cell Junction Organization (GO|GO:0034330). The two gene-sets are consistent with the usual targets for miR-126 but the Hypergeometric test failed to capture equally important, known target, gene-sets. Both gene-sets had the same four overlapping genes but out of the four, only two genes were differentially expressed: Integrin Alpha 6 (*ITGA6*) and Integrin-Linked Kinase.

When miR prediction was performed with the Mann-Whitney U test (set to a *p*-value cut-off of 0.05), exactly three enriched gene-sets were identified: (1) Cell Junction Organization (REACTOME|REACT_20676.1), (2) Interphase (GO|GO:0051325), and (3) Interphase of Mitotic Cell Cycle (GO|GO:0051329). The overlap between miR-126 and REACTOME|REACT_20676.1 contained only two genes, both of which were up-regulated. The overlap between miR-126,

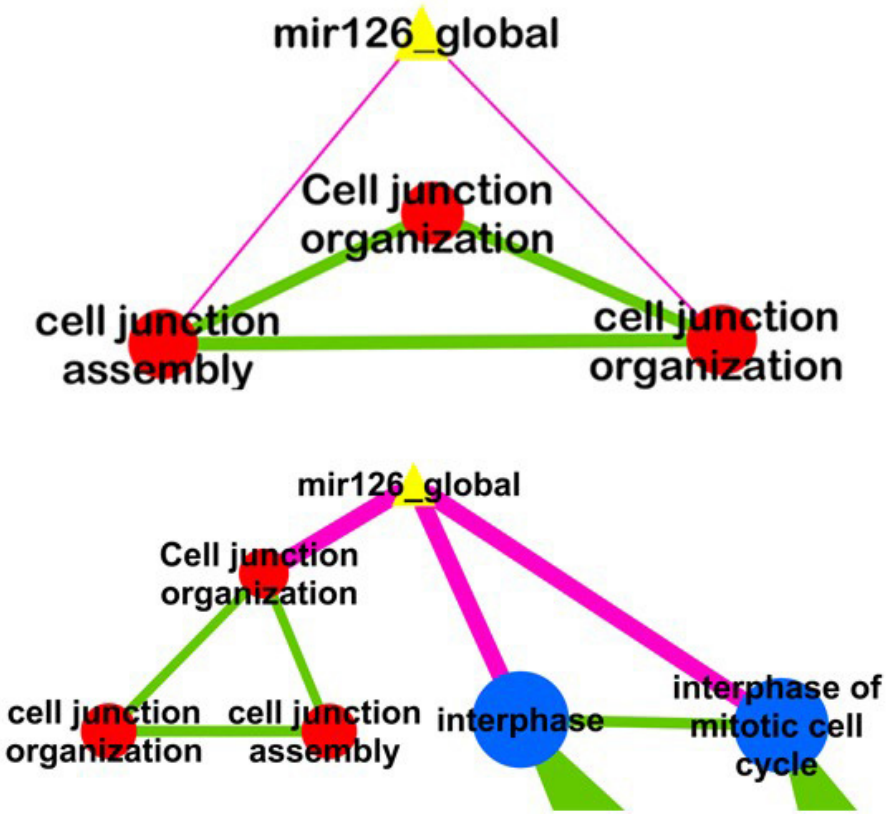


**Figure 2.** Pink edges indicate miR-126 targets. Green edges indicate overlap between enriched gene-sets. (A) Top. Predicted miR-126 targets with Hypergeometric test set at a *p*-value cut-off of 0.05. Setting an arbituary *p*-value cut-off of 0.05 resulted in the identification of exactly two enriched gene-sets: (1) Cell Junction Assembly (GO|GO:0034329) and (2) Cell Junction Organization (GO|GO:0034330. (B) Bottom. Predicted miR-126 targets with Mann-Whitney U test set, set at a *p*-value cut-off of 0.05. A *p*-value cut-off of 0.05 resulted in the identification of exactly those enriched gene-sets: (1) Cell Junction Organization (REACTOME|REACT_20676.1), (2) Interphase (GO|GO:0051325, and (3) Interphase of Mitotic Cell Cycle (GO|G):0051329).

GO|GO:0051325, and GO|GO:0051329 consisted of three up-regulated genes, one of which exhibited markedly higher expression than the others. Similar to the test performed at the 0.25 cut-off, the Mann-Whitney U test selectively assimilated targets in which the overlapping genes were differentially expressed but which would have failed had the Hypergeometric test been performed first (i.e., with a 0.05 cut-off). The other targets exhibit the same issues of regulation inconsistency that have already been outlined. The genes making up the overlap between miR-126 and the two targets, REACTOME|REACT_20676.1 and GO|GO:0051325, are all up-regulated even though the overall pathways linked to miR-126 are down-regulated. The overall effect of miR-126 on the pathways is one of repression, but since the genes it affects have the opposite change in expression, the relationship between miR-126 and the pathway is more complex. Future research will focus on developing a way to explicitly identify pathways whose overall change in expression is opposite that of the specific genes being targeted by the miR.

## Discussion

Stated simply, the Hypergeometric test is used to determine whether a particular overlap between an miR gene-set and an enriched gene-set is of biological interest. The test calculates the likelihood of obtaining the observed overlap simply by chance (i.e., by randomly sampling the universe of up-regulated or down-regulated genes). If obtaining the observed overlap is highly unlikely due to chance, then the overlap may have some biological significance and as such merits further examination. The Mann-Whitney U test, on the other hand, is used to answer a very different question than that addressed by the Hypergeometric test. It is suited for answering questions like: does the enriched gene-set have more up-regulated or down-regulated genes than the miR gene-set? Thus, the Mann-Whitney U test identifies target genes that are guaranteed to be differentially expressed. However, performing the Mann-Whitney U test by itself, without performing the Hypergeometric test first, means that some of the targets identified might not be worth looking at [15]. For example, PD-1's designation as a target indicates that a wide variety of tests might need to be done in conjunction with the Mann-Whitney U test in order to obtain biologically useful results. Upon examination of the other targets, a recurring theme was that the specific genes which miR-126 targeted were the ones that were down-regulated, whereas the entire gene-set or pathway was up-regulated. From a biological standpoint, this could indicate that miR-126 induces repression and that its up-regulation causes inhibition of most of the genes that make up the pathway. However, the test's inability to explicitly identify targets where the expression change of the overlapping genes is in line with the overall change in expression of the target gene-set is problematic for users of the app. Future work on the app should be directed towards adding support for one-sided Mann-Whitney U tests. In addition, the visual style will have to be modified such that subtle variations in overlap can be readily identified.

When miR gene-set prediction was performed on data from the study by Lechman and colleagues, lower *p*-values yielded smaller numbers of significant gene-sets for both tests. However, none of the potentially interesting miRs that had been highlighted in the study were present in the final list of miRs for any of the low *p*-value cut-offs. Exactly 24 miRs were found to be significant when signature gene-set discovery was performed with the Mann-Whitney U test at a *p*-value cut-off of 0.001. The number of miRs identified by the Hypergeometric test was roughly the same (around 19). The precise function of these miRs was not been verified as they have only been briefly mentioned in the literature. Further research is needed to elucidate their exact function.

## Conclusion

At high *p*-value cut-offs, the Hypergeometric test's flaws and weaknesses are apparent. Targets for which the overlapping genes exhibit no change in expression are selected even though these targets have no biological significance. The Mann-Whitney U test has proven to be a worthy addition to the roster of statistical tests provided by the app. Its use of rank in calculating a statistic

allows for more sensitive tests to be performed. However, the Mann-Whitney U test is not perfect. Its latitude and range is reduced considerably when compared to the Hypergeometric test. Furthermore, its reliability in instances where the overlap is small is also lacking. Investigating the precise nature of the distributions of the overlapping genes will prove vital for the correct identification of relevant targets.

## References

1. Huand D, Sherman B, Lempicki RA. Bioinformatics enrichment tools: paths towards the comprehensive functional analysis of large gene lists. Nucleic Acids Res 2009;37(1):1-13.
2. Carmona-Saez P, Chagoyen M, Tirado F, Carazo JM, Pascual-Montano A. GENECODIS: a web-based tool for finding significant concurrent annotations in gene lists. Genome Biol 2007;8(1):R3.
3. Huang DW, Sherman BT, Lempicki RA. Systematic and integrative analysis of large gene lists using DAVID bioinformatics resources. Nature Protocols 2008;4(1):44-57.
4. Robinson PN, Wollstein A, Bohme U, Beattie B. Ontologizing gene-expression microarray data: characterizing clusters with gene ontology. Bioinformatics 2004 Apr 12;20(6)979-81.
5. Zheng Q, Wang XJ. GOEAST: a web-based software toolkit for gene ontology enrichment analysis. Nucleic Acids Res 2008 Jul 1;36(Web Server issue):W358-63.
6. Shannon P, Markiel A, Ozier O, Baliga N, Wang J, Ramage D, Amin N, Schwikowski B, Ideker T. Cytoscape: a software environment for integrated models of biomolecular interaction networks. Genome Res 2003;13(11):2498-2504.
7. Merico D, Isserlin R, Stueker O, Emili A, Bader G. Enrichment map: a network-based method for gene-set enrichment visualization and interpretation. PLOS One 2010;5(11):1-12.
8. Mann HB, Whitney DR. On a test of whether one of two random variables is stochastically larger than the other. The Annals of Mathematical Statistics 1947; 50-60.
9. Wackerly D, Mendenhall W, Scheaffer R. Mathematical statistics with applications.: Cengage Learning; 2007.
10. Lechman ER, Gentner B, Van Galen P, Giustacchini A, Saini M, Boccalatte FE, Hiramatsu H, Restuccia U, Bachi A, Voisin V, Bader GD, Dick JE, Naldini L. Attenuation of miR-126 activity expands HSC in vivo without exhaustion. Cell Stem Cell 2012;11(6)799-811.
11. Crawford M, Brawner E, Batte K, Yu L, Hunter MG, Otterson GA, Nuovo G, Marsh CB, Nana-Sinkam SP. MicroRNA-126 inhibits invasion in non-small cell lung carcinoma cell lines. Biochem Biophys Res Commun 2008;373(4)607-12.
12. Feng R, Chen X, Yu Y, Su L, Yu B, Li J, Cai Q, Yan M, Liu B, Zhu Z. miR-126 functions as a tumour suppressor in human gastric cancer. Cancer Lett 2010;298(1):50-63.
13. Kim W, Lee Y, McKenna ND, Yi M, Simunovic F, Wang Y, Kong B, Rooney RJ, Seo H, Stephens RM, Sonntag KC. miR-126 contributes to Parkinson's disease by dysregulating the insulin-like growth factor/phosphoinositide 3-kinase signaling. Neurobiol Aging 2014;35(7):1712-21.
14. Riley JL. PD-1 signaling in primary T cells. Immunol Rev 2009;229(1):114-25.
15. Hahne F, Huber W, Gentleman R, Falcon S. Bioconductor case studies: Springer Science & Business Media 2010;205-18.

JULS REVIEWS

# Brugada Syndrome: Epidemiology, Etiopathogenesis, and Treatment

Ahmad Kamal M. Hamid

Department of Physiology, Faculty of Medicine, University of Toronto, Toronto, ON, Canada

## Abstract

**Brugada Syndrome (BrS) is a genetic cardiac disease that may unfold by physiological or environmental triggers. It affects about 0.05% of the population and has an annual mortality rate of 10%. BrS is an adult-onset disease and occurs more commonly in males. The first clinical manifestation of BrS is sudden cardiac death with no structural defects discernable using routine diagnostic tools (e.g., echocardiography, angiography, and ventriculography). Two competing pathophysiological mechanisms of the disease have been proposed: (1) a repolarization model, which involves a channelopathy; and (2) a depolarization model, which involves a conduction delay due to minor structural defects. A third developmental model has been proposed to unify both of the previous models and is related to a neural crest cell aberration that leads to a slower conduction in the right ventricular outflow tract and a transmural heterogeneity of repolarization. This model is supported by evidence implicating both genetic mutations and structural derangements, and suggests that the repolarization and depolarization models can occur concurrently. However, further investigation is warranted to support the neural crest model. Moreover, the strong positive correlation between testosterone levels and BrS incidence in males points to a new, possible therapeutic approach: targeting the pathway involved in testosterone-driven enhancement of $I_{to}$ (transient outward current) and reduction of $I_{Ca\text{-}L}$ (L-type $Ca^{2+}$ current) may restore electrical homogeneity and ameliorate BrS prognosis. Future studies should investigate the possibility that BrS is an oligogenic disease as the syndrome is correlated with common genetic polymorphisms identified using genome wide-associations.**

## Introduction

With a global prevalence of about 1 in 2500 and an annual mortality rate of 10%, Brugada Syndrome (BrS) is a serious cause of sudden cardiac death; it has also been linked to sudden unexplained nocturnal death syndrome (SUNDS) [1-3]. Often, the first clinical manifestation of the syndrome is sudden cardiac arrest (SCA); other symptoms include recurrent episodes of polymorphic ventricular tachycardia, ventricular fibrillation, and syncope [4]. The pathophysiological mechanism of BrS remains controversial, with two competing hypotheses proposed in the literature. One mechanism is a classical channelopathy (repolarization) model, and the second mechanism is a conduction delay (depolarization) model that incorporates minor structural defects [1]. Recently, a new model has been proposed; it attempts to unify both models on the basis of an aberration in myocardial development [5].

About fourteen genes are linked to BrS, seven of which are associated with the cardiac voltage-gated $Na^+$ channel [6-10]. The mutational background of BrS appears to be very complex with a myriad of mutations identified in each of the correlated genes. For instance, there are over 300 BrS-linked mutations in the α-subunit of the voltage-gated $Na^+$ channel type V (*SCN5A*) [11]. Similarly, the physiological and environmental triggers for BrS are also diverse, ranging from electrolyte imbalance to hyperpyrexia [12].

Based on its characteristic ST segment elevation on the electrocardiogram (ECG), a consensus has been developed among physicians to diagnose BrS [8, 13]. However, risk stratification for asymptomatic patients is still unclear, and available treatments require significant improvements [1, 13]. Nevertheless, as BrS is predominantly regarded as a disorder of the heart's electrical system, pharmacologic intervention aiming to rebalance electrical currents appears to hold promise for future treatments [4, 14]. This paper will provide an overview compendium of the syndrome, highlighting general epidemiological trends in the population, the main proposed pathophysiologic mechanisms, the genetic and environmental basis of the disease, and promising therapeutic avenues.

## Epidemiology

### Geographic Prevalence

BrS type I ECG pattern, characterized by an ST segment elevation with a negative T wave, has a high occurrence in Southeast Asia (4 and 3.6 in 2000 in Japan and the Philippines, respectively) and the Middle East (1.6, 7.2, and 3.6 in 2000 in Turkey, Iran, and Pakistan, respectively) and a low occurrence in Northern and Western Europe and North America [1, 3]. For instance, the BrS pattern prevalence is 0.022 in 2000 in Denmark, and 0.24 in 2000 in the USA [1, 3]. The high prevalence of the BrS pattern in Southeast Asia may be explained by a haplotype variant

comprised of six polymorphisms in the *SCN5A* promoter with an allele frequency of 22% in ethnically Asian subjects, in contrast to 0% in ethnically white and black subjects [15]. In addition, a study showed that Southeast Asian refugees living in the USA have a high incidence of SUNDS along with other BrS markers, which suggests that the basis for geographic differences is unlikely to be a location-specific environmental factor, but a combination of genetic and culture-specific or other environmental factors [16].

## Symptoms and Mortality

The initial symptom in 30% of symptomatic BrS patients is SCA [4]. The annual incidence rate of arrhythmic events is 0.5-4% in patients with no previously aborted SCA and 0.4-1% in asymptomatic patients, where these overlapping groups constitute ~ 90% and ~ 60% of the patient population, respectively [3]. BrS is responsible for at least 20% of deaths due to idiopathic SCA (with no obvious structural heart defects) and 4-12% of total sudden cardiac deaths [1, 4, 17]. Using the Cox proportional hazards model, a study has shown that age- and gender-standardized mortality via unexpected death was 21.9% for subjects displaying a Brugada ECG pattern ($n$ = 32) and 0.42% for control subjects ($n$ = 4,756); the odds ratio was 52.63 [18]. Due to its circadian dependence and pathological nature, it has also been suggested that BrS may underlie SUNDS [1, 3]. For instance, polymorphic ventricular tachycardia and ventricular fibrillation tend to occur during evenings in BrS patients [4]. In fact, a study concluded that the two syndromes are identical at the genetic, phenotypic, and functional levels [19]. Overall, the mortality rate for both symptomatic and asymptomatic BrS patient populations is approximately 10% per year [2].

## Age and Gender

BrS displays an adult onset (~35 years of age), however, patients as young as 1 year and as old as 84 years have been diagnosed with BrS [4, 17]. Many epidemiological studies have supported a male preponderance of the syndrome, with an adult male-to-female ratio of 9:1. However, children exhibited no gender difference with respect to BrS prevalence [1, 4, 17]. An increased transient outward potassium current ($I_{to}$) in males, and a difference in hormonal status may account for this asymmetric gender distribution [1]. The lack of gender difference in the pediatric population supports the latter hypothesis, due to similar levels of testosterone (TST) in both genders at a young age [1]. In fact, a recent study by Barajas-Martínez and colleagues provided evidence for the co-occurrence of the hypotheses [20]. The study showed that 1 μM of TST increased the expression of $K_V$4.3/KCND3 (a voltage-gated $K^+$ channel) by 547.51% and accelerated its recovery from inactivation, which led to an increase in $I_{to}$ from 11.8 ± 1.6 pA/pF (current density) to 18.7 ± 3.2 pA/pF in human induced pluripotent stem cell-derived cardiomyocytes (hiPSC-CM) [20]. Nevertheless, a possible limitation of this study is the use of embryoid body technology in which immature phenotypes are often observed, and may lead to a potential deficiency in antagonistic pathways that suppress TST-induced $I_{to}$ [21]. In addition, the cells had a depolarized maximum diastolic potential around -65.4 ± 10.3 mV caused by a low $I_{K1}$ (inward rectifier $K^+$ current) and a very slow recovery of inactive $I_{to}$ channels [20]. The change in gating kinetics of the $K_V$4.3 channels (possibly by under or overexpression of regulatory proteins) and the increase in diastolic membrane potential may have affected the channels' sensitivity to TST leading to an overestimation of the increase in $I_{to}$ density.

In support of the above findings, the collective evidence from two separate studies examining the incidence rates of BrS and investigating the effect of aging on TST levels in human males suggest a positive correlation between TST levels and BrS ($r$ = 0.88) (**Figure 1**) [18, 22]. The data shows that the proportion of men with hypogonadism (rHG), characterized by a total serum TST < 11.3 nm $L^{-1}$, peaks at the fourth decade of life concomitant with a culmination of BrS prevalence in males. Moreover, rHG and BrS prevalence in males both plateau after 40 years of age before declining at 60 years of age. Females showed lower BrS prevalence with no discernable age-dependence. Another study by Matsuo and colleagues reported that the ECG pattern characteristic of BrS disappeared after two asymptomatic BrS patients underwent surgical castration due to prostate cancer, which corroborates the implication of TST in the syndrome [23]. Altogether, the literature suggests that increased BrS prevalence in males may be explained by their increased TST levels, which may elevate cardiac $I_{to}$ current and facilitate the syndrome's progression.

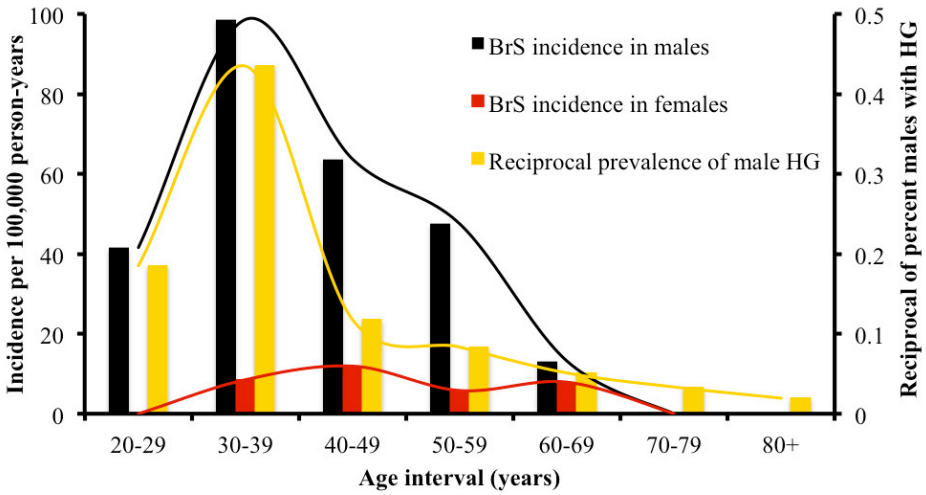


**Figure 1.** The incidence of Brugada Syndrome (BrS) for both genders and the reciprocal prevalence of male hypogonadism (HG) as a function of age. The bars and the curves denote the same data in different representations.

## Limitations

A major limitation in many BrS epidemiological studies is that the Brugada ECG pattern is not specific for BrS patients. In fact, the same pattern can be observed in patients suffering from a myocardial infarction, severe electrolyte imbalance, or mediastinal tumours [3]. Given the sporadic nature of the Brugada ECG pattern, frequent ECG monitoring is necessary to accurately estimate the syndrome's prevalence [18]. In addition, most epidemiological studies are retrospective. Here, BrS is characterized by idiopathic ventricular fibrillation and the lack of data on structural heart defects may affect these results [3, 18].

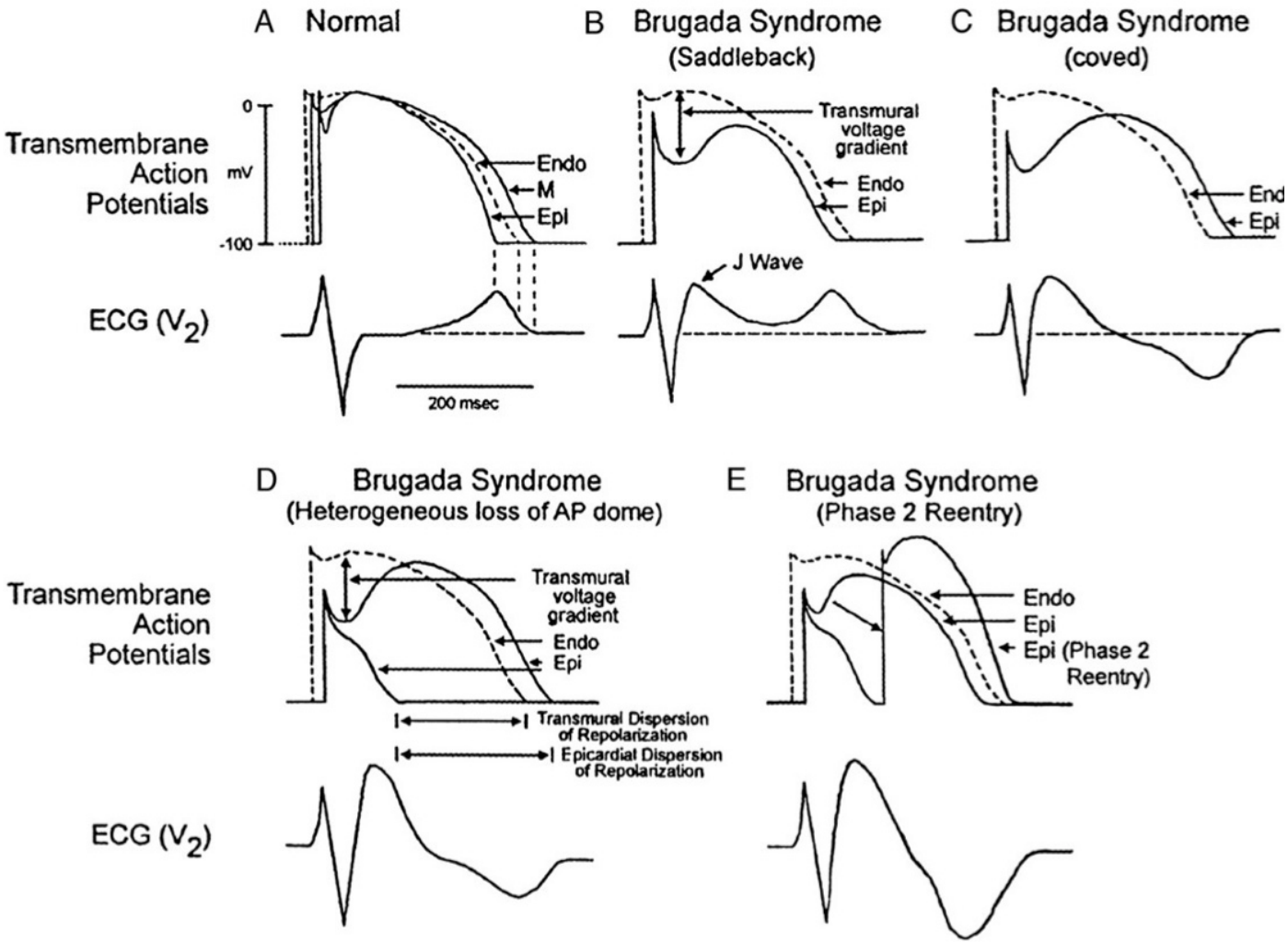


**Figure 2.** The repolarization model of Brugada Syndrome (BrS) pathophysiology and arrhythmogenesis. (A) shows the normal action potential of the endocardial (Endo), M and epicardial (Epi) cells (top) and the normal ECG V2 trace (bottom). (B) and (C) demonstrate the two types of ECG observed patterns in BrS patients. (D) shows the epicardial dispersion of repolarization while (E) illustrates phase 2 re-entry arrhythmia [24].

## Pathophysiology

An electrocardiographic characteristic of BrS is an ST segment elevation in the right precordial leads (V1-V3). It is often highly variable, changing from beat to beat and from day to day [24]. The two types of ST elevations are the saddle-back and the coved-type. Both types have a J point elevation that results from an extracellular current travelling towards the right precordial leads. This may be due to a voltage change propagating inwards either across the cardiac transmural layers or towards an internal cardiac anatomical structure. Unlike the saddle-back, the coved-type ST elevation has a negative T wave which indicates an opposite propagation of the voltage change (**Figure 2A**, **2B** & **2C**).

In BrS, SCA often results from polymorphic ventricular tachyarrhythmia whereas the monomorphic type rarely occurs [24]. The type of arrhythmia developed in BrS is thought to be re-entry arrhythmia rather than an early after-depolarization (EAD) arrhythmia, delayed after-depolarization (DAD) arrhythmia, or an altered automaticity arrhythmia. Decelerated impulse propagation, high readiness of ventricular tachycardia/fibrillation (VT/VF) inducibility in electrophysiological studies (EPS), and the polymorphicity of the resulting arrhythmia support a re-entry type arrhythmia [24]. The lack of QT interval prolongation in BrS renders the possibility of a causative EAD unlikely [24]. DAD is also not likely to be implicated, as catecholamines increase intracellular $Ca^{2+}$ in this type of arrhythmia and thereby ameliorate ST segment elevation [24]. Furthermore, the sudden onset and the polymorphic nature of the tachyarrhythmia observed with BrS renders altered automaticity another unlikely type of arrhythmia in the syndrome [24]. The proposed pathophysiological mechanisms underlying the symptoms of BrS include a repolarization model, a depolarization model, a structural defect model, and a neural crest model [24, 25].

### The Repolarization Model

Normally, the $I_{to}$-driven action potential notch, exhibited by the epicardial cells more profoundly than by the endocardial cells, generates a transmural voltage gradient responsible for the slight J point elevation observed in an ECG inscription [26]. Due to a higher expression of $I_{to}$ in the epicardium, it is markedly affected by a reduction in the depolarizing $Na^+$ current observed in the heart of BrS patients. At -30 mV of the action potential phase 1 (early rapid repolarization phase), the epicardial cells display an all-or-none heterogeneous repolarization phenomenon [1, 24]. Cells that undergo early repolarization then exhibit a loss of the action potential dome, rendering a significantly shorter

action potential duration (**Figure 2D** top) [1]. Consequently, an epicardial dispersion of repolarization may ensue, leading to a transmural voltage gradient where an initial repolarization wave spreads from the epicardium to the endocardium giving rise to further J point elevation [1]. Subsequently, if $I_{Na}$ is high enough to maintain the brevity of the epicardial action potential relative to the endocardium, the next repolarization wave originates from the epicardial cells that did not undergo early repolarization to the endocardium yielding a positive T wave observed in the saddle-back ST elevation pattern (**Figure 2B** bottom) [2]. However, if $I_{Na}$ is lower, the epicardial action potential may be prolonged beyond the repolarization of the endocardium, and the repolarization wave would then originate from the endocardium to the non-early repolarized epicardial cells yielding a negative T wave observed in the coved-type ST elevation pattern (**Figure 2C**) [2].

The resultant transmural dispersion of repolarization creates a vulnerable window where an extrasystole can initiate re-entry arrhythmia (**Figure 2E**) [2]. Furthermore, the epicardial dispersion of repolarization permits the action potential dome to spread from normally repolarized cells to cells with early repolarization [1]. This may then trigger a local re-excitation by means of a re-entry arrhythmia that leads to a closely coupled extrasystole that has been shown to cause circus movement re-entry [1, 2].

Numerous studies have demonstrated evidence in favour of the repolarization model [24, 27-30]. For instance, $I_{to}$ heterogeneity between the epicardium and the endocardium as well as the transmural layers supports the possibility of differential effects of reduced $I_{Na}$ on the action potential morphologies [24]. Moreover, some studies have shown that an increased parasympathetic stimulation occurs prior to VF episodes, which has been shown to exacerbate ST elevation by means of reducing the L-type $Ca^{2+}$ current [24]. In contrast, sympathetic stimulation depresses ST elevation and inhibits the development of VF, which is further supported by observations of pathological norepinephrine recycling in some BrS patients [24]. There is evidence that 4-aminopyridine, an $I_{to}$ inhibitor, recovers the spike-and-dome morphology and inhibits electrical heterogeneity [24]. Quinidine, which has anticholinergic and $I_{to}$ blocking effects, also prevents arrhythmias [24].

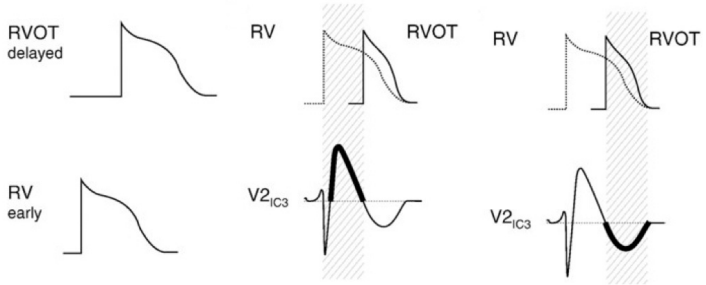


**Figure 3.** The depolarization model of Brugada Syndrome. RV and RVOT denote the right ventricle and the right ventricular outflow tract, respectively. V2IC3 denotes the ECG electrode. The two diagrams on the left qualitatively demonstrate the chronological difference between the RVOT and RV action potentials. In the top middle and top right diagrams, the dotted and solid lines denote the action potentials of the RV and RVOT, respectively. In the bottom middle and bottom right diagrams, the bold lines indicate the resultant ECG phenomenon due to the corresponding difference in RV and RVOT action potentials shaded in diagonal stripes in the top diagrams [24].

## The Depolarization Model

In this pathophysiological model, the mechanism does not revolve around a difference in action potential morphology, but rather conduction velocity [24]. Here, a conduction delay in the right ventricular outflow tract (RVOT) results in the action potential reaching the right ventricle (RV) first (**Figure 3**) [24]. At this time interval, the membrane potential in the RV is more positive than that in the RVOT allowing it to serve as an initiator of depolarization in the RVOT [24]. Therefore, an intercellular depolarization wave would propagate from the RV to the RVOT and an extracellular current would travel from the opposite direction yielding a closed-loop circuit [24]. During this phase, an electrocardiographic electrode at the RVOT level would inscribe a positive deflection representing the elevated J wave [24]. In the next phase, the depolarized RVOT is more positive than the repolarized RV, causing a reciprocation of the above currents and a negative inscription on the ECG trace representing the negative T wave observed in the coved-type BrS pattern [24].

In this model, arrhythmogenesis occurs as a result of the disparity between the electrical properties of the RVOT and the RV. This bears similarity to a model developed to explain arrhythmogenesis in regional transmural ischemia, where a depolarization wave front propagating from the RV would decelerate through the RVOT but maintain its pace on its border [24]. By the time the RVOT wave reaches the level of a specific normal-tissue zone parallel to it, the normal tissue would have already repolarized from the quickly propagating border wave, and the RVOT wave can then travel through the border zone to the already-repolarized tissue and emerge back from the site of origin as a re-entrant wave [24].

Evidence lending support to the depolarization model includes the high occurrence of ventricular late potentials in BrS patients, which suggests delayed conduction velocity and provides a substrate for re-entry arrhythmia [24, 32]. The presence of RVOT conduction slowing as per body surface mapping studies, localization of arrhythmogenicity to the RVOT area, and development of structural derangements and fibrosis in BrS patients further support this model [24]. Late potentials are also a strong predictor of VT/VF inducibility and are often concomitant with ST elevations [24]. Similar to the repolarization model, BrS-linked mutations in $Na^+$ channels and $I_{Na}$ blocker-induced deterioration are also consistent with the depolarization model, as they correspond to conduction slowing [24]. Nevertheless, the depolarization model does not provide an explanation for the saddle-type ECG pattern.

## The Neural Crest Model

This model attempts to provide a unifying pathophysiological mechanism that supports the coexistence of the above models [5]. The hypothesis proposes that the RVOT conduction slowing and transmural heterogeneity of repolarization observed in BrS patients is caused by an abnormal expression of the neural crest cells (NCCs), a group of migratory cells that contribute to the development of multiple tissue lineages at the embryonic stage [5]. Specifically, NCCs may be involved in the morphogenesis of the RVOT free wall, aortopulmonary septum, aortic arch, AV node, bundle of His, bundle branches, some atrial tissue, and pulmonary veins [5]. As Connexin 43 (Cx43) expression exhibits transmural heterogeneity and is directly proportional to NCC migratory speed, this model suggests that a possible abnormal expression in Cx43

can alter the transmural electrical properties and exacerbate the effect in the RVOT due to abnormal NCC migration [5]. In turn, aberrant Cx43 provides the possibility of concurrent conduction slowing and abnormal repolarization. This model may possibly explain the underlying mechanism of roughly 70% of BrS patients, where a genomic $Na^+$ channel mutation is not present [33].

Although BrS is commonly characterized by the absence of structural heart defects, recent evidence suggests possible mild structural derangements that are only detectable by histological methods [24]. Studies of BrS patients have reported RV enlargement, increased adipose tissue, and abnormal RV wall motion in areas of high VT/VF inducibility during an EPS – where premature complexes occur [24]. Interestingly, an electron beam computer tomography study showed that disopyramide (a class Ia $Na^+$ channel blocker) administration accentuates motion abnormalities resulting from structural derangements in the RVOT in 62% of BrS patients ($n$ = 13, $p$ < 0.01) [34]. Structural derangements also include fibrosis and epicardial fatty infiltration [35]. It has also been argued that functional derangements may lead to structural ones. For instance, a subject with compound heterozygosity for two $Na^+$ channel mutations (*SCN5A*) suffered from acute degeneration in the specialized conduction system [24]. Moreover, *SCN5A*$^{-/+}$ mice display increasing cardiac fibrosis as a function of age [24]. Therefore, although there is ample evidence of structural abnormalities causing BrS, genetic mutations may still be the primary cause of the syndrome.

### Other Possibilities

Aside from the neural crest model, another proposed cause of conduction slowing in the RVOT is the presence of localized remnant nodal-like cells from developmental abnormalities [24]. Since the RVOT and the atrioventricular region differentiate from a common cell group but are functionally different, residual slow-conducting atrioventricular cells that employ L-type $Ca^{2+}$ channels for the action potential upstroke phase in the RVOT can provide the substrate for arrhythmia and exhibit improvement upon isoproterenol administration due to an increased $I_{Ca\text{-}L}$ [24]. It may even explain the male predominance as males have lower $I_{Ca\text{-}L}$ expression [24].

## Genetic Etiology

While some pathogenic models propose that a mutation occurs at the somatic level in patients suffering from BrS, it is commonly accepted that BrS is a hereditary genetic autosomal dominant disorder with incomplete penetrance and a high level of sporadicity (≤ 60%) [6, 8, 17, 33, 36]. It is estimated that 15-30% of BrS cases correspond to a mutation in the *SCN5A* gene, while 11-12% correspond to mutations in the *CACNA1C* and the *CACNB2* genes [8]. In the *SCN5A* gene alone, over 300 mutations have been found in BrS patients [11]. In addition, 11 other genes have been loosely correlated with BrS, namely *GPD1L*, *SCN1B*, *SCN3B*, *KCNE3*, *KCNJ8*, *KCND3*, *CACNA2D1*, *MOG1*, *HCN4*, *SCN10A*, and *HEY2* (**Table 1**) [6, 7]. The majority of the known mutations have been shown to alter normal ion channel function, emphasizing the nature of BrS as a channelopathy. In this section of the review, the role of multiple genes implicated in BrS will be

**Table 1.** The genes implicated in the mutational background of Brugada syndrome and the pathophysiological model(s) they support.

| Gene | Protein | Relevant function[a] | Model(s) supported |
|---|---|---|---|
| SCN5A | α-subunit of the voltage-gated $Na^+$ channel $Na_v1.5$ | Facilitating $I_{Na}$ during phase 0 of the cardiac AP | Depolarization and repolarization models |
| SCN1B | β1 and β1b subunits of the voltage-gated $Na^+$ channel $Na_v1.5$ | Enhancing $I_{Na}$ | Depolarization and repolarization models |
| SCN3B | β3 subunit of the voltage-gated $Na^+$ channel $Na_v1.5$ | Enhancing $I_{Na}$ | Depolarization and repolarization models |
| SCN10A | α-subunit of the voltage-gated $Na^+$ channel $Na_v1.8$ | $Na_v1.5$ transcription and a controversial role in conduction velocity | Depolarization and repolarization models |
| MOG1 | Multicopy suppressor Of ts Gsp1 | Trafficking $Na_v1.5$ to the cell surface | Depolarization and repolarization models |
| HEY2 | Hes-related family bHLH transcription factor with YRPW motif 2 | Repressing $Na_v1.5$ expression to establish a transmural gradient | Depolarization and repolarization models |
| CACNA1C | Pore-forming $\alpha_{1c}$-subunit of the voltage-gated $Ca^{2+}$ channel $Ca_v1.2$ | Facilitating $I_{Ca\text{-}L}$ during phase 2 of the cardiac AP and excitation-contraction coupling | Depolarization and repolarization models |
| CACNB2 | $Ca_v\beta2$ subunit of the voltage gated $Ca^{2+}$ channel $Ca_v1.2$ | Enhancing $I_{Ca\text{-}L}$ and trafficking the $Ca_v1.2$ α-subunit to the cell surface | Repolarization model |
| CACNA2D1 | α2δ1 auxiliary subunit for the voltage gated $Ca^{2+}$ channel $Ca_v1.2$ | Enhancing $I_{Ca\text{-}L}$ | Repolarization model |
| KCNE3 | β-subunit of the voltage gated $K^+$ channels $K_v4.3$ (MiRP2) | Reducing $I_{to}$ | Repolarization model |
| KCNE5 | β-subunit of the voltage gated $K^+$ channels $K_v4.3$ (MiRP4) | Reducing the $I_{to}$ $K^+$ current | Repolarization model |
| KCNJ8 | α-subunit of the inwardly-rectifying ATP-sensitive $K^+$ channel $Kir_{6.1}$ | Facilitating $I_{K\text{-}ATP}$ | Repolarization model |
| ABCC9 | The sulfonylurea receptor regulatory subunit of the inwardly-rectifying ATP-sensitive $K^+$ channels $Kir_{6.1}$ and $Kir_{6.2}$ | Reducing $I_{K\text{-}ATP}$ | Repolarization model |
| GJA1[b] | Gap junction protein α-1 (connexin 43, Cx43) | Facilitating cardiac impulse propagation and signalling during development | Neural crest model |
| HCN4 | Hyperpolarization activated cyclic nucleotide-gated potassium channel 4 (HCN4) | Generating the rhythmogenic funny current ($I_f$) in pacemaker cells | None |

[a] AP denotes the action potential.
[b] GJA1 is yet to be directly associated with Brugada syndrome.

visited with specific examples of mutations and their contribution to the syndrome's overall pathophysiology.

### *SCN5A*—Voltage-gated Na+ Channel Type V α Subunit

*SCN5A* was the first gene with mutations linked to BrS. It encodes for the pore-forming α-subunit of the cardiac voltage-gated $Na^+$ channel ($Na_V1.5$) responsible for the depolarizing $I_{Na}$ current during phase 0 of the action potential [8]. The gene is 80 kb in length and is comprised of 28 exons situated at the 3p21 locus [8]. In most BrS patients with an aberration in this gene, the mutated *SCN5A* gene results in a loss of function concomitant with a decrease in $I_{Na}$ due to a reduced expression or an alteration in the voltage and/or time dependence of the channel (activation, inactivation, and reactivation) [8]. Examples of such mutations include (1) G351V, which increases $I_{Na}$ decay; (2) R367H, G1406R, and R1432G, which abolish $I_{Na}$; (3) Y1795H, which reduces $I_{Na}$ decay, increases persistence of late $I_{Na}$ but, most strongly, increases inactivation; and (4) G514C, which reduces $I_{Na}$ and voltage-dependent inactivation, yielding an isolated, conduction-slowing symptom, free of tachyarrhythmia [8, 37]. However, the genetic basis of BrS is even more complex and somewhat obscure. For example, some mutations that give rise to BrS lead to distinct phenotypes in related individuals, such as G1406R and these modifying factors are largely unknown [8].

The outcome of the *SCN5A* mutations depends on the interplay between the effects and their magnitudes on the different gating parameters of the $Na^+$ channel [8]. Since over 300 *SCN5A* mutations are associated with BrS, there is a wide array of possible biophysical mechanisms responsible for the observed phenotype [11]. For example, it has been suggested that a G351V mutation leads to a seven fold decrease in $I_{Na}$ either due to an increased steric hindrance at the pore, caused by the valine residue (reduced permeability), or a conformational change due to its hydrophobic side chain (change in gating kinetics and/or permeability) [38]. However, a mutation-caused aberration in *SCN5A* gene processing/protein trafficking is also possible [38].

### *GPD1L*—Glycerol-3-phosphate Dehydrogenase 1-like Protein

*GPD1L* encodes for the glycerol-3-phosphate dehydrogenase 1-like protein (G3PD1L) and is comprised of 8 exons contained in 62 kb at the 3p24-p22 locus [8]. A strong association between a *GPD1L* mutation (A280V) and BrS was found based on 46 family members that exhibited 37% penetrance [8, 39, 40]. In Human Embryonic Kidney 293 (HEK-293) cells, it was observed that the mutation reduced $I_{Na}$ by 50% and also decreased $Na_V1.5$ cell surface expression [8, 40].

G3PD1L is an enzyme responsible for the conversion of glycerol-3-phosphate (G3P) to dihydroxyacetone phosphate (DHAP) [9]. A study reported that G3PD1L is physically associated with the α-subunit of the $Na_V1.5$ cardiac channel, either directly or indirectly, by channel-interacting proteins (ChIPs) [9]. Based on co-immunoprecipitation, SDS-PAGE, and activity assay experiments, the authors show that the A280V *G3PD1L* mutation does not reduce the association of the protein to the channel but rather decreases its catalytic activity [9]. Therefore, the mechanism by which the A280V *G3PD1L* mutation decreases $I_{Na}$ is such that the mutation reduces the conversion of G3P to DHAP, and the accumulating G3P increases the levels of lysophosphatidic acid, phosphatidic acid, and diacylglycerol [9]. Diacylglycerol then activates protein kinase C (PKC), which then inhibits the $Na_V1.5$ channel by phosphorylating it at S1503 and possibly other sites [9]. This pathway is an important link between the metabolic state of the cell and its excitability, and it can account for the high variability of the ECG pattern observed in a single BrS patient [9, 40]. For instance, reduced oxygen levels in ischemic hearts activate glycogenolysis and accelerate glycolysis which function to increase the levels of NADH by means of the glyceraldehyde-3-phosphate dehydrogenase enzyme. Decreased oxygen levels also inhibit the electron transport chain thereby decreasing the rate of mitochondrial inward transfer of NADH [41]. The result is an accumulated cytosolic NADH that can inhibit the conversion of G3P to DHAP as G3PD1L requires the reduction of NAD+ to NADH [9, 41, 42]. This leads to an oxygen-depletion-mediated negative bathmotropic effect to reduce energy expenditure.

For BrS of this etiology, a drug such as a glycerol-3-phosphate dehydrogenase (GPD) allosteric activator or breakdown inhibitor can prevent $Na_V1.5$ channel inhibition by reducing G3P in patients suffering from a *GPD1L* mutation [43]. Since the pathway for dysfunctional G3PD1L-mediated BrS has now largely been elucidated, other drugs can target any enzyme in the pathway leading to PKC activation.

### *CACNA1C*—Voltage-gated $Ca^{2+}$ Channel Type L $\alpha_{1C}$-Subunit

The *CACNA1C* gene encodes for multiple isoforms of the pore-forming α1c-subunit of $Ca_V1.2$, the L-type voltage-gated $Ca^{2+}$ channel, and it has been associated with BrS [8]. The gene contains 50 exons and spans 640 kb at the 12p13.33 locus [8]. This long-lasting slowly inactivating channel plays a major depolarizing role in phase 2 (plateau phase) of the cardiac action potential and couples excitation with contraction [8]. Two of the observed missense heterozygous mutations in the *CACNA1C* are G490R and A39V [8]. While neither mutation leads to an abnormal trafficking, both decrease $I_{Ca\text{-}L}$ [8]. Since the G490 residue is situated at the linker between the first and second domains of the channel, a mutation in this residue can alter the channels interaction with the $Ca_V\beta2$-subunit, which would normally enhance $I_{Ca\text{-}L}$ [8]. An $I_{Ca\text{-}L}$-linked BrS supports both the repolarization and depolarization models as reductions in the $Ca^+$ current can cause less depolarization and has been suggested to slow conduction [44].

### *CACNB2*—Voltage-gated $Ca^{2+}$ Channel β2-Subunit

*CACNB2*, involved in the pathogenesis of BrS, encodes for the $Ca_V\beta2$-subunit of the $Ca_V1.2$ channel discussed above [8]. The gene contains 14 exons over 421 kb at the 10p12 locus [8]. In addition to the role of $Ca_V\beta2$ in increasing $I_{Ca\text{-}L}$, it is also involved in the trafficking the channel's α-subunit to the plasma membrane by interacting with the phosphatidylinositol-3-kinase pathway [8]. Nevertheless, the missense mutation S481L found in a BrS patient did not lead to a $Ca_V1.2$ trafficking defect but rather to a decrease in the stimulatory effect of $Ca_V\beta2$ on the channel (as explained above), causing a reduced $I_{Ca\text{-}L}$ [8].

### *SCN1B*—Voltage-gated $Na^+$ Channel Type I β-Subunit

At the 19q13.1 locus, the 6-exon 9.8-kb *SCN1B* gene encodes two differently-spliced $Na_v1.5$ β-subunit isoforms, β1 and β1b [8]. Both isoforms are transmembrane proteins with an extracellular N-terminus, containing an immunoglobulin-like domain defining the difference between β1 and β1b, and the intracellular C-terminus [8]. The general function of the β1- and β1b-subunits is to increase $I_{Na}$ through the $Na_v1.5$ channel. Both subunits shift the voltage-dependence of activation and inactivation of the channel leftward (to more negative potentials) [8]. Currently, among the identified heterozygous mutations with incomplete penetrance are E87Q in the β1-subunit and E87Q and W179X in the β1b-subunit [45]. The E87Q mutation is in the extracellular domain of both isoforms and results in a decrease of $I_{Na}$ by abolishing the leftward shift in voltage-dependence of activation. This supports the notion that the extracellular domain is responsible for gating regulation [45]. However, the W179X mutation in the β1b-subunit results in a premature stop codon. As a result, a truncated protein is formed which fails to incorporate into the sarcolemma [45]. Therefore, since the subunits increase $I_{Na}$, the W179X mutation phenotype is assumed to be mediated by haploinsufficiency [45].

*SCN3B*, a 25.6-kb 6-exon gene at the 11q23 locus encodes for another $Na_v1.5$ β-subunit, $Na_vβ3$ [8]. Similar to β1, $Na_vβ3$ acts to increase the $I_{Na}$ current, however, through a different kinetic mechanism [8]. An L10P mutation found in a Caucasian male suffering from BrS, has been shown to decrease $I_{Na}$ and the trafficking of the $Na_v1.5$ channel [8].

### *KCNE3*—Voltage-gated $K^+$ Channel Subfamily E Regulatory β3-Subunit

The *KCNE3* gene encodes for MiRP2, a β-subunit of the voltage gated $K^+$ channels [8]. *KCNE3* consists of 3 exons spanning 13 kb at the 11q13-q14 locus, with only the third exon translated to protein [8]. MiRP2 acts as a negative regulator of the $K_v4.3$ channels, which are responsible for the transient outward $I_{to}$ current that facilitates the early repolarization of the cardiac action potential [46]. Mutations, such as R99H and T4A in MiRP2, are also associated with BrS as they cause a gain of function in the $K_v4.3$ channel [46]. Loss-of-function mutations in the *KCNE5*, which codes for another $K_v4.3$ inhibitory β-subunit have also been shown to cause BrS [47].

### Other BrS-Related Mutations

Many other mutations have been correlated with BrS. These include mutations in *KCNJ8*, which codes for the $K_{ATP}$ ($Kir_{6.1}$) channels in the heart. A missense mutation in this gene has been shown to increase $I_{K\text{-}ATP}$ leading to an increased early repolarization current by means of a reduced ATP sensitivity [48, 49]. *ABCC9*, another susceptibility gene, encodes for the sulfonylurea receptor subunit SUR2A that associates with $Kir_{6.1}$ and $Kir_{6.2}$ to inhibit them in an ATP-dependent manner [50-52]. Gain-of-function mutations in *KCND3*, which codes for the α-subunit of $K_v4.3$, have also been reported to cause BrS by increasing $I_{to}$ [46]. Three mutations in *CACNA2D1*, a gene that codes for the $I_{Ca\text{-}L}$-enhancing α2δ1 disulfide-linked auxiliary subunit for the L-type voltage-gated $Ca_{2+}$ channel $Ca_v1.2$, have also been found in some BrS patients [53, 54].

Furthermore, it has been proposed that *HCN4* is a susceptibility gene for BrS as it codes for HCN4 channels which are ubiquitously expressed in the ventricles and nodal cells [55]. It was established that HCN4 normally plays a critical role in preventing bradycardia-induced ventricular arrhythmia typically found in BrS patients. Ventricular HCN4 channels are activated during diastolic hyperpolarization and become deactivated following the upstroke of the action potential. Since their reversal potential is about -30 mV, this results in a decaying outward current during the plateau phase of the action potential [55]. Under longer diastolic intervals, more HCN4 channels become activated yielding an increased decaying outward current. Ultimately, this leads to an HCN4-mediated shortening of the action potential duration [55]. Hence, HCN4 protects from ventricular arrhythmia by preventing action potential prolongation, which would otherwise permit the reactivation of $I_{Ca\text{-}L}$ facilitating early after-depolarization and subsequent arrhythmia [55, 56]. In a BrS patient with no *SCN5A* mutations, a four-base insertion was detected at the junction of exon 2 and intron 2 of *HCN4*, which led to a frame-shift mutation at codon 404 and the translation of a truncated inactive HCN4 channel [55]. In some BrS patients, a reduced $I_f$ (HCN4 current) increases the incidence of bradycardia-induced SCA explaining the link of the syndrome to SUNDS [55].

It has been recently established that *MOG1*, a gene that plays a role in the trafficking of the $Na_v1.5$ channel to the cell surface, is also a susceptibility gene for BrS [10]. In a genome-wide association study, SCN10A was associated with BrS based on polymorphisms in the patient population. *SCN10A* codes for the $Na_v1.8$ channel, which was recently detected in the working myocardium. A study showed that an enhancer positioned in the *SCN10A* gene modulates the expression of *SCN5A* by interacting with its promoter [7, 57]. In the same study, *HEY2* (hes-related family bHLH transcription factor with *YRPW* motif 2) polymorphisms were also associated with BrS patients [7]. *HEY2* encodes for a transcriptional repressor in the sub-epicardium of the developing heart. In addition to many other functions, *HEY2* represses the expression of the $Na_v1.5$ channel in the epicardium in order to establish the expression gradient observed in the adult normal heart [7]. Heterozygous *Hey2* knockout mice exhibit no cardiac structural defects, an increased conduction velocity, an enhanced Nav1.5 function, and a prolonged repolarization in the RVOT [7]. Therefore, it is most probable that a gain-of-function mutation in HEY2 may slow down conduction velocity in the RVOT as well as steepen the transmural expression gradient characteristic of BrS. The above genome-wide association study also shows that common genetic polymorphisms known to modulate ECG conduction indices can predispose individuals to BrS. This finding suggests the possibility that BrS is an oligogenic disease.

In essence, a large and diverse mutational background underlies BrS accounting for the controversy in the pathophysiology of the disease. Generally, mutations appear to decrease depolarizing $Na^+$ or $Ca^{2+}$ current, increase early repolarizing transient outward $K^+$ current, steepen the transmural expression gradient, or decrease the conduction velocity in the RVOT. Conduction velocity slowing in the RVOT can be caused by loss-of-function or gain-of-function mutations in the channels or their regulatory subunits or by altered expression or trafficking of the channels to the cell surface.

## Environmental Factors

BrS ECG patterns as well as its clinical manifestations can be induced by several non-genetic factors in otherwise asymptomatic patients or individuals not suffering from BrS. Thus, it is important to distinguish between BrS and a BrS pattern when assessing patients [58]. As previously discussed, it is widely accepted that most, if not all, of BrS cases are likely due to a reduction in depolarizing current or an increase in early repolarizing current. Therefore, it would be reasonable to expect that drugs or factors attenuating depolarization or enhancing repolarization through the corresponding channels can lead to either the unmasking of BrS in asymptomatic patients or the induction of the BrS clinical manifestation in healthy subjects. Indeed, there are numerous factors and drugs that can trigger BrS including antiarrhythmics, anesthetics, analgesics, psychotropics, antiepileptics, antiemetics, vagotonics, cocaine, cannabinoids, lithium, alcohol, fever, $I_{K\text{-}ATP}$ activators, and severe electrolyte imbalance [12, 58-62]. Similar to the diverse mutational background of BrS, the environmental and physiological factors involved in inducing the disease follow multiple pathways that will be delineated in this section of the review.

### $Na^+$ Channel Blockers

A large majority of the drugs and factors induce the BrS pattern by blocking cardiac $Na^+$ channels, thereby either exacerbating the haploinsufficiency due to the inherent early repolarization heterogeneity in asymptomatic BrS patients, or sufficiently reducing $I_{Na}$ to exhibit an ST segment elevation in healthy individuals. Such drugs include some antiarrhythmics (e.g., flecainide, procainamide, and ajmaline), anesthetics (e.g., bupivacaine and ketamine), analgesics (e.g., procaine benzylpenicillin and tramadol), psychotropics (e.g., tricyclic antidepressants, amitriptyline, clomipramine, imipramine, doxepin, dosulepin, desipramine, nortriptyline, and quetiapine), antiepileptics (e.g., oxcarbazepine), antiemetics (e.g., metoclopramide), lithium, and cocaine [17, 59, 61, 63-65]. However, some of these drugs, like quetiapine, do not have a well-established $Na^+$ channel blockade effect while others, such as the anesthetic propofol, induce BrS by causing other conditions, namely acidosis, hyperkalemia, and fever [59, 66].

### $Na^+$ Channel Modulators

Other drugs and factors exert a similar effect on the heart by inactivating $Na^+$ channels. For instance, hyperthermic or hyperpyrexic patients exhibit a 20 times higher prevalence of coved-type BrS pattern compared to afebrile patients [67]. Using a two-pulse protocol with a conditioning pre-pulse of variable length, one study showed that slow inactivation is more enhanced at higher temperatures (21°C vs. 36°C) for an SCN5A channel with a D1714G mutation [68]. In another study, a T1620M *SCN5A* mutation resulted in a significant enhancement in the high-temperature-induced decrease in fast inactivation kinetics (22°C vs. 32°C), as well as the overall current decay kinetics (22°C to 42°C) [69]. It has also been reported that an F1344S *SCN5A* mutation induces temperature sensitivity causing a rightward shift of voltage-dependence of activation (to more positive potentials) and a decrease in the slope factor (leading to $I_{Na}$ reduction) at higher temperatures (23°C vs. 40.5°C) [70].

In contrast, another study suggested that since some heterozygous BrS patients who have a severely reduced to completely abolished $I_{Na}$ from the mutant SCN5A channel continue to display temperature-sensitivity, the biophysical properties of the wild type $Na^+$ channels are responsible for the fever-induced BrS patterns [71]. This study also found that the activation and inactivation kinetics of the SCN5A channel are both accelerated at a higher temperature (42°C) [71]. Using mathematical modelling and computer simulations, it was shown that the very small fraction of $Na^+$ channels that are still active after phase 1 of the cardiac action potential contribute an essential depolarizing current that, if reduced (due to faster inactivation kinetics), can lead to a premature repolarization and the consequent BrS symptoms discussed in its pathophysiology [71].

Multiple studies have found that an increase in temperature enhances the inactivation kinetics of wild type *SCN5A*. Although the mechanism of fever-sensitivity is mutation-dependent, the biophysical properties of the wild type channel differentially confer fever-induced coved-type BrS patterns in all BrS patients with a reduced $I_{Na}$ [68, 69, 71]. The reduced $I_{Na}$ may either be due to a haploinsufficiency of *SCN5A*, a decreased $I_{Na}$ of mutant SCN5A, dominant negative effect on wild type SCN5A channels (e.g. L325R mutation), or an increased repolarizing current [71].

Hyperkalemia and hypercalcemia are other factors that can accelerate the $Na^+$ channel inactivation rate [61, 72]. It is well established that a high concentration of extracellular $K^+$ can result in an inactivation of the $Na^+$ channels due to a depolarization block [61]. Increased extracellular $Ca^{2+}$ on the other hand, has been shown to increase intracellular $Ca^{2+}$-calmodulin complexes, which can then bind to the carboxy-terminal IQ domain of the cardiac $Na^+$ channel to reduce $I_{Na}$ [72]. $Ca^{2+}$ ions can also act on the extracellular portion of voltage-gated $Na^+$ channel: $Ca^{2+}$ can shift the voltage-dependence of the channel activation (requiring more depolarized potentials) by interacting with the negative charges on its surface thereby altering the function of the voltage-sensor [73]. $Ca^{2+}$ ions can also decrease single-channel conductance by interacting with the π-system of T401 (Nav1.4) in the outer pore of the channel [73].

### Other Current-Modulating Factors

Other agents and conditions can also induce BrS by simple mechanisms. Hypokalemia increases $I_{to}$ (steeper $K^+$ concentration gradient). $I_{K\text{-}ATP}$ activators increase early repolarization. Hyponatremia decreases $I_{Na}$; vagotonic agents decrease $I_{Ca\text{-}L}$ and increase $I_K$; alcohol decreases $I_{Ca\text{-}L}$ and exhibits vagotonic effects; and cannabinoids exhibit late vagotonic effects [12, 58-60, 62, 74].

## Diagnosis and Treatment

### Diagnosis

At present, the most recent medical consensus on diagnosing BrS is based on observed ECG patterns [13]. Although there are two distinct morphologies of BrS patterns as discussed above, there are three types. Type I exhibits a coved-type (negative T wave) ST segment elevation equivalent to 2 mm or more (≥ 0.2 mV) (**Figure 4**). Type II displays a saddle-back morphology with an ST segment elevation of 2 mm or more (≥ 0.2 mV), and an ST segment trough elevation of 1 mm or more (≥ 0.1 mV) accompanied by a positive or biphasic T wave. Type III may contain the coved-type or saddle-back

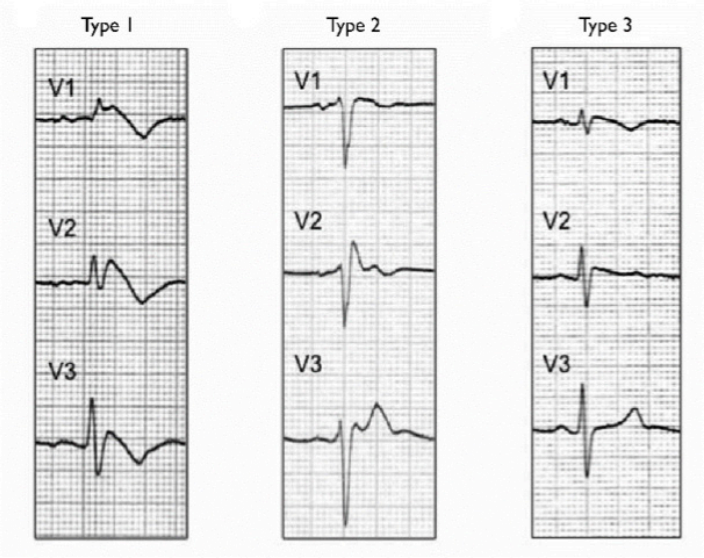


**Figure 4.** The three types of ECG patterns from precordial leads V1-V3 used in the diagnosis of BrS. Type 1, coved-type ST segment elevation; type 2, saddle-back high ST segment elevation; type 3, saddle-back intermediate ST segment elevation [1].

morphology, however, with an ST segment elevation less than 1 mm (< 0.1 mV) in 2 or more precordial leads (V1-V3) [8]. With regard to the diagnostic criteria, BrS is diagnosed either if type I ECG pattern is observed with or without a Class I antiarrhythmic drug (intravenously administered) or if the type II or type III ECG patterns are observed and can be converted to a type I ECG pattern subsequent to the intravenous administeration of a Class I antiarrhythmic drug [13].

### Treatment

The treatment of BrS includes an implantable cardioverter-defibrillator (ICD), certain pharmacological agents, and radiofrequency catheter ablation as per the Heart Rhythm Society (HRS), European Heart Rhythm Association (EHRA), and Asia Pacific Heart Rhythm Society expert consensus [13]. If a patient has suffered from a previous cardiac arrest or a sustained VT (patient class I), then an ICD is recommended [13]. If the patient did not suffer from the aforementioned but has a spontaneous type I ECG pattern and a medical history of ventricular-arrhythmia-caused syncope (patient class IIa), then an ICD can be useful [13]. If the patient suffers from none of the above but has an inducible ventricular fibrillation on an EPS (patient class IIb), then an ICD may be considered [13]. Finally, if a patient does not suffer from any of the above, is asymptomatic, has a pharmacologically-induced type I ECG pattern and a family history of sudden cardiac death (patient class III), then an ICD implantation is not indicated [13]. The complex ICD-need assessment above is to ensure optimal patient lifestyle since an ICD implantation has several disadvantages. For instance, surgical complications include hemorrhage, pneumothorax, vascular perforations, cardiac tamponade, and infections [1]. Technical complications include lead fracture, battery exhaustion, and false defibrillations [1]. Functional complications include inappropriate therapy. Several studies have demonstrated that a considerable percentage of the BrS-ICD patient populations received false shocks [4].

Given the numerous complications associated with ICD therapy, many studies propose pharmacological agents that can reinstate the current balance in cardiomyocytes [1]. The most commonly agreed-upon drug is the Class Ia antiarrhythmic, quinidine [1]. Quinidine's effects are mostly facilitated by its $I_{to}$ and $I_{Kr}$ (rapid delayed rectifier current) blocking properties, which prevent phase 2 re-entry arrhythmia in BrS patients [1]. However, quinidine also has pro-arrhythmic properties, such as blocking the fast inward $I_{Na}$, and has been shown to lead to torsades de pointes arrhythmia (with a 2-8% risk) exclusively in the initial phase of the treatment, unless later interacted with by other drugs and factors, such as hypokalemia [1, 4]. Other side effects for quinidine include diarrhea, thrombocytopenia and hepatitis [1]. Additional proposed drugs include isoproterenol, which can enhance $I_{Ca\text{-}L}$ (shown to help treat electrical storm in BrS) and is recommended for some class IIa BrS patients; cilostazol, which inhibits phosphodiesterase III to provide similar sympathomimetic effects and reduces $I_{to}$ due to its heart rate elevating effects; and tedisamil, which differs from quinidine in its lower $I_{Na}$ blockade potency [4, 13, 75]. Other studies are beginning to shed light on the therapeutic potential of radiofrequency catheter ablation for BrS patients: it was reported that in the high-risk population, ablation can prevent the recurrence of VF, syncope, and sudden cardiac arrest in the short-term and epicardial substrate ablation in the RVOT can prevent VF inducibility [76-80].

## Conclusions

Since its discovery, BrS has been extensively studied. While much of its clinical and electrophysiological characteristics have been elucidated, no single model has been regarded as the sole explanatory mechanism for its pathophysiology. Although the wide variety of genetic mutations favour the repolarization model, the presence of structural derangements in all patients supports the depolarization model. However, some evidence suggests that genetic mutations can lead to structural defects and both can contribute to the pathophysiology of BrS. Further investigation is required to support the neural crest model. The recent association of common genetic polymorphisms to BrS and their ability to confer arrhythmogenic susceptibility is another topic that requires further study, as it could indicate that the syndrome is in fact oligogenic. In addition, the collective evidence suggests that although fever is likely to exacerbate clinical manifestations in all BrS patients due to a further decrease in $I_{Na}$, the severity of the effects is mutation-dependent.

With regard to its treatment, a variety of pharmacological therapeutics should be investigated. Due to the strong correlation between TST levels and BrS incidence via increasing $I_{to}$, further studies are required to determine the pathway involved and subsequently develop potential pharmacological inhibitors. Specific inhibition of early repolarizing current channels (e.g., $K_V1.5$) may also prove invaluable for the treatment of BrS, as it can prevent premature repolarization. Although the HRS/EHRA expert consensus does not consider genetic testing a valuable tool in impacting treatment, as it has no prognostic value, it may help provide a more appropriate therapeutic approach. For instance, a GPD allosteric activator or breakdown inhibitor may be a better treatment alternative for a patient with a mutated GPD1L than quinidine, which has many side effects.

## Acknowledgements

I would like to express my profound gratitude to Professor Peter H. Backx (Department of Physiology, Faculty of Medicine, University of Toronto) for his invaluable guidance and instruction.

## References

1. Jellins J, Milanovic M, Taitz DJ, Wan SH, Yam PW. Brugada syndrome. Hong Kong Med J 2013;19(2):159-67.
2. Naccarelli GV, Antzelevitch C. The Brugada syndrome: clinical, genetic, cellular, and molecular abnormalities. Am J Med 2001;110(7):573-81.
3. Postema PG. About Brugada syndrome and its prevalence. Europace 2012;14(7):925-8.
4. Khan A, Mittal S, Sherrid MV. Current review of Brugada syndrome: from epidemiology to treatment. Anadolu Kardiyol Derg 2009;9(Suppl 2):12-16.
5. Elizari MV, Levi R, Acunzo RS, Chiale PA, Civetta MM, Ferreiro M, Sicouri S. Abnormal expression of cardiac neural crest cells in heart development: a different hypothesis for the etiopathogenesis of Brugada syndrome. Heart Rhythm 2007;4(3):359-65.
6. Crotti L, Marcou CA, Tester DJ, Castelletti S, Giudicessi JR, Torchio M, Medeiros-Domingo A, Simone S, Will ML, Dagradi F, Schwartz PJ, Ackerman MJ. Spectrum and prevalence of mutations involving BrS1-through BrS12-susceptibility genes in a cohort of unrelated patients referred for Brugada syndrome genetic testing: implications for genetic testing. J Am Coll Cardiol 2012;60(15):1410-18.
7. Bezzina CR, Barc J, Mizusawa Y, Remme CA, Gourraud JB, Simonet F, Verkerk AO, Schwartz PJ, Crotti L, Dagradi F, Guicheney P, Fressart V, Leenhardt A, Antzelevitch C, Bartkowiak S, Borggrefe M, Schimpf R, Schulze-Bahr E, Zumhagen S, Behr ER, Bastiaenen R, Tfelt-Hansen J, Olesen MS, Kääb S, Beckmann BM, Weeke P, Watanabe H, Endo N, Minamino T, Horie M, Ohno S, Hasegawa K, Makita N, Nogami A, Shimizu W, Aiba T, Froguel P, Balkau B, Lantieri O, Torchio M, Wiese C, Weber D, Wolswinkel R, Coronel R, Boukens BJ, Bézieau S, Charpentier E, Chatel S, Despres A, Gros F, Kyndt F, Lecointe S, Lindenbaum P, Portero V, Violleau J, Gessler M, Tan HL, Roden DM, Christoffels VM, Le Marec H, Wilde AA, Probst V, Schott JJ, Dina C, Redon R. Common variants at SCN5A-SCN10A and HEY2 are associated with Brugada syndrome, a rare disease with high risk of sudden cardiac death. Nat Genet 2013 Sep;45(9):1044-9.
8. Hedley PL, Jørgensen P, Schlamowitz S, Moolman-Smook J, Kanters JK, Corfield VA, Christiansen M. The genetic basis of Brugada syndrome: a mutation update. Hum Mutat 2009;30(9):1256-66.
9. Valdivia CR, Ueda K, Ackerman MJ, Makielski JC. GPD1L links redox state to cardiac excitability by PKC-dependent phosphorylation of the sodium channel SCN5A. Am J Physiol Heart Circ Physiol 2009;297(4):H1446-52.
10. Kattygnarath D, Maugenre S, Neyroud N, Balse E, Ichai C, Denjoy I, Dilanian G, Martins RP, Fressart V, Berthet M, Schott JJ, Leenhardt A, Probst V, Le Marec H, Hainque B, Coulombe A, Hatem SN, Guicheney P. MOG1: a new susceptibility gene for Brugada syndrome. Circ Cardiovasc Genet 2011 Jun;4(3):261-8.
11. Zeng Z, Zhou J, Hou Y, Liang X, Zhang Z, Xu X, Xie Q, Li W, Huang Z. Electrophysiological characteristics of a SCN5A voltage sensors mutation R1629Q associated with Brugada syndrome. PLoS One 2013 Oct 22;8(10):e78382.
12. Junttila MJ, Gonzalez M, Lizotte E, Benito B, Vernooy K, Sarkozy A, Huikuri HV, Brugada P, Brugada J, Brugada R. Induced Brugada-type electrocardiogram, a sign for imminent malignant arrhythmias. Circulation 2008 Apr 8;117(14):1890-3.
13. Priori SG, Wilde AA, Horie M, Cho Y, Behr ER, Berul C, Blom N, Brugada J, Chiang CE, Huikuri H, Kannankeril P, Krahn A, Leenhardt A, Moss A, Schwartz PJ, Shimizu W, Tomaselli G, Tracy C. Executive summary: HRS/ EHRA/APHRS expert consensus statement on the diagnosis and management of patients with inherited primary arrhythmia syndromes. Heart Rhythm 2013 Dec 10;10(12):e85-e108.
14. Tsuchiya, T. Role of pharmacotherapy in Brugada syndrome. Indian Pacing Electrophysiol J 2004;4(1):26-32.
15. Bezzina CR, Shimizu W, Yang P, Koopmann TT, Tanck MW, Miyamoto Y, Kamakura S, Roden DM, Wilde AA. Common sodium channel promoter haplotype in Asian subjects underlies variability in cardiac conduction. Circulation 2006 Jan 24;113(3):338-44.
16. Baron RC, Thacker SB, Gorelkin L, Vernon AA, Taylor WR, Choi K. Sudden death among Southeast Asian refugees. An unexplained nocturnal phenomenon. JAMA 1983;250(21):2947-51.
17. Yap YG, Behr ER, Camm AJ. Drug-induced Brugada syndrome. Europace 2009;11(8):989-94.
18. Matsuo K, Akahoshi M, Nakashima E, Suyama A, Seto S, Hayano M, Yano K. The prevalence, incidence and prognostic value of Brugada type electrocardiogram: a population-based study of four decades. J Am Coll Cardiol 2001 Sep;38(3):765-70.
19. Vatta M, Dumaine R, Varghese G, Richard TA, Shimizu W, Aihara N, Nademanee K, Brugada R, Brugada J, Veerakul G, Li H, Bowles NE, Brugada P, Antzelevitch C, Towbin JA. Genetic and biophysical basis of sudden unexplained nocturnal death syndrome (SUNDS), a disease allelic to Brugada syndrome. Hum Mol Genet 2002 Feb 1;11(3):337-45.
20. Barajas-Martínez H, Hu D, Urrutia J, Wu Y, Panama BK, Goodrow RJ Jr, Sicouri S, Di Diego JM, Treat JA, Desai M, Doss MX, Antzelevitch C. Chronic exposure to testosterone increases expression of transient outward current in human induced pluripotent stem cell (hiPSC)-derived cardiomyocytes (CM). Heart Rhythm 2013 Nov;10(11):1741.
21. Knollmann, B. C. Induced pluripotent stem cell-derived cardiomyocytes: boutique science or valuable arrhythmia model? Circ Res 2013;112(6):969-76.
22. Harman SM, Metter EJ, Tobin JD, Pearson J, Blackman MR. Longitudinal effects of aging on serum total and free testosterone levels in healthy men. J Clin Endocrinol Metab 2001;86(2):724-31.
23. Matsuo K, Akahoshi M, Seto S, Yano K. Disappearance of the Brugada-type electrocardiogram after surgical castration: a role for testosterone and an explanation for the male preponderance. Pacing Clin Electrophysiol 2003;26(7 Pt 1):1551-3.
24. Meregalli PG, Wilde AA, Tan HL. Pathophysiological mechanisms of Brugada syndrome: depolarization disorder, repolarization disorder, or more? Cardiovasc Res 2005;67(3):367-78.
25. Brugada P, Brugada J, Roy D. Brugada Syndrome 1992-2012: 20 years of scientific excitement, and more. Eur Heart J 2013;34(47):3610-15.
26. Yan GX, Antzelevitch C. Cellular basis for the electrocardiographic J wave. Circulation 1996;93(2):372-9.
27. Yan GX, Antzelevitch C. Cellular basis for the Brugada syndrome and other mechanisms of arrhythmogenesis associated with ST-segment elevation. Circulation 1999 Oct 12;100(15):1660-6.
28. Antzelevitch C, Yan GX, Shimizu W. Transmural dispersion of repolarization and arrhythmogenicity: the Brugada syndrome versus the long QT syndrome. J Electrocardiol 1999;32(Suppl): 158-65.
29. Di Diego JM, Sun ZQ, Antzelevitch C. I(to) and action potential notch are smaller in left vs. right canine ventricular epicardium. Am J Physiol 1996;271(2 Pt 2):H548-61.
30. Liu DW, Gintant GA, Antzelevitch C. Ionic bases for electrophysiological distinctions among epicardial, midmyocardial, and endocardial myocytes from the free wall of the canine left ventricle. Circ Res 1993 Mar;72(3):671-87.
31. Janse MJ, Kléber AG. Electrophysiological changes and ventricular arrhythmias in the early phase of regional myocardial ischemia. Circ Res 1981 Nov;49(5):1069-81.
32. Jarrett JR, Flowers NC. Signal-averaged electrocardiography: history, techniques, and clinical applications. Clin Cardiol 1991;14(12):984-94.
33. Brugada, P. On the intriguing phenotypic manifestations of Brugada syndrome and the diagnostic value of the electrocardiogram. J Am Coll Cardiol 2011 Nov 22;58(22):2299-2300.
34. Takagi M, Aihara N, Kuribayashi S, Taguchi A, Kurita T, Suyama K, Kamakura S, Takamiya M. Abnormal response to sodium channel blockers in patients with Brugada syndrome: augmented localised wall motion abnormalities in the right ventricular outflow tract region detected by electron beam computed tomography. Heart 2003 Feb;89(2):169-74.
35. Coronel R, De Groot JR, Veldkamp MW, Casini S, Koopman T.T, Bhuiyan Z, CR Bezzina. Electrophysiologic, genetic and histopathologic characterization of the explanted heart of a patient with Brugada syndrome. Heart Rhythm 2004;1(1):S6.
36. Campuzano O, Brugada R, Iglesias A. Genetics of Brugada syndrome. Curr Opin Cardiol 2010;25(3):210-15.
37. Tan HL, Bink-Boelkens MT, Bezzina CR, Viswanathan PC, Beaufort-Krol GC, van Tintelen PJ, Van den Berg MP, Wilde AA, Balser JR. A sodium-channel mutation causes isolated cardiac conduction disease. Nature 2001 Feb 22;409(6823):1043-7.
38. Vatta M, Dumaine R, Antzelevitch C, Brugada R, Li H, Bowles NE, Nademanee K, Brugada J, Brugada P, Towbin JA. Novel mutations in domain I of SCN5A cause Brugada syndrome. Mol Genet Metab 2002 Apr;75(4):317-24.
39. Weiss R, Barmada MM, Nguyen T, Seibel JS, Cavlovich D, Kornblit CA, Angelilli A, Villanueva F, McNamara DM, London B. Clinical and molecular heterogeneity in the Brugada syndrome: a novel gene locus on chromosome 3. Circulation 2002 Feb 12;105(6):707-13.
40. London B, Michalec M, Mehdi H, Zhu X, Kerchner L, Sanyal S, Viswanathan PC, Pfahnl AE, Shang LL, Madhusudanan M, Baty CJ, Lagana S, Aleong R, Gutmann R, Ackerman MJ, McNamara DM, Weiss R, Dudley SC Jr. Mutation in glycerol- 3-phosphate dehydrogenase 1 like gene (GPD1-L) decreases cardiac Na+ current and causes inherited arrhythmias. Circulation 2007 Nov 13;116(20):2260–8.
41. Zhou L, Stanley WC, Saidel GM, Yu X, Cabrera ME. Regulation of lactate production at the onset of ischaemia is independent of mitochondrial NADH/NAD+: insights from in silico studies. J Physiol 2005;569(Pt 3):925-37.
42. Wahr JA, Olszanski D, Childs KF, Bolling SF. Dichloroacetate enhanced myocardial functional recovery post-ischemia: ATP and NADH recovery. J Surg Res 1996;63(1):220-4.
43. Albertyn J, Hohmann S, Thevelein JM, Prior BA. GPD1, which encodes glycerol-3-phosphate dehydrogenase, is essential for growth under osmotic stress in Saccharomyces cerevisiae, and its expression is regulated by the high-osmolarity glycerol response pathway. Mol Cell Biol 1994;14(6):4135-44.
44. Gan TY, Qiao W, Xu GJ, Zhou XH, Tang BP, Song JG, Li YD, Zhang J, Li FP, Mao T, Jiang T. Aging-associated changes in L-type calcium channels in the left atria of dogs. Exp Ther Med 2013;6(4):919-24.
45. Watanabe H, Koopmann TT, Le Scouarnec S, Yang T, Ingram CR, Schott JJ, Demolombe S, Probst V, Anselme F, Escande D, Wiesfeld AC, Pfeufer A, Kääb S, Wichmann HE, Hasdemir C, Aizawa Y, Wilde AA, Roden DM, Bezzina CR. Sodium channel β1 subunit mutations associated with Brugada syndrome and cardiac conduction disease in humans. J Clin Invest 2008 Jun;118(6):2260-8.
46. Nakajima T, Wu J, Kaneko Y, Ashihara T, Ohno S, Irie T, Ding WG, Matsuura H, Kurabayashi M, Horie M. KCNE3 as the genetic basis of Brugada-pattern electrocardiogram. Circ J 2012;76(12):2763-72.
47. Ohno S, Zankov DP, Ding WG, Itoh H, Makiyama T, Doi T, Shizuta S, Hattori T, Miyamoto A, Naiki N, Hancox JC, Matsuura H, Horie M. KCNE5 (KCNE1L) variants are novel modulators of Brugada syndrome and idiopathic ventricular fibrillation. Circ Arrhythm Electrophysiol 2011 Jun;4(3):352-61.
48. Barajas-Martínez H, Hu D, Ferrer T, Onetti CG, Wu Y, Burashnikov E, Boyle M, Surman T, Urrutia J, Veltmann C, Schimpf R, Borggrefe M, Wolpert C, Ibrahim BB, Sánchez-Chapula JA,

Winters S, Haïssaguerre M, Antzelevitch C. Molecular genetic and functional association of Brugada and early repolarization syndromes with S422L missense mutation in KCNJ8. Hearth Rhythm 2012 Apr;9(4):548-55.
49. Medeiros-Domingo A, Tan BH, Crotti L, Tester DJ, Eckhardt L, Cuoretti A, Kroboth SL, Song C, Zhou Q, Kopp D, Schwartz PJ, Makielski JC, Ackerman MJ. Gain-of-function mutation S422L in the KCNJ8-encoded cardiac K(ATP) channel Kir6.1 as a pathogenic substrate for J-wave syndromes. Heart Rhythm 2010 Oct;7(10):1466-71.
50. Bienengraeber M, Alekseev AE, Abraham MR, Carrasco AJ, Moreau C, Vivaudou M, Dzeja PP, Terzic A. ATPase activity of the sulfonylurea receptor: a catalytic function for the KATP channel complex. FASEB J 2000 Oct;14(13):1943-52.
51. Hu D, Barajas-Martínez H, Terzic A, Park S, Pfeiffer R, Burashnikov E, Wu Y2, Borggrefe M4, Veltmann C4, Schimpf R4, Cai JJ5, Nam GB6, Deshmukh P7, Scheinman M8, Preminger M9, Steinberg J10, López-Izquierdo A11, Ponce-Balbuena D11, Wolpert C4, Haïssaguerre M12, Sánchez-Chapula JA11, Antzelevitch C13. ABCC9 is a novel Brugada and early repolarization syndrome susceptibility gene. Int J Cardiol 2014 Feb 15;171(3):431-42.
52. Burke MA, Mutharasan RK, Ardehali H. The sulfonylurea receptor, an atypical ATP-binding cassette protein, and its regulation of the KATP channel. Circ Res 2008;102(2):164-76.
53. Burashnikov E, Pfeiffer R, Barajas-Martinez H, Delpón E, Hu D, Desai M, Borggrefe M, Häissaguerre M, Kanter R, Pollevick GD, Guerchicoff A, Laiño R, Marieb M, Nademanee K, Nam GB, Robles R, Schimpf R, Stapleton DD, Viskin S, Winters S, Wolpert C, Zimmern S, Veltmann C, Antzelevitch C. Mutations in the cardiac L-type calcium channel associated with inherited J-wave syndromes and sudden cardiac death. Heart Rhythm 2010 Dec;7(12):1872-82.
54. Bourdin B, Shakeri B, Tétreault MP, Sauvé R, Lesage S, Parent L. Functional characterization of CaV α2δ mutations associated with sudden cardiac death. J Biol Chem 2014;290(5):2854-69.
55. Ueda K, Hirano Y, Higashiuesato Y, Aizawa Y, Hayashi T, Inagaki N, Tana T, Ohya Y, Takishita S, Muratani H, Hiraoka M, Kimura A. Role of HCN4 channel in preventing ventricular arrhythmia. J Hum Genet 2009 Feb;54(2):115-21.
56. Veldkamp MW, Verkerk AO, van Ginneken AC, Baartscheer A, Schumacher C, De Jonge N, De Bakker JM, Opthof T. Norepinephrine induces action potential prolongation and early afterdepolarizations in ventricular myocytes isolated from human end-stage failing hearts. Eur Heart J 2001 Jun;22(11):955-63.
57. Van den Boogaard M, Smemo S, Burnicka-Turek O, Arnolds DE, van de Werken HJ, Klous P, McKean D, Muehlschlegel JD, Moosmann J, Toka O, Yang XH, Koopmann TT, Adriaens ME, Bezzina CR, de Laat W, Seidman C, Seidman JG, Christoffels VM, Nobrega MA, Barnett P, Moskowitz IP. A common genetic variant within SCN10A modulates cardiac SCN5A expression. J Clin Invest 2014 Apr;124(4):1844-52.
58. Alvarez PA, Vázquez Blanco M, Lerman J. Brugada type 1 electrocardiographic pattern induced by severe hyponatremia. Cardiology 2011;118(2):97-100.
59. Letsas KP, Kavvouras C, Kollias G, Tsikrikas S, Korantzopoulos P, Efremidis M, Sideris A. Drug-induced Brugada syndrome by noncardiac agents. Pacing Clin Electrophysiol 2013 Dec;36(12):1570-7.
60. Romero-Puche AJ, Trigueros-Ruiz N, Cerdán-Sánchez MC, Pérez-Lorente F, Roldán D, Vicente-Vera T. Brugada electrocardiogram pattern induced by cannabis. Rev Esp Cardiol (Engl Ed) 2012;65(9):856-8.
61. Ersan T, Emir D, Mustafa A. Pseudo Brugada pattern due to hyperkalemia. J Clin Exp Cardiolog 2012;S10:001.
62. Gazzoni GF, Borges, AP, Bergoli, LC, Soares JL, Kalil C, Bartholomay E. Brugada-like electrocardiographic changes induced by hypokalemia. Arq Bras Cardiol 2013;100(3):e35-7.
63. Khaire SS, Nagarajarao H, Quin EM, Borganelli SM, Marshall RC. Electrocardiographic Brugada pattern induced by quietiapine overdose. J Investig Med 2012;60(1):322-3.
64. El-Menyar A, Khan M, Al Suwaidi J, Eljerjawy E, Asaad N. Oxcarbazepine-induced resistant ventricular fibrillation in an apparently healthy young man. Am J Emerg Med 2011 Jul;29(6):693.e1-3.
65. Bonilla-Palomas JL, López-López JM, Moreno-Conde M, Gallego de la Sacristana A, Gámez-López AL, Villar-Ráez A. Type I Brugada electrocardiogram pattern induced by metoclopramide. Europace 2011;13(9):1353-1534.
66. Tan HH, Hoppe J, Heard K. A systematic review of cardiovascular effects after atypical antipsychotic medication overdose. Am J Emerg Med 2009;27(5):607-16.
67. Adler A, Topaz G, Heller K, Zeltser D, Ohayon T, Rozovski U, Halkin A, Rosso R, Ben-Shachar S, Antzelevitch C, Viskin S. Fever-induced Brugada pattern: how common is it and what does it mean? Heart Rhythm 2013 Sep;10(9):1375-82.
68. Amin AS, Verkerk AO, Bhuiyan ZA, Wilde AA, Tan HL. Novel Brugada syndrome-causing mutation in ion-conducting pore of cardiac Na+ channel does not affect ion selectivity properties. Acta Physiol Scand 2005;185(4):291-301.
69. Dumaine R, Towbin JA, Brugada P, Vatta M, Nesterenko DV, Nesterenko VV, Brugada J, Brugada R, Antzelevitch C. Ionic mechanisms responsible for the electrocardiographic phenotype of the Brugada syndrome are temperature dependent. Circ Res 1999 Oct 29;85(9):803-9.
70. Keller DI, Huang H, Zhao J, Frank R, Suarez V, Delacrétaz E, Brink M, Osswald S, Schwick N, Chahine M. A novel SCN5A mutation, F1344S, identified in a patient with Brugada syndrome and fever-induced ventricular fibrillation. Cardiovasc Res 2006 Jun 1;70(3):521-9.
71. Keller DI, Rougier JS, Kucera JP, Benammar N, Fressart V, Guicheney P, Madle A, Fromer M, Schläpfer J, Abriel H. Brugada syndrome and fever: genetic and molecular characterization of patients carrying SCN5A mutations. Cardiovasc Res 2005 Aug 15;67(3):510-19.
72. Zeb M, McKenzie DB, Naheed B, Gazis T, Morgan JM, Staniforth AD. Hypercalcaemia and a Brugada-like ECG: an independent risk factor for fatal arrhythmias. Resuscitation 2010;81(8):1048-50.
73. Santarelli VP, Eastwood AL, Dougherty DA, Ahern CA, Horn R. Calcium block of single sodium channels: role of a pore-lining aromatic residue. Biophys J 2007;93(7):2341-9.
74. Verrier RL, Antzelevitch C. Autonomic aspects of arrhythmogenesis: the enduring and the new. Curr Opin Cardiol 2004;19(1):2-11.
75. Maury P, Hocini M, Haissaguerre M. Electrical storms in Brugada syndrome: review of pharmacologic and ablative therapeutic options. Indian Pacing Electrophysiol J 2005;5(1):25-34.
76. Haïssaguerre M, Extramiana F, Hocini M, Cauchemez B, Jaïs P, Cabrera JA, Farré J, Leenhardt A, Sanders P, Scavée C, Hsu LF, Weerasooriya R, Shah DC, Frank R, Maury P, Delay M, Garrigue S, Clémenty J. Mapping and ablation of ventricular fibrillation associated with long-QT and Brugada syndromes. Circulation 2003 Aug 26;108(8):925-8.
77. Darmon JP, Bettouche S, Deswardt P, Tiger F, Ricard P, Bernasconi F, Saoudi N. Radiofrequency ablation of ventricular fibrillation and multiple right and left atrial tachycardia in a patient with Brugada syndrome. J Interv Card Electrophysiol 2004 Dec;11(3):205-9.
78. Nakagawa E, Takagi M, Tatsumi H, Yoshiyama M. Successful radiofrequency catheter ablation for electrical storm of ventricular fibrillation in a patient with Brugada syndrome. Circ J 2008;72(6):1025-9.
79. Morita H, Zipes DP, Morita ST, Lopshire JC, Wu J. Epicardial ablation eliminates ventricular arrhythmias in an experimental model of Brugada syndrome. Heart Rhythm 2009;6(5):665-71.
80. Nademanee K, Veerakul G, Chandanamattha P, Chaothawee L, Ariyachaipanich A, Jirasirirojanakorn K, Likittanasombat K, Bhuripanyo K, Ngarmukos T. Prevention of ventricular fibrillation episodes in Brugada syndrome by catheter ablation over the anterior right ventricular outflow tract epicardium. Circulation 2011 Mar 29;123(12):1270-9.
81. Ackerman MJ, Priori SG, Willems S, Berul C, Brugada R, Calkins H, Camm AJ, Ellinor PT, Gollob M, Hamilton R, Hershberger RE, Judge DP, Le Marec H, McKenna WJ, Schulze-Bahr E, Semsarian C, Towbin JA, Watkins H, Wilde A, Wolpert C, Zipes DP. HRS/EHRA expert consensus statement on the state of genetic testing for the channelopathies and cardiomyopathies this document was developed as a partnership between the Heart Rhythm Society (HRS) and the European Heart Rhythm Association (EHRA). Heart Rhythm 2011 Aug;8(8):1308-39.

UNIVERSITY OF TORONTO
FACULTY OF MEDICINE

# Thinking about Graduate Studies in the Life Sciences, Biomedical Research, Rehabilitation Sciences, or Community Health?

**Visit the Graduate and Life Sciences Education (GLSE) and the 15 departmental websites. Talk to our departmental graduate coordinators.**

*Programs*

*Funding*

*Career Opportunities*

*Biomedical Research Networking*

**IT IS NEVER TOO EARLY TO BE INFORMED !**

**For more information visit:**
**http://www.facmed.utoronto.ca/programs/graduate.htm**

JULS REVIEWS

# Genomic Imprinting: Mechanisms and Disease Implications

Tamara Kleiman and Cathy Su

University of Toronto, Toronto, ON, Canada

## Abstract

Genomic imprinting, a *cis*-acting epigenetic phenomenon, was discovered less than thirty years ago. Imprinted genes display mono-allelic expression, meaning that alleles from one parent are preferentially expressed at an imprinted gene locus. Thus, embryos derived from only one parent are rarely viable. The imprinting mechanism is complex: imprints are typically found in gene clusters, may be passed to offspring despite waves of genome-wide demethylation known to occur in the zygote, and act on genes that vary widely in function. By studying genomic imprinting we have learned about the function of epigenetic machinery, including methylases, chromatin remodelling complexes, and non-coding RNAs. Most imprinted genes function in development and growth, thus loss of imprinting can result in serious diseases ranging from genetic syndromes to kidney cancer. In this review, current research into the mechanisms of genomic imprinting are addressed and summarized.

## Introduction

Genomic imprinting describes the process by which alleles of certain genes are differentially expressed through epigenetic regulation based on their parental origin. Imprinting was first recognized in two different labs over thirty years ago, both of which attempted to grow parthenogenic and androgenic mouse embryos. In one experiment, an activated egg was injected with a pronucleus taken from a fertilized egg [1]. In the other experiment, one pronucleus of a 1-cell embryo was replaced by a pronucleus from the opposite parent taken from a different embryo [2]. Both labs found that although parthenogenic and androgenic embryos commence embryogenesis, they usually fail to complete it. The inability of a single parental genome to support development implies that both maternal and paternal genomes support separate, yet essential activities.

In seeking to explain the difference between the parental genomes, insulin-like growth factor 2 (*Igf2*) of distal chromosome 7, which has a crucial role in embryogenesis, was the first imprinted gene discovered [3]. Nuclease protection assays (which detect RNA of a known sequence) and *in situ* hybridization had revealed that *Igf2* was only expressed by its paternal allele [3]. Since then, over 200 imprinted genes have been found in mammals [4]. These genes mainly seem to govern development and growth; loss of imprinting at key loci is therefore implicated in diseases such as cancer [5].

Imprints are established through cytosine methylation, small RNAs, splice variants, and histone modification – all distinctively *cis*-regulatory epigenetic processes. Imprints are transmitted based on parent of origin, meaning that imprints on the parental genome are completely erased before new imprints are established in gametes. It's speculated that recognition machinery for establishing imprints is unique between the oocyte and sperm in order to facilitate differential *de novo* methylation [6]. Several factors have been associated with the imprint, yet only methylated cytosines persevere in the germline of the organism following global demethylation of the genome during embryogenesis [6].

5-methylcytosine is formed by methylation of cytosines at CpG sites, sites at which C and G nucleotides are directly adjacent. This methylation stabilizes the genome, lowering rates of genetic recombination [7]. Regions dense with CpGs and longer than 500 base pairs (bp) in length are called CpG islands, and contain many 5-methylcytosines [8]. Imprinted genes are rich in CpG islands [8], within which we can find differentially methylated regions (DMRs), which occur between the parental copies and contain the control elements (i.e., silencers, enhancers, etc.) of imprinted genes [10]. These regions can then be defined as imprinting control regions (ICRs) if their deletion leads to a loss of imprinting [11]. An ICR is typically a few kilobases (kb) in length and drives the imprinting of genes in its vicinity by turning gene expression on or off, depending on its parent-of-origin-specific epigenetic state [9].

Imprinted genes are rarely isolated on a given chromosome. Eighty percent of the roughly 150 imprinted genes in mice form the main 16 imprinted gene clusters in mice, each of which contains at least two genes [7]. Each cluster is regulated by an ICR and expresses at least one long non-coding RNA (lncRNA) [11]. The two prevailing models of how these ICRs work are the insulator model and the lncRNA model. In the insulator model, an insulator governs regulatory elements, which control a group of imprinted genes [7]. In the lncRNA model, it is a long non-coding RNA that mediates silencing [7].

Both the mechanism and purpose of genomic imprinting are yet to be fully understood; nonetheless research in this area

is important because of the significant health consequences of imprinting. This review brings together recent research on the mechanism and applications of genomic imprinting.

## The Imprinting Life Cycle

Imprints are established within ICRs in germ cells during gametogenesis. In male gametes, this establishment of imprints occurs prenatally in prospermatogonia [12]. Female imprints are established postnatally during oocyte maturation [13]. In either case, methyl groups are introduced by *de novo* DNA methyltransferases DNMT3A and DNMT3B [7]. Following the establishment of the imprints, they must be maintained after fertilization and while the organism develops. This entails that the pre-existing imprinted DNA resists a genome-wide demethylation wave that takes place after fertilization and prior to blastulation [14]. The corresponding unimprinted DNA, meanwhile, needs to resist another *de novo* methylation wave that coincides with the differentiation of morula cells into the inner cell mass and trophoblast cells of the blastocyst [10]. DNA (cytosine-5)-methyltransferase 1 has been postulated as playing a role during this maintenance stage [10], but the details as to how exactly ICRs manage to resist these waves are still unknown. Following the establishment stage, the next stage of the life cycle is erasure. The erasure phase serves to reset all programming in the germline of the developing embryo [15]. This occurs between embryonic days 8.5 and 11.5 in mice, before the primordial germ cells have migrated to the genital ridge and before sex determination [10].

## The Imprinting Mechanism: Insulator Model

The cluster of genes located at distal chromosome 7 in mice, which includes the aforementioned imprinted gene *Igf2* [7], follows the insulator model and therefore will be used as a case study. This same cluster of genes includes the lncRNA-encoding *H19* [11], which is also imprinted: its promoter is methylated on the paternal chromosome. There is a region upstream of *H19* that exhibits both epigenetic markings (methylation on the paternal version) and control overexpression of these nearby imprinted genes; therefore it has been denoted ICR1 [16]. Experiments involving primary embryo fibroblasts that were disomic for either maternal or paternal distal chromosome 7 revealed the way ICR1 controls imprinted gene expression. These embryos were treated with DNase I, dimethyl sulphate, or ultraviolet (UV) light [16]. This made protein activity on DNA visible, and following analysis with ligation-mediated polymerase chain reaction (PCR), it was observed that four 21-bp repeats demonstrated activity of the CCCTC-binding factor, or CTCF [16]. CTCF is a zinc finger protein known to mediate insulator activity [17]. On the maternal chromosome, both ICR1 and *H19* are unmethylated [18]. Therefore CTCF may bind to ICR1, preventing *H19*'s downstream enhancer from accessing the *Igf2* promoter [16]. As a result, the enhancer upregulates the transcription of *H19* instead [16]. On the paternal chromosome, both *H19* and ICR1 are methylated [18]. Therefore CTCF does not bind to ICR1, and the enhancer only upregulates *Igf2* expression [16]. In brief, ICR1 activity is inversely related to

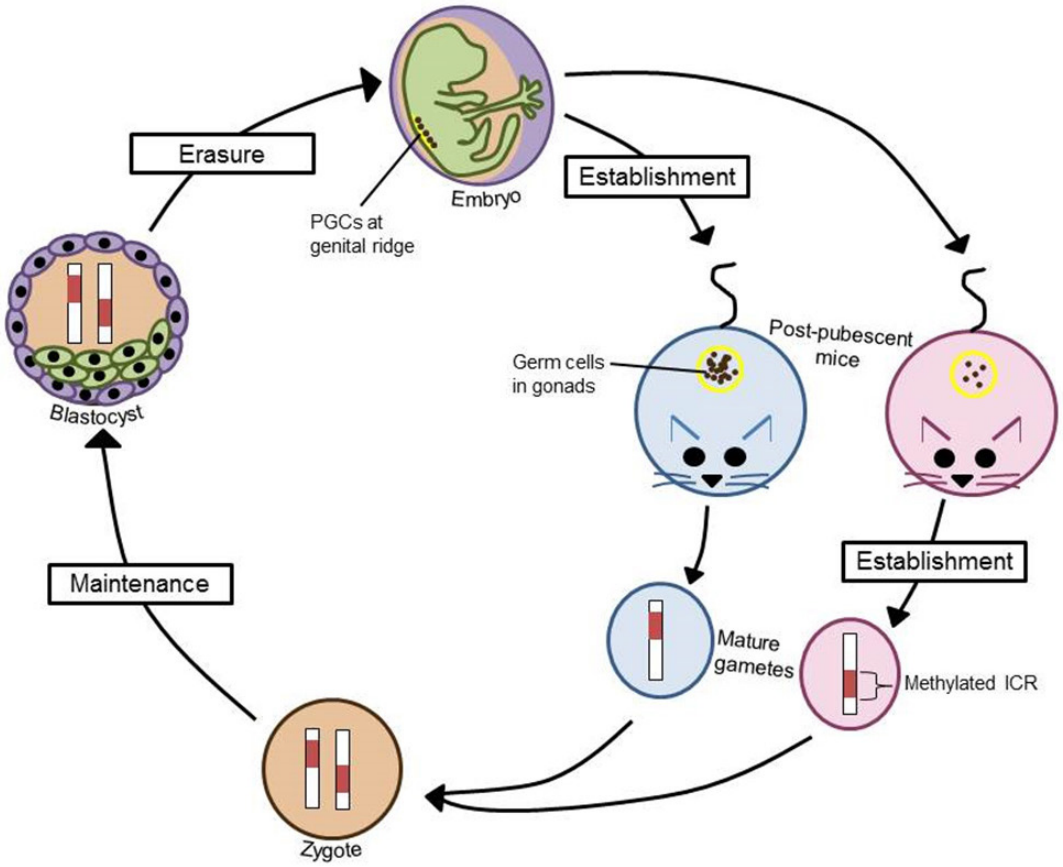


**Figure 1.** The life cycle of methylation imprints. Represented by three distinct stages: establishment, maintenance, and erasure. Gametes and their progenitors are indicated by blue for males, and pink for females. In the blastocyst, purple represents trophoblast cells (which develop into the placenta) and green represents the inner cell mass (which develop into the fetus). Note that the female and male gametes show the same chromosome; therefore, sex-specific methylation (red box) will not be seen in the same region.

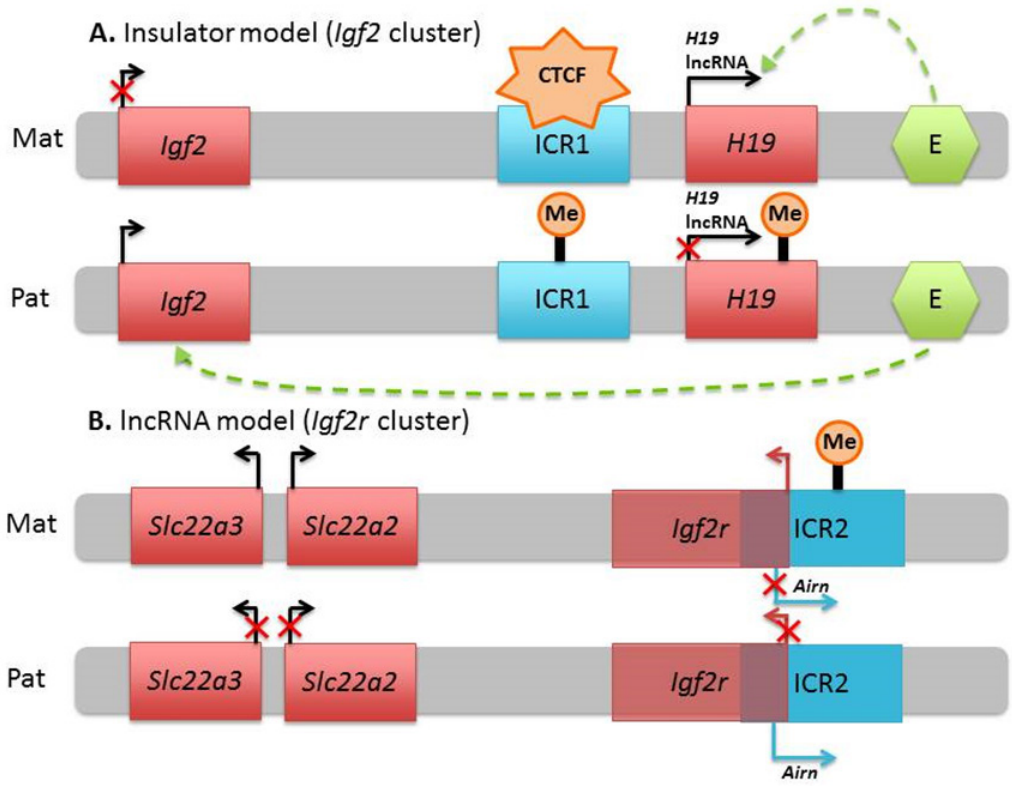


**Figure 2.** Two current models of the imprinting mechanism. (A) The insulator model, as demonstrated by the insulin-like growth factor 2 (*Igf2*) cluster. *Igf2* is paternally expressed in a reciprocal fashion to maternally expressed *H19*, which codes for an lncRNA. Enhancers can upregulate from up to 1 Mbp away, as *H19*'s downstream enhancer does to *Igf2* on the paternal chromosome. ICR1 acts as an insulator, as CTCF binding to it prevents *H19*'s downstream enhancer from accessing the *Igf2* promoter. When ICR1 is methylated, CTCF cannot access it and therefore does not "block" the enhancer. (B) The more common lncRNA model as demonstrated by insulin-like growth factor 2 receptor gene (*Igf2*) and members of the organic cation transporter family: *Slc22a2* and *Slc22a3*. All of these genes are maternally expressed. Within ICR2 is the promoter for *Airn* lncRNA, which overlaps *Igf2r* on the opposing strand. When ICR2 is not methylated, the transcription of *Airn* prevents access of RNA polymerase II to *Igf2r*, *Slc22a2*, *Slc22a3*.

*Igf2* expression, and directly related to *H19* expression. This results in *Igf2* expression on the paternal chromosome only, and *H19* expression on the maternal.

## The Imprinting Mechanism: lncRNA Model

This model is the more common, and direct, model of imprinting. The cluster containing maternally expressed insulin-like growth factor 2 receptor (*Igf2r*) will be used to illustrate it. The ICR of this cluster, which will be referred to as ICR2, was discovered through the construction of a yeast artificial chromosome (YAC) containing the 400-kb "*Igf2r* locus" [19]. The YAC was transferred to a mouse, and its imprinting was maintained despite the new chromosomal surroundings of the locus. This serves to indicate that the region must contain the components necessary to imprint the cluster [19]. ICR2 contains a promoter for the lncRNA-encoding *Airn*, therefore its epigenetic state directly affects the expression of *Airn* [20]. *Airn* acts as an antisense transcript to *Igf2r*, repressing it by way of antisense RNA interference. Since ICR2 is demethylated on the paternal chromosome only, *Airn* only interferes with the paternal copy of *Igf2r* [20]. Therefore, *Airn* and *Igf2r* have a reciprocal relationship such that *Airn* is expressed paternally while *Igf2r* is expressed maternally.

## Diseases related to genomic imprinting

Imprinted genes are vulnerable to mutations because of their mono-allelic expression. Mutations on the active parental allele cannot be compensated for by the other parental allele, in contrast to regularly expressed genes. Exceptionally high expression of an active, non-mutated allele (often caused by uniparental disomy by which the offspring receives two copies of the same chromosome from the same parent) can also prove to be harmful. Perhaps unsurprisingly, many of the seven well-characterized imprinted gene clusters happen to be associated with a human disease [21]. These so-called "imprinting diseases" are some of the most prevalent amongst all congenital human diseases. Moreover, many of these diseases represent severe development disorders that are typically diagnosed during childhood. These imprinting diseases are usually the result of abnormal expression of the ICR-associated lncRNA of a specific gene cluster [22].

Amongst all currently recognized imprinting diseases, Prader-Willi Syndrome (PWS) and Angelman Syndrome (AS) are of the best understood. These diseases are often discussed simultaneously because they are both associated with the imprinted gene cluster at 15q11q13 in humans, which exhibits a highly complex expression pattern. In particular, they are related to the abnormal expression of *SNURF-SNRPN* lncRNA at this locus [23]. This lncRNA is somewhat misnamed; although the majority of its products post-RNA splicing is indeed small non-coding RNAs, it also encodes one of two proteins: small nuclear ribonucleoprotein polypeptide N (SNPRN) and SNRPN upstream reading frame (SNURF) proteins. SNRPN is a spliceosomic protein involved in pre-mRNA splicing, while SNURF's function is not currently understood [23]. *SNURF-SNRPN* lncRNA is bicistronic, therefore the protein expressed depends on the open reading frame used on any given transcript

[23]. The PWS-ICR contains the promoter for this lncRNA, and that promoter is not methylated on the paternal chromosome [24]. Therefore, *SNURF-SNRPN* lncRNA and the proteins it encodes, as well as the various ncRNAs it hosts, are all paternally expressed.

PWS has an occurrence of 1:20,000 live births and is generally identified by symptoms that include mild to moderate mental retardation, incomplete sexual development, obesity, short stature, and an obsessive-compulsive personality [25]. Recall that it is associated with abnormal expression of *SNURF-SNRPN* lncRNA; this lncRNA hosts 29 tandem repeats of the C/D box small nucleolar RNA (snoRNA), *SNORD116* [26]. In fact, PWS is primarily caused by lack of expression of this cluster of snoRNAs – generally caused by a large deletion of paternal origin at 15q11q13, or less commonly, maternal uniparental disomy (UPD) 15 [26].

AS, which occurs in 1:15,000 live births, is characterized by limited to absent speech, severe mental retardation, sleep disorder, seizures, microcephaly, and an uncommonly happy disposition [25]. As with PWS, AS is associated with the expression of *SNURF-SNRPN* – but in this case, it is only affected by the lncRNA's expression in neuronal cells. In neurons, by an unknown mechanism, *SNURF-SNRPN* lncRNA can be transcribed to reach a longer length (>500 kb) than in other cells [24]. It now includes the antisense transcript to ubiquitin-protein ligase E3A (*UBE3A*): *UBE3A-ATS* [24]. Since *SNURF-SNRPN* lncRNA and all of its products (hence, *UBE3A-ATS* in neuronal cells) are paternally expressed, *UBE3A* is not expressed on the paternal chromosome

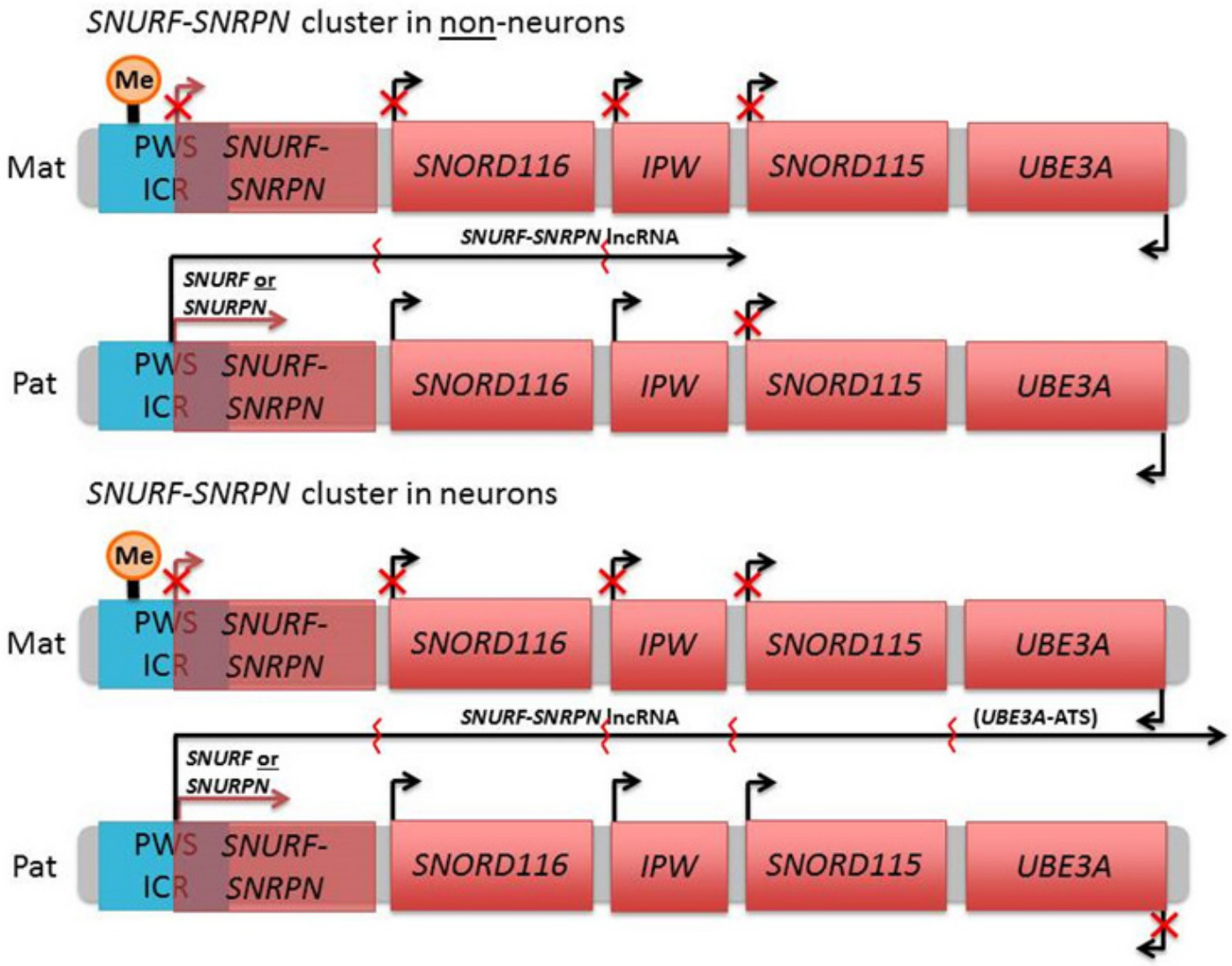


**Figure 3.** The SNURF-SNRPN cluster at 15q11q13: The affecting region for Prader-Willi syndrome (PWS) and Angelman syndrome (AS). This cluster follows the lncRNA model as PWS-ICR contains the promoter for *SNURF-SNRPN* lncRNA. Further, the expression of this lncRNA affects the expression of nearby imprinted genes. *SNURF-SNRPN* lncRNA is best viewed as a long pre-mRNA transcript, as post-RNA splicing produces, among other things, the bicistronic *SNURF-SNRPN* mRNA. In addition, the lncRNA transcript is host to tandem repeats of C/D box snoRNAs, *SNORD116* and *SNORD115*, and ncRNA *IPW*. The lncRNA, and its products, are expressed paternally due to methylation on the maternal copy of PWS-ICR. In non-neurons, the lncRNA transcript includes *IPW* product but does not extend past it. In neurons, by an unknown mechanism, the transcript extends further to encode the *SNORD115* cluster and the antisense transcript to *UBE3A*. PWS has been shown to be caused primarily by lack of expression of *SNORD116*. This can occur in both neurons and non-neurons when the patient has a paternal deletion of this region, or maternal UPD 15. AS is caused by a deficiency of UBE3A in neurons, as UBE3A deficiency in non-neurons is unlikely due to its lack of imprinting. Neuronal deficiency of UBE3A is caused by the inverse of the mutations that cause PWS: either a large maternal deletion of this region, or paternal UPD 15.

in neurons due to antisense interference [24]. As AS is caused by a loss of expression of *UBE3A*, which itself is caused by expression of the longer paternally expressed *SNURF-SNRPRN* lncRNA of neurons, the genetic lesion that produces AS is the inverse of what causes PWS. In particular, AS patients typically have either a maternal deletion of this imprinted gene cluster or paternal UPD 15 [26].

## Future directions

It has now become clearer that genomic imprinting affects the growth, metabolism, and survival of mammals. A few key attributes characterize imprinted genes: they are differentially methylated between the two parental copies and controlled by ICRs that may work through insulators or long non-coding RNAs. However, there is still much we do not understand about genomic imprinting. In regards to mechanisms, the imprinting life cycle involves erasure and re-establishment of imprints, but imprints from each parental genome are transmitted faithfully from the gamete to the zygote. We do not know how this happens.

Though it was not covered in this review, the question of why imprinting may have evolved arises, as it can allow expression of recessive alleles at a locus if the organism is heterozygous [27]. More than a dozen hypotheses have emerged to explain its evolutionary origin, all of which have been theoretically or experimentally validated in some way, but with contrasting conclusions [28]. In the end, there may not exist a single satisfactory explanation for why imprinting occurs, though such an explanation would aid us in finding and characterizing imprinted genes.

Future work in these two areas will be important to help understand genomic imprinting, so that we may in turn understand the many diseases associated with loss of imprinting, as well as the role of epigenetics as a whole in health and disease.

## References

1. Surani MA, Barton SC, Norris ML. Development of reconstituted mouse eggs suggests imprinting of the genome during gametogenesis. Nature 1984 Apr 5;308(5959):548–50.
2. McGrath J, Solter D. Completion of mouse embryogenesis requires both the maternal and paternal genomes. Cell 1984 May;37(1):179–83.
3. DeChiara TM, Robertson EJ, Efstratiadis A. Parental imprinting of the mouse insulin-like growth factor II gene. Cell 1991 Feb 22;64(4):849–59.
4. Wilkinson LS, Davies W, Isles AR. Genomic imprinting effects on brain development and function. Nat Rev Neurosci 2007 Nov;8(11):832–43.
5. Sakatani T, Kaneda A, Iacobuzio-Donahue CA, Carter MG, de Boom Witzel S, Okano H, Ko MS, Ohlsson R, Longo DL, Feinberg API. Loss of imprinting of Igf2 alters intestinal maturation and tumorigenesis in mice. Science 2005;307(5717):1976–8.
6. Vilkaitis G, Suetake I, Klimasauskas S, Tajima S. Processive methylation of hemimethylated CpG sites by mouse Dnmt1 DNA methyltransferase. J Biol Chem 2005;280(1):64–72.
7. Barlow DP, Bartolomei MS. Genomic imprinting in mammals. Cold Spring Harb Perspect Biol 2014 Feb;6(2). doi:10.1101cshperspect.a018382.
8.Paulsen M, El-Maarri O, Engemann S, Strödicke M, Franck O, Davies K, Reinhardt R, Reik W, Walter J. Sequence conservation and variability of imprinting in the Beckwith-Wiedemann syndrome gene cluster in human and mouse. Hum Mol Genet 2000 Jul 22;9(12):1829–41.
9. MacDonald WA, Mann MRW. Epigenetic regulation of genomic imprinting from germ line to preimplantation. Mol Reprod Dev 2014 Feb;81(2):126–40.
10. Morgan HD, Santos F, Green K, Dean W, Reik W. Epigenetic reprogramming in mammals. Hum Mol Genet 2005 Apr 15;14 Spec No 1:R47–58.
11. Cai X, Cullen BR. The imprinted H19 non-coding RNA is a primary microRNA precursor. RNA 2007 Mar;13(3):313–16.
12. Ueda T, Abe K, Miura A, Yuzuriha M, Zubair M, Noguchi M, Niwa K, Kawase Y, Kono T, Matsuda Y, Fujimoto H, Shibata H, Hayashizaki Y, Sasaki H. The paternal methylation imprint of the mouse H19 locus is acquired in the gonocyte stage during foetal testis development. Genes Cells 2000 Aug;5(8):649–59.
13. Bourc'his D, Xu GL, Lin CS, Bollman B, Bestor TH. Dnmt3L and the establishment of maternal genomic imprints. Science 2001 Dec 21;294(5551):2536–9.
14. Monk M, Boubelik M, Lehnert S. Temporal and regional changes in DNA methylation in the embryonic, extraembryonic, and germ cell lineages during mouse embryo development. Development 1987 Mar;99(3):371–82.
15. Feng S, Jacobsen SE, Reik W. Epigenetic reprogramming in plant and animal development. Science 2010 Oct 29;330(6004):622–7.
16. Szabó P, Tang SH, Rentsendorj A, Pfeifer GP, Mann JR. Maternal-specific footprints at putative CTCF sites in the H19 imprinting control region give evidence for insulator function. Curr Biol 2000 May 18;10(10):607–10.
17. Bell AC, West AG, Felsenfeld G. The protein CTCF is required for the enhancer blocking activity of vertebrate insulators. Cell 1999 Aug 6;98(3):387–96.
18. Reik W, Walter J. Genomic imprinting: parental influence on the genome. Nat Rev Genet 2001 Jan;2(1):21–32.
19. Wutz A, Smrzka OW, Schweifer N, Schellander K, Wagner EF, Barlow DP. Imprinted expression of the Igf2r gene depends on an intronic CpG island. Nature 1997 Oct 16;389(6652):745–9.
20. Latos PA, Pauler FM, Koerner MV, Şenergin HB, Hudson QJ, Stocsits RR, Allhoff W, Stricker SH, Klement RM, Warczok KE, Aumayr K, Pasierbek P, Barlow DP. Airn transcriptional overlap, but not its lncRNA products, induces imprinted Igf2r silencing. Science 2012 Dec 14;338(6113):1469–72.
21. Thorvaldsen JL, Bartolomei MS. SnapShot: imprinted gene clusters. Cell 2007 Sep 7;130(5):958.
22. Horsthemke B. In brief: genomic imprinting and imprinting diseases. J Pathol 2014 Apr;232(5):485–7.
23. Runte M, Hüttenhofer A, Gross S, Kiefmann M, Horsthemke B, Buiting K. The IC-SNURFSNRPN transcript serves as a host for multiple small nucleolar RNA species and as an antisense RNA for UBE3A. Hum Mol Genet 2001 Nov 1;10(23):2687–700.
24. Autuoro JM, Pirnie SP, Carmichael GG. Long non-coding RNAs in imprinting and X chromosome inactivation. Biomolecules 2014;4(1):76–100.
25. Rangasamy S, D'Mello SR, Narayanan V. Epigenetics, autism spectrum, and neurodevelopmental disorders. Neurotherapeutics 2013 Oct;10(4):742–56.
26. Buiting K. Prader-Willi syndrome and Angelman syndrome. Am J Med Genet C Semin Med Genet 2010 Aug 15;154C(3):365–76.
27. Moore T, Mills W. Evolutionary theories of imprinting - enough already! Adv Exp Med Biol 2008;626:116–22.
28. Spencer HG, Clark AG. Non-conflict theories for the evolution of genomic imprinting. Heredity (Edinb) 2014 Aug;113(2):112–18.

JULS REVIEWS

# A Cure for Ebola: Is Monoclonal Antibody Therapy the Solution?

Dhia Azzouz[1] and Louiza Azzouz[2]
[1]Department of Chemistry, University of Toronto, ON, Canada
[2]Marc Garneau Collegiate Institute, ON, Canada

## Abstract

**The Ebola virus of the *Filoviridae* family is a pathogen that affects humans, as well as non-human primates. The Ebola virus causes hemorrhagic fever and can be potentially fatal. The readily-transmissible nature of the Ebola virus makes it a great public health threat. There are currently no approved vaccines or therapies available to treat infected patients. The current Ebola outbreak, which began in December 2013, has led to 9442 deaths in West Africa, 1 death in North America, and many other reported cases at the time of submission [1]. If Ebola containment is slow in Guinea, Liberia, and Sierra Leone, The World Bank estimates that the loss of GDP in these countries would correspond to US$7.4 billion in 2014, and US$25.2 billion in 2015 [2]. As such, it is becoming increasingly important to find a treatment for Ebola. One of the current possible treatments is monoclonal antibody (a therapeutic agent that can be used to target many immunologically mediated diseases) therapy, although its promise as a cure for Ebola is limited. This review will discuss the current state of knowledge in using monoclonal antibody therapy to treat Ebola, as well as its overall likelihood of success.**

## Introduction

Monoclonal antibodies (mAbs) are therapeutic agents that can target many immunologically mediated diseases [3] (**Figure 1**). They offer the therapeutic advantage of binding to, and attacking, only those cells which are involved with the immunopathogenesis of certain diseases, as is the case for the Ebola virus [4]. Antibody recognition of surface markers on lymphocytes (especially T-cells) has been successfully manipulated in animals as well as in clinical allograft rejection [4]. Monoclonal antibodies, whose efficacy is determined by their half-lives and isotopes, can block important receptors for antigens, adhesion factors, and growth factors [3, 5]. Passive immunotherapy using mAbs has been fairly successful in treating diseases such as Marburg virus (MARV) and Zaire Ebola virus (ZEBOV) in test animals [6-9]. In non-human primates, monoclonal antibody therapy has been shown to slow the progress of viremia and help improve clinical outcomes [6, 10]. One unresolved issue is that neutralizing antibodies have not yet been proven to be successful in determining the efficacy of vaccines against diseases caused by filoviruses [7, 11-13], leading to considerable doubt surrounding the value of mAb therapy for treatment of Ebola [14, 15].

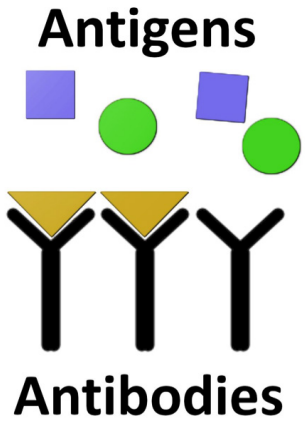


**Figure 1.** Antigens bind to specific antibodies.

## Background on the Ebola Virus and its Pathogenesis

The Ebola virus (EBOV) is a systematic viral infection that spreads rapidly to mononuclear phagocytic cells in tissues such as the liver and spleen [16]. This is followed by its spreading to fibroblasts, hepatocytes, and parenchymal cells of other organs [16]. Necrosis in the spleen, liver, and lymphoid tissue is observed in infected individuals [16]. The initial symptoms include fever, fatigue, headache, sore throat, and muscle pain, followed by vomiting and diarrhea [16, 17]. In non-human primate models, it was found that the EBOV can enter the body orally or conjunctively [17]. Further studies have shown that EBOV can enter the body through mucous-membrane interactions, skin abrasions, and pharyngeal contamination from swallowing [17]. Ebola has been contracted by humans eating infected forest animals [17]. EBOV is often mistaken for other diseases (like malaria, bacterial infection, or yellow fever) which have similar symptoms and are more common in the same geographical regions, but with lower mortality rates [16]. The Ebola virus infects many different cell types and its entry has been found to be pH-dependent [18]. Viral entry into host cells is important for determining pathogenicity, the ability of the virus to cause disease [19]. In one study, particles similar to those found in Ebola, which were formed from glycoproteins GP1, GP2, and VP40 (a matrix protein), were found to enter through clathrin-

mediated endocytosis and micropinocytosis [20]. In another study, Ebola-enveloped glycoprotein (GP) exposed on pseudotyped HIV was rendered incapable of entering cells by clathrin inhibitors, suggesting that EBOV enters cells through clathrin-mediated endocytosis [18]. There are several identified Ebola strains, including the Cote d'Ivoire, Sudan, and notably the Zaire Ebola virus, with mortality rates of up to 90% [20].

## Potential Treatment: KZ52

One neutralizing mAb that was once regarded as a potential treatment for EBOV was KZ52, which was found to inhibit cathepsin cleavage of GP [21]. Parren *et al.* demonstrated that it protected *Cavia porcellus* (guinea pigs) against ZEBOV in a dose-dependent manner, despite high levels of viremia suggesting that KZ52 acts through a mechanism independent of targeting viremia [9]. A disadvantage of KZ52 is that it was found to have optimal results when administered within an hour of the infection, which is rarely when Ebola is detected [9]. However, Oswald *et al.* found that *Macaca mulatta* (rhesus macaques) treated with KZ52 prior to, and after, being subjected to ZEBOV did not survive [13].

## Potential Treatment: MB-003

Wilson *et al.* discovered fourteen mAbs from extracted hybridomas. They were the result of fusion of P3X63Ag8.653 myeloma cells with spleen cells from mice that were injected with Venezuelan equine encephalitis virus replicons that encoded the GP from the Ebola Zaire strain [22, 23]. The mAbs 13F6-1-2, 6E3-1-1, 6D8-1-2, 12B5-1-1, 13C6-1-1, 12E12-1-1, 6D3-1-1, 8C10-1-1, and 3H8-1-1 were administered in 100 µg doses, and most had different effects on mice survival rates [6]. Survival rates due to mAb administration decreased as doses decreased [6].

Olinger *et al.* developed treatment trials applicable in humans, as murine mAbs (13C6, 13F6, and 6D8) were de-immunized with human constant regions to form c13C6, h-13F6, and c6D8 [27]. The mAbs were originally produced in Chinese hamster ovary (CHO) cells, but this was neither a scalable nor cost-effective method [29]. Instead, rapid antibody manufacturing platform (RAMP) is a system that allows for quick and scalable production of mAbs [24]. magnICON is a pro-viral expression system in which deconstructed viral vectors were utilised by *Nicotiana benthamiana*-based RAMP to produce the mAbs [25]. Experiments were performed on rhesus macaques to compare the effects of mAbs produced from CHO cells (CHO-MB-003) versus from RAMP (RAMP-MB-003) [27]. Macaques subjected to CHO-MB-003 (50 mg/kg) an hour after infection with ZEBOV were protected from 100 plaque-forming units (PFU) of ZEBOV, an amount lethal in untreated rhesus macaques [27]. In another treatment, the amount of ZEBOV administered was increased to 1000 PFU, and rhesus macaques were either administered CHO-MB-003 (50 mg/kg) or RAMP-MB-003 (16.7 mg/kg) [27]. The concentration of RAMP-MB-003 was selected using data from previous experiments which found that RAMP-MB-003 was three times more potent than CHO-MB-003 [26, 27]. Only 1 of the 2 rhesus monkeys that were administered CHO-MB-003 an hour after the infection survived, but all 3 rhesus monkeys that were administered RAMP-MB-003 survived [27]. These macaques had no detectable virus levels. In another treatment, rhesus macaques were administered RAMP-MB-003 1 or 2 days after infection, and 4 of the 6 rhesus macaques survived [27].

While these results are very promising, the experimental method did not take into consideration that the time of infection is unknown in human infections. MB-003 was studied by Pettitt *et al.* in order to determine its efficacy under more realistic time conditions, where 7 rhesus macaques were infected with 1067 PFU of ZEBOV [30]. Once viremia detection tested positive and the rhesus macaques showed an increase in body temperature greater than 1.5 ºC, RAMP-MB-003 (50 mg/kg) was administered [28]. The survival rate of these macaques was found to be 43% [28]. The ability of MB-003 to be administered at later times while significantly increasing survival rates highlights the therapeutic potential of MB-003 for realistic Ebola infection times [28].

## Potential Treatment: ZMAb

A study by Qiu *et al.* generated eight mAbs against ZEBOV GPs by injecting mice with a ZEBOV vaccine VSVΔG/ZEBOVGP [29]. The mAbs produced were 1H3, 2G4, 4G7, 5D2, 5E6, 7C9, 7G4, and 10C8 (**Figure 2**) [29]. The 8 mAbs were administered 1 day before and 1 day after infection in mice, at doses of 100 µg [29]. All of the mAbs, increased survival rate from 0% to 100% when administered 1 day after infection, except for 2G4, which led to a survival rate of 83% [20]. Furthermore, mAbs 4G7, 5D2, 5E6, 7C9, and 7G4 improved survival rates to 100% when administered 1 day prior to infection (10C8, 1H3, and 2G4 led to a survival rate of 83.3%, 50.0%, and 33.3%, respectively) [29].

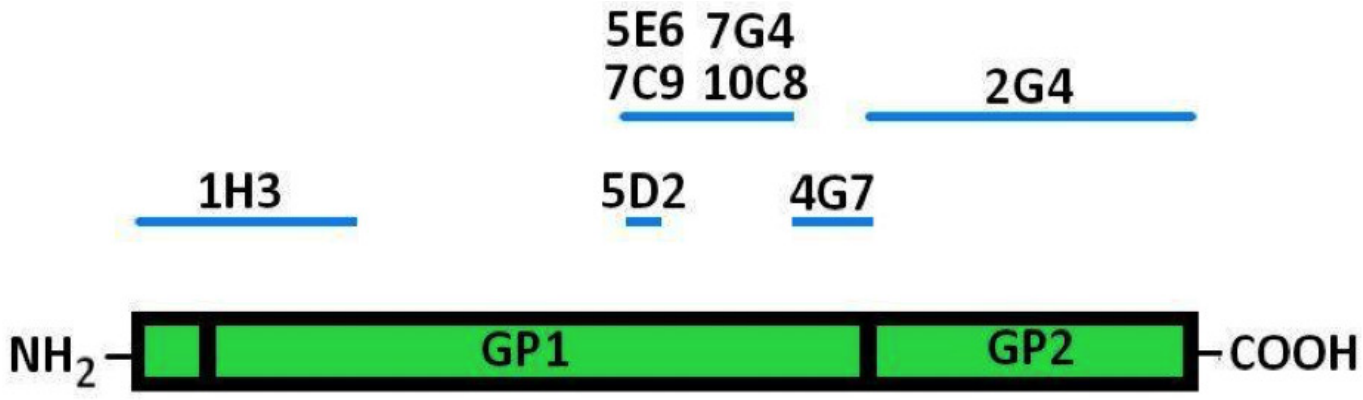


**Figure 2.** Proposed binding sites of ZEBOV GP mAbs.

Qiu *et al.* tested the 8 mAbs on guinea pigs in another experiment [30]. Each mAb administered at 100 μg doses led to partial protection when administered 1 day after infection, but there was a large increase in the time between infection and death in treated guinea pigs compared to the control group and treated mice [30]. Overall, the 8 mAbs alone did not perform well compared to KZ52 in guinea pigs [30]. However, a combination of 4G7, 1H3, and 2G4 led to a 50% survival rate when the mAb was administered 1 day prior to, and 1 day after infection; 100% survival rate when administered 2 days after infection; and 67% survival rate when administered 3 days after infection (compared to 0% survival rate in the control group) [30]. Taken together, these results suggest that a cocktail of mAbs have demonstrated promising results.

The efficacy of the mAb cocktail on infected non-human primates (NHPs) needed to be demonstrated; hence Qui *et al.* conducted another study where equal amounts of mAbs 4G7, 1H3, and 2G4 were combined into a mAb cocktail labelled ZMAb [31]. One advantage of using ZMAb over KZ52 was its ability to recognize three epitopes on GP, as opposed to only one by KZ52 [31]. ZMAb was administered to *Macaca fascicularis* (cynomolgus macaques) at a 25 mg/kg concentration [31]. When administered 24 hours after infection with ZEBOV, the survival rate increased to 100% (compared to 0% in the control group), but decreased to 50% when administered 48 hours after infection [31].

Research has shown that ZMAb is a more effective potential treatment than KZ52, as it demonstrated partial to complete curing of ZEBOV on NHPs [31]. However, in order to extend the period of time between infection and treatment, ZMAb was used as a treatment with DEF201 and adenovirus-vectored interferon-α (Ad-IFN) ($1\times 10^9$ PFU) [32, 33]. DEF201 is made up of consensus human alpha interferon (IFN-α), a cytokine whose formation and release is triggered by pathogen presence, expressed on recombinant human adenovirus of serotype 5 (AdHu5) which is a common gene therapy vector [34]. Qui *et al.* conducted experiments where $2 \times 10^8$ PFU DEF201 and 10 mg of ZMAb were administered together, and noted that the survival rate was 100% when they were administered four to seven days after infection [32]. When they combined ZMAb (50mg/kg) and Ad-IFN and administered the mixture three days after infection, it resulted in survival rates of 75% and 100% in cynomolgus macaques and rhesus macaques, respectively [32]. Survival rate was 50% when Ad-IFN was administered 1 day after infection, followed by the administration of ZMAb three days later [33].

The ability of ZMAb to provide sustained immunity was tested. Qui *et al.* conducted an experiment where animals that had previously survived infection due to monoclonal antibody therapy [31, 33] were re-infected with EBOV 10 weeks or 13 weeks after the initial infection [35]. It was found that all the cynomolgus macaques re-infected after 10 weeks survived, whereas 66% of the cynomolgus macaques re-infected after 13 weeks survived [35]. These findings support the possibility of sustained immunity after administration of ZMAb [35].

## Potential Treatment: ZMapp

In order to improve the results obtained when administering ZMAb, the mAbs were chimerized with human constant regions to form cZMAb which was comprised of c1H3, c2G4, and c4G7 [2]. Qui *et al.* combined components from cZMAb and MB-003 in the hopes of creating an even more effective mAb cocktail [36]. The combination of mAbs c13C6, c2G4, and m4G7 (murine m4G7 was used rather than c4G7 in the first experiment due to limited availability of c4G7) was found to be the most effective, as it increased the survival rate of infected rhesus macaques who received treatment three days after infection, improving survival rates from 0% to 100% [36]. Further experiments on the mAbs cocktail containing c13C6, c2G4, and c4G7, trademarked as ZMapp by MappBio Pharmaceuticals, revealed that ZMapp increased the survival rate from 0% to 100% for rhesus macaques treated up to five days after infection [36]. It was noted that many of the treated monkeys were experiencing advanced symptoms of ZEBOV such as fever and viremia prior to treatment with ZMapp [36]. Enzyme-linked immunosorbent assay and neutralising antibody assays have indicated that ZMapp, which was created to treat ZEBOV, also cross-reacts with the Guinean Ebola strain, the variant responsible for the 2014 West Africa Ebola outbreak [36].

## Future Directions

While great progress has been recently made towards finding a cure for Ebola, the potential treatments are yet to be tested in clinical trials in order to confirm that monoclonal antibody therapy, is in fact, the route for an Ebola cure.

## Conclusions

Many attempts have been made to develop a treatment for Ebola using monoclonal antibody therapy, despite the skepticism towards its therapeutic value. Even though many monoclonal antibody treatments have arisen, the primary issue is the short viral incubation time and rapid treatment administration used in these studies. One recent monoclonal antibody cocktail combining two treatments that demonstrated a lot of potential, ZMapp, highlighted effective recovery for rhesus macaques who were given treatment five days after infection with the Zaire Ebola strain - a more realistic time frame than the other antibody treatments. Furthermore, ZMapp cross-reacts with Guinean Ebola - the variant accountable for the 2014 West Africa Ebola outbreak [36]. Although this mAb cocktail is the most promising therapy thus far, clinical trials have yet to take place to determine efficacy in humans. Nonetheless, monoclonal antibody therapy still remains a promising method for developing a treatment for Ebola.

## References

1. Center for Disease Control and Prevention [Internet] 2014 [cited 2014 Dec 26]. Available from: http://www.cdc.gov/vhf/ebola/outbreaks/2014-west-africa/case-counts.html
2. The World Bank Group [Internet] 2014 [cited 2014 Dec 26]. Available from: https://openknowledge.worldbank.org/bitstream/handle/10986/20396/912190WPsee0a00070385314B00PUBLIC0.pdf?sequence=1
3. Soulillou JP, Peyronnet P, Le Mauff B, Hourmant M, Olive D, Mawas C, Delaage M, Hirn M, Jacques Y. Prevention of rejection of kidney transplants by monoclonal antibody directed against interleukin 2. Lancet 1987;1(8546):1339–42.
4. Mathieson P, Cobbold P, Hale G, Clark M, Oliveira D, Lockwood CM, Waldmann H. Monoclonal-antibody therapy in systemic vasculitis. N Engl J Med 1990;323(4):250-4.
5. Waldmann H. Manipulation of T-cell responses with monoclonal antibodies. Annu Rev Immunol 1989;7:407–44.
6. Hevey M, Negley D, Geisbert J, Jahrling P, Schmaljohn A. Antigenicity and vaccine potential of Marburg virus glycoprotein expressed by baculovirus recombinants. Virology 1997;239(1):206–16.
7. Wilson JA, Hevey M, Bakken R, Guest S, Bray M, Schmaljohn AL, Hart MK. Epitopes involved in antibody-mediated protection from Ebola virus. Science 2000; 287(5458):1664–6.
8. Gupta M, Mahanty S, Bray M, Ahmed R, Rollin P. Passive transfer of antibodies protects

immunocompetent and imunodeficient mice against lethal Ebola virus infection without complete inhibition of viral replication. J Virol 2001;75(10); 4649–54.
9. Parren P, Geisbert T, Maruyama T, Jahrling P, Burton D. Pre- and post-exposure prophylaxis of Ebola virus infection in an animal model by passive transfer of a neutralizing human antibody. J Virol 2002;76(12): 6408–12.
10. Mupapa K, Massamba M, Kibadi K, Kuvula K, Bwaka A, Kipasa M, Colebunders R, Muyembe-Tamfum JJ. Treatment of Ebola hemorrhagic fever with blood transfusions from convalescent patients. International Scientific and Technical Committee. J Infect Dis 1999;179(Suppl 1):S18–23.
11. Hevey M, Negley D, Pushko P, Smith J, Schmaljohn A. Marburg virus vaccines based upon alphavirus replicons protect guinea pigs and nonhuman primates. Virology 1998;251(1): 28–37.
12. Jones SM, Feldmann H, Ströher U, Geisbert JB, Fernando L, Grolla A, Klenk HD, Sullivan NJ, Volchkov VE, Fritz EA, Daddario KM, Hensley LE, Jahrling PB, Geisbert TW. Live attenuated recombinant vaccine protects nonhuman primates against Ebola and Marburg viruses. Nature Med 2005;11(7):786–90.
13. Oswald WB, Geisbert TW, Davis KJ, Geisbert JB, Sullivan NJ, Jahrling PB, Parren PW, Burton DR. Neutralizing antibody fails to impact the course of Ebola virus infection in monkeys. PLoS Pathog 2007;3(1):e9.
14. Jahrling PB, Geisbert JB, Swearengen JR, Larsen T, Geisbert TW. Ebola hemorrhagic fever: evaluation of passive immunotherapy in nonhuman primates. J Infect Dis 2007;196(Suppl 2):S400-3.
15. Mohamadzadeh M, Chen L, Schmaljohn A. How Ebola and Marburg viruses battle the immune system. Nat Rev Immunol 2007;7(7):556-67.
16. Mike B, Siddhartha M. Ebola hemorrhagic fever and septic shock. J Infect Dis 2003;188(11):1613-7.
17. Peters C, Peters J. An introduction to Ebola: the virus and the disease. J Infect Dis 1999;179(Suppl 1):ix-xvi.
18. Bhattacharyya S, Warfield KL, Ruthel G, Bavari S, Aman MJ, Hope TJ. Ebola virus uses clathrin-mediated endocytosis as an entry pathway. Virology 2010;401(1):18-28.
19. Aleksandrowicz P, Marzi A , Biedenkopf N, Beimforde N, Becker S, Hoenen T, Feldmann H, Schnittler HJ. Ebola virus enters host cells by macropinocytosis and clathrin-mediated endocytosis. J Infect Dis 2011;204(Suppl 3):S957-67.
20. Breman JG, Piot P, Johnson KM, White MK, Mbuyi M, Sureau P, Heymann DL, Van Nieuwenhove S, McCormick JB, Ruppol JP, Kintoki V, Isaacson M, Van Der Groen G, Webb PA, Ngvete K. The epidemiology of Ebola hemorrhagic fever in Zaire, 1976. Ebola virus haemorrhagic fever 1978;56(2):103-24.
21. Shedlock DJ, Bailey MA, Popernack PM, Cunningham JM, Burton DR, Sullivan NJ. Antibody-mediated neutralization of Ebola virus can occur by two distinct mechanisms. Virology 2010;401(2):228-35.
22. Pushko P, Parker M, Geisbert J, Negley D, Schmaljohn A, Sanchez A, et al. Venezuelan equine encephalitis virus replicon vector: immunogenecity studies with Ebola NP and GP genes in guinea pigs. In: Brown F, Burton D, Doherty P, Mekalanos J, Norrby E, editors. Vaccines 97. Cold Spring Harbor, N.Y: Cold Spring Harbor Laboratory Press; 1997. pp. 253-8.
23. Stiles BG, Lidgerding BC, Sexton FW, Guest SB. Production and characterization of monoclonal antibodies against Naja naja atra cobrotoxin. Toxicon 1991;29(10):1195-204.
24. Pogue G P, Vojdani F, Palmer KE, Hiatt E, Hume S, Phelps J, Long L, Bohorova N, Kim D, Pauly M, Velasco J, Whaley KJ, Zeitlin L, Garger SJ, White E, Bai Y, Haydon H, Bratcher B. Production of pharmaceutical-grade recombinant aprotinin and a monoclonal antibody product using plant-based transient expression systems. Plant Biotechnol J 2010;8(5):638–54.
25. Giritch A, Marillonnet S, Engler C, van Eldik G, Botterman J, Klimyuk V, Gleba Y. Rapid high-yield expression of full-size IgG antibodies in plants coinfected with noncompeting viral vectors. P Natl Acad Sci USA 2006;103(40):14701–6.
26. Zeitlin L, Pettitt J, Scully C, Bohorova N, Kim D, Pauly M, Hiatt A, Ngo L, Steinkellner H, Whaley KJ, Olinger GG. Enhanced potency of a fucose-free monoclonal antibody being developed as an Ebola virus immunoprotectant. P Natl Acad Sci USA 2011;108(51):20690–4.
27. Olinger GG Jr, Pettitt J, Kim D, Working C, Bohorov O, Bratcher B, Hiatt E, Hume SD, Johnson AK, Morton J, Pauly M, Whaley KJ, Lear CM, Biggins JE, Scully C, Hensley L, Zeitlin L. Delayed treatment of Ebola virus infection with plant-derived monoclonal antibodies provides protection in rhesus macaques. P Natl Acad Sci USA 2012;109(44):18030-5.
28. Pettitt J, Zeitlin L, Kim do H, Working C, Johnson JC, Bohorov O, Bratcher B, Hiatt E, Hume SD, Johnson AK, Morton J, Pauly MH, Whaley KJ, Ingram MF, Zovanyi A, Heinrich M, Piper A, Zelko J, Olinger GG. Therapeutic intervention of Ebola virus infection in rhesus macaques with the MB-003 monoclonal antibody cocktail. Sci Transl Med 2013;5(199):199ra113.
29. Qiu X, Alimonti JB, Melito PL, Fernando L, Ströher U, Jones SM. Characterization of Zaire ebolavirus glycoprotein-specific monoclonal antibodies. Clin Immunol 2011;141(2):218-27.
30. Qiu X, Fernando L, Melito PL, Audet J, Feldmann H, Kobinger G, Alimonti JB, Jones SM. Ebola GP-specific monoclonal antibodies protect mice and guinea pigs from lethal Ebola virus infection. PLoS Negl Trop Dis 2012;6(3):e1575.
31. Qiu X, Audet J, Wong G, Pillet S, Bello A, Cabral T, Strong JE, Plummer F, Corbett CR, Alimonti JB, Kobinger GP. Successful treatment of Ebola virus-infected cynomolgus macaques with monoclonal antibodies. Sci Transl Med 2012;4(138):138ra81. doi:10.1126/scitranslmed.3003876.
32. Qiu X, Wong G, Fernando L, Ennis J, Turner JD, Alimonti JB, Yao X, Kobinger GP. Monoclonal antibodies combined with adenovirus-vectored interferon significantly extend the treatment window in Ebola virus-infected guinea pigs. J Virol 2013;87(13):7754-7.
33. Qiu X, Wong G, Fernando L, Audet J, Bello A, Strong J, Alimonti JB, Kobinger GP. mAbs and Ad-vectored IFN-α therapy rescue Ebola-infected nonhuman primates when administered after the detection of viremia and symptoms. Sci Transl Med 2013;5(207):207ra143.
34. Julander JG, Ennis J, Turner J, Morrey JD. Treatment of yellow fever virus with an adenovirus-vectored interferon, DEF201, in a hamster model. Antimicrob Agents Ch 2011;55:2067–73.
35. Qiu X1, Audet J, Wong G, Fernando L, Bello A, Pillet S, Alimonti JB, Kobinger GP. Sustained protection against Ebola virus infection following treatment of infected nonhuman primates with ZMAb. Sci Rep 2013 Nov 28;3:3365. doi:10.1038/srep03365.
36. Qiu X, Wong G, Audet J, Bello A, Fernando L, Alimonti JB, Fausther-Bovendo H, Wei H, Aviles J, Hiatt E, Johnson A, Morton J, Swope K, Bohorov O, Bohorova N, Goodman C, Kim D, Paul MH, Velasco J, Pettitt J, Olinger GG, Whaley KJ, Xu B, Strong JE, Zeitlin L, Kobinger GP. Reversion of advanced Ebola virus disease in nonhuman primates with ZMapp. Nature 2014;514(7520):47-53.

JULS REVIEWS

# The Role of T-Cell Immunoglobulin and Mucin Domain (TIM) Proteins in Virus Cell Entry and HIV-1 Virion Egress

Nidaa Rasheed[1], Dia Azzoux[1], Sudarshan Bala[1], PeiXuan Chen[1], Saad Khan[1], Lie Yun Kok[1], Cheng Min Sung[1], Skye Daley[1], Dohyun Kim[1], Vivian Xie[1], Natalie J. Galant[2] and Imre G. Csizmadia[1,3]

[1]Department of Chemistry, University of Toronto, Ontario
[2]Department of Medical Biophysics, University of Toronto, Ontario
[3]Department of Chemistry and Chemical Informatics, University of Szeged, Hungary

## Abstract

**Incidence rates of infection by human immunodeficiency virus (HIV), a cause of progressive immune system failure, have been increasing over the past years. Recent studies have shown that T cell (or transmembrane) immunoglobulin and mucin domain (TIM) proteins, expressed naturally by the body's hematopoietic and kidney epithelial cells, strongly inhibit HIV type 1 (HIV-1) virion release. TIM proteins inhibit HIV-1 virion release by accumulating viral particles on the cell surface through interactions with the virion-associated phosphatidylserine (PS) binding sites. On the other hand, it has been shown that TIM proteins can also promote the entry of enveloped viruses such as Hepatitis A, Ebola, and Dengue, suggesting that TIM proteins act as cellular receptors that interact with viral proteins to mediate virus entry. The following review focuses on the recent and controversial findings surrounding the function of TIM family proteins in viral pathogenesis.**

## Introduction

Cell surface receptors play an important role in human health and disease. They are specialized membrane proteins on the cell surface to which molecules bind for cell-to-cell communication. With respect to viral pathogenesis, cell surface receptors are responsible for mediating or inhibiting transit of the virus in and out of host cells. One class of receptors that has been recently linked to viral entry and egress is the family of T-cell (or transmembrane) immunoglobulin and mucin domain (TIM) proteins [1, 2]. TIM family proteins are a class of cell surface Type I transmembrane receptors that contain exposed IgV, mucin, and stalk domains [3]. Recent studies have shown that TIM-1 is able to inhibit the proliferation and migration of human immunodeficiency virus type 1 (HIV-1) cells, a retrovirus that attacks the immune system leading to the development of Acquired Immune Deficiency Syndrome (AIDS). This occurs via phosphatidylserine (PS), a ligand that binds to the IgV domain of the protein [4]. PS is held on the cytosolic side of the membrane by an enzyme called flippase, which allows PS to move freely in between the extracellular and intracellular side of the membrane on the cell. When a cell undergoes apoptosis or is infected with a virus, flippase moves the PS to the outer surface of the membrane and becomes a signal for macrophages to engulf the cell [5-7]. When the HIV-1 cells try to exocytose from the infected host cell, the TIM-1 proteins on that host cell bind to the flipped PS of the cells that are budding off, thus causing them to accumulate and inhibiting them from spreading. Other studies have demonstrated that the TIM proteins are also capable of inducing the entry of virus particles into the host cell using similar mechanisms, revealing contradictory results [1, 2]. This review will focus on the contribution of TIM proteins to enhancing both pathogen virulence and host immunity.

## Structure and Immunomodulatory Functions of TIM Proteins

The TIM proteins are Type I transmembrane proteins that possess an N-terminal Ig domain of the V type, which is responsible for the recognition, binding, and adhesion of certain cells [3]. The Ig domain is linked to the mucin domain, and the stalk domain links these two components to the transmembrane domain [3]. The cytoplasmic tail attached to the transmembrane domain is believed to be involved in facilitating intracellular responses in the cytosol, and can range in length from 38-65 residues [3]. A schematic of a generic TIM receptor is given in **Figure 1**.

Three TIM genes are found in the human genome: TIM-1, TIM-3, and TIM-4 [4]. Each TIM family member affects unique cellular functions [5]. TIM proteins are expressed on the surface of hematopoietic cells from the lymphoid and myeloid lineages, as well as kidney epithelial cells [1]. During viral infections and in tumor cells, these proteins can also be observed on stromal and epithelial cells near the site of infection or tumor growth

**Table 1.** Summary of the function, ligand, and site of expression of human TIM proteins (TIM-1, TIM-3, and TIM-4) in regulating immune responses, specifically through their interactions with T cells.

| Human TIM Proteins | Site of Expression | Ligand | Functional Effects | Reference |
|---|---|---|---|---|
| **TIM-1** | Epithelial and T helper 2 (Th2) cells | Phosphatidylserine and TIM-4 | T cell proliferation and cytokine production | [3][14] |
| **TIM-3** | Activated T helper cells (Th1), dendritic and macrophage cells | Galectin-9 | Inhibitory signals resulting in cell apoptosis | [14][15] |
| **TIM-4** | Macrophages and dendritic cells | TIM-1 | Acts co-stimulatory with TIM-1 to facilitate T cell activation | [16][17] |

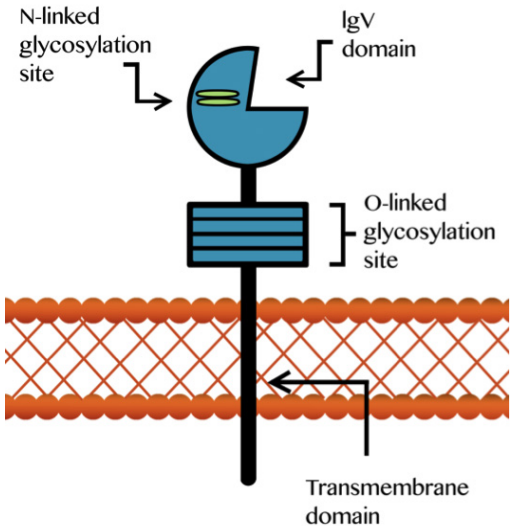


**Figure 1.** A generic representation of TIM proteins, in which specific ligands have been described for the IgV domains. All members of the family possess an IgV domain that is capable of N-linked glycosylation. Following is a mucin domain that contains many sites for O-linked glycosylation. Furthermore, there may also be some sites for N-linked glycosylation present immediately above the transmembrane domain. Following the transmembrane domain is a cytoplasmic tail, in which TIM-1 and TIM-3 have tyrosine-kinase phosphorylation motifs [1].

[10]. Initial polymorphisms in the TIM protein locus were positively linked to the development of asthma and apoptosis of cells [7-9]. However, recent studies suggest that TIM proteins may enhance or inhibit the activity of viruses. A summary of human TIM protein expression, ligand binding, and function is provided in **Table 1**.

## TIM-1 and TIM-4 Enhance T-cell Function and Clearance of Apoptotic Cells

TIM-1 proteins are expressed at low levels in naïve T-cells and are dramatically up-regulated after activation [11-13]. The function of the TIM-1 protein, demonstrated through the use of transient expression in HEK-293 T-cells, which are human embryonic kidney cells grown in tissue culture, is regulated by cytoplasmic tail phosphorylation or co-stimulation with TIM-4 to trigger T-cell proliferation and cytokine production [14-16]. TIM-1 has several ligands of its own, which include TIM-4 and PS. Though TIM-4 is not expressed in T-cells, it is present on antigen presenting cells. Its main ligand is TIM-1 and it activates the TIM1-TIM4 complex enhancing T-cell response [15, 17, 18]. The interaction between the two proteins occurs through the Ig domains and is regulated by the mucin domains, as well as cytoplasmic tails [19, 20]. The cytoplasmic tail of TIM-1 contains two tyrosines, one of which is a site for phosphorylation that, after ligation, triggers biochemical pathways downstream, including signaling for the production of interleukins. In humans, only the cytoplasmic tail of TIM-1 and TIM-3 can be phosphorylated [14].

## TIM-3 Inhibits T-cell Response and Increases Apoptosis

TIM-3 is preferentially expressed on T helper 1 (Th1) cells as well as on dendritic cells [20-22], and generates an inhibitory signal resulting in the apoptosis of Th1 cells [23, 24]. Recent studies have shown that some Th1-mediated inflammatory diseases that are negatively regulated by TIM proteins are experimental autoimmune encephalomyelitis (EAE), type I diabetes mellitus, and acute graft-versus-host diseases [22, 24, 25]. Zhu *et al.* has identified that the S-type lectin galectin-9 binds to the carbohydrate moiety on TIM-3 [26]. When bound together, TIM-3 stimulates the apoptosis of Th1 cells by terminating Th1 immunity. In inactivated immune systems, galectin-9 is mostly expressed on naïve CD4+ T effector cells and $CD4^+$ CD25 $T_{reg}$-cells, commonly known as regulatory T-cells. Upon activation of the immune system, galectin-9 is down-regulated on $CD4^+$ cells, but remains constant on $T_{reg}$-cells. This sustained expression on $T_{reg}$-cells is hypothesized to mediate suppression by inhibition of effector T-cells that express TIM-3 [26]. Furthermore, blocking the interaction between TIM-3 and its ligand has been shown to enhance the development of autoimmune diseases and inhibited the induction of tolerance, which is associated with reduced mortality from the disease [26]. TIM-3 proteins have also been observed to have similar inhibitory functions in HIV-1 infection [24]. Clinical studies conducted by Jones *et al.* [27] found that TIM-3 is a repressor for HIV-1 specific T-cell responses and that TIM-3 can also act as a negative co-stimulator of Th1 cells, often resulting in cell death [3, 21].

## TIM-Phosphatidylserine Interactions Inhibit the Spread of HIV-1

HIV-1 progressively impairs the function of infected $CD8^+$ and $CD4^+$ T-cells by diminishing cytokine production, cytotoxic activity, and proliferative capacity, rendering them functionally inactive [3]. HIV-1 is a retrovirus, meaning it carries a single-stranded RNA as its genetic material. First it fuses with the human, or host, cell and then it uses the reverse transcriptase enzyme to copy its RNA into DNA in order to infect the cell. The virus uses the host cell's machinery to replicate itself during the process of reverse transcription, while the new copies of HIV-1 cells then leave the host cell by budding off in order to infect other cells [3].

Human TIM-1 was initially discovered as the receptor for Hepatitis A virus (HAV), and has been recently shown to function as a receptor or entry cofactor for Ebola virus (EBOV) and Dengue virus [28-31]. Recently, TIM-1 proteins have also been

shown to strongly inhibit HIV-1 release through interactions with viral PS [3, 31]. PS has been found to be in the inner leaflet part of the membrane of HIV-1 particles and is essential for HIV-1 assembly; however, after infection, the PS has been shown to be present on the outer surface of these cells [23, 33-35]. This is one of the hallmark events associated with apoptosis or viral infection, thus exposing the PS to phagocytic cells that have specific receptors for it [5-7].

After infecting the host cell, HIV-1 particles bud off from the host in order to spread to other cells in the body. As the infected cell goes through exocytosis it picks up the PS present on the plasma membrane of the infected host cell. Li *et al.* has found that, because of the ability of TIM-1 to bind to PS, the protein is able to stop HIV-1 egress by inhibiting viral cells from leaving the infected host cell after they go through exocytosis [24]. This occurs through the interaction formed between the TIM-1 on the infected host cell and the PS on the newly formed HIV-1 cell that buds off following exocytosis. When the TIM-1 protein interacts with PS expressed on the same surface, it can be incorporated into the viral particle; therefore, it is able to block the new HIV-1 virion from migrating as well as use it to further block other infected cells. The interaction can form a tether to keep the HIV-1 particles at the infected cells, preventing it from affecting other T-cells (**Figure 2**). Once the agglutination of the HIV-1 cells becomes significant, such that the host is able to recognize the cells as being abnormal, other immune cells such as macrophages are able to rapidly phagocytize the infected cell – thus, limiting the infection and preventing it from spreading [26].

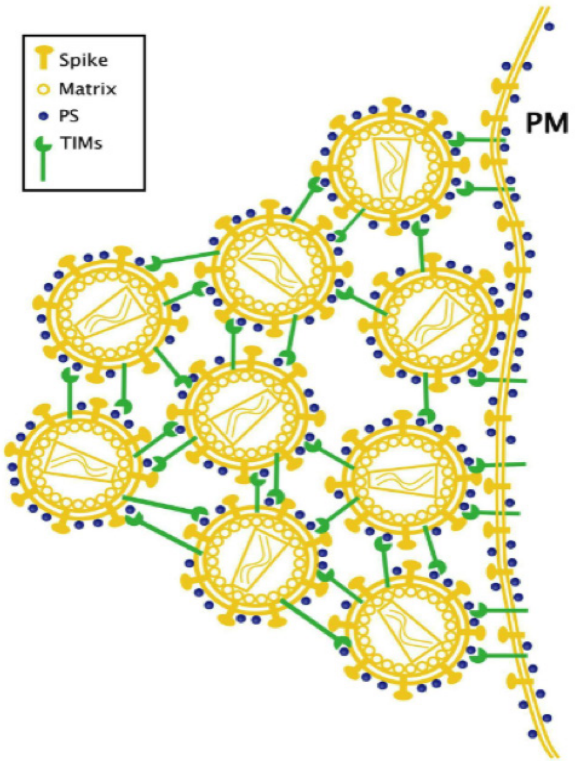


**Figure 2.** Suggested representation of the interaction between TIM-1 and HIV-1 virions. The interaction between phosphatidylserine (PS), on released HIV-1 virions, with the IgV domain of TIM-1, on the surface of the infected host cell, produces a tether to keep the HIV-1 particles at the infected cells, preventing them from migrating [24].

## TIM-Phosphatidylserine Interactions Enhance Virus Entry

Although the TIM family has diverse functions in regulating immunity in mice and humans [21, 35], many studies have also reported its ability to increase the body's susceptibility to viral infection. Jamielity *et al.* [7] showed that TIM-1 promotes the infection of cells by retroviruses and virus-like particles, and is associated with a range of viral entry proteins. The *Filoviridae* family of viruses contains Ebolavirus and Marburgvirus, both of which cause hemorrhagic fevers in humans [32]. A recent study performed by Kondratowicz *et al.* [23] showed that TIM-1 binds to the receptor-binding domain of the Zaire Ebola virus (EBOV) glycoprotein (GP). Using African green monkey kidney (Vero) cells, previously used in many studies to investigate EBOV infection [33-35], the authors demonstrated that infection led to a high surface expression of TIM-1. In addition, it was found that ectopic expression of TIM-1 in poorly permissive cells enhanced EBOV infection by 10- to 30-fold. Conversely, the reduction of cell-surface expression of TIM-1 by RNA interference decreased infection of highly permissive Vero cells [23]. The binding of the IgV domain to the PS on viral membrane caused the accumulation of viruses on the receiving cell surface, followed by internalization of viruses into endosomes [7, 36].

This ability to mediate virus entry has been mapped to specific domains of TIM proteins. Neither the transmembrane nor the cytoplasmic domains of TIM family proteins are required for viral entry [20]. This was demonstrated in experiments by replacing these two domains of TIM-1 protein with glycosylphosphatidylinositol (GPI) anchors, resulting in the same viral transduction efficiency as wild type TIM-1 protein [20]. In addition, TIM-3, despite the ability of its IgV domain to bind to virion-associated PS, does not effectively enhance the internalization of other enveloped viruses [36]. This suggests that specific characteristics of the IgV domain may affect the efficiency of viral entry into host cells [7, 20, 35]. The hypothesis that viral transduction efficiency could be due to higher affinity of IgV domain to PS in TIM-1 than TIM-3 was indicated by DeKruyff *et al.* [36] and tested by Moller-Tank and colleagues [20]. The results showed that TIM-1 or TIM-4 with IgV domain of TIM-3 had a similar efficiency of viral entry to wild type TIM-1 or TIM-4, while TIM-3 with IgV domain of TIM-1 was as inefficient as normal TIM-3 [20]. This suggests that although the presence of an IgV domain is crucial for viral entry, the affinity of this domain for PS is not a factor determining entry efficiency [20].

## Conclusions

This review has highlighted the roles of TIM proteins in both the inhibition of HIV-1 virion proliferation and in the enhancement of viral entry into host cells. Many experiments have supported a model where TIM proteins, specifically TIM-1, can use virion-associated PS binding sites to inhibit HIV-1 release. Interactions between TIM and its ligands are still under investigation, and the exact mechanism by which the TIM proteins can enhance viral particle entry remains unknown. It will be worthwhile to determine if there are additional ligands for the mucin domains that are common to all of the TIM family proteins. Furthermore, future research should focus on the biological consequences of having a build-up of viral particles on the infected cell resulting from its interaction with TIM proteins. The function of TIM-1 proteins

may be modulated through traditional protein drug approaches, including enhancing the interactions between TIM proteins and the virion through the use of antibody or soluble receptors in order to further inhibit HIV-1 virion release in the body. Ultimately, TIM proteins may prove to be valuable targets for HIV-1, Ebola, Hepatitis A, and Dengue antiviral therapy.

## References


1. Kuchroo K, Umetsu T, DeKruyff H, Freeman J. The TIM gene family: Emerging roles in immunity and disease. Nat Rev Immunol 2003;3(6):454–62.
2. Freeman J, Casasnovas M, Umetsu T, DeKruyff H. TIM genes: A family of cell surface phosphatidylserine receptors that regulate innate and adaptive immunity. Immunol Rev 2010;235(1):172–89.
3. Kane P. TIM Proteins and Immunity. J Immunol 2010;184(6): 2743–9.
4. Li M, Ablan SD, Miao C, Zheng YM, Fuller MS, Rennert PD, Maury W, Johnson MC, Freed EO, Liu SL. TIM-family proteins inhibit HIV-1 release. PNAS 2014;111(35):E3699-E3707.
5. Qing J, Xiao H, Zhao L, Qin G, Hu L, Chen Z. Construction and characterization of an enhanced GFP-tagged TIM-1 fusion protein. J Microbiol Biotechnol 2014; 24(4):568-76.
6. Baghdadi M, Jinushi M. The impact of the TIM gene on tumor immunity and immunosuppression. Cell & Molecular Immunology 2014;11:41-8.
7. Jamielty S, Wang JJ, Chan YK, Ahmed AA, Li W, Monahan S, Bu X, Farzan M, Freeman GJ, Umetsu DT, DeKruyff RH, Choe H. TIM-family proteins promote infection of multiple enveloped viruses through virion-associated phosphatidylserine. PLoS Pathog 2013 Mar;9(3):e1003232.
8. McIntire J, Umetsu E, Macaubas C, Hoyte G, Cinnioglu C, Cavalli-Sforza LL, Barsh GS, Hallmayer JF, Underhill PA, Risch NJ, Freeman GJ, DeKruyff RH, Umetsu DT. Immunology: Hepatitis A virus link to atopic disease. Nature 2003;425(6958):576.
9. Umetsu T, Umetsu E, Freeman J, DeKruyff H. TIM gene family and their role in atopic diseases. Curr Top Microbiol Immunol 2008;321:201–15.
10. Chiba S, Baghdadi M, Akiba H, Yoshiyama H, Kinoshita I, Dosaka-Akita H, Fujioka Y, Ohba Y, Gorman JV, Colgan JD, Hirashima M, Uede T, Takaoka A, Yagita H, Jinushi M. Tumor-infiltrating DCs suppress nucleic acid-mediated innate immune responses through interactions between the receptor TIM-3 and the alarmin HMGB1. Nat Immunol 2012; 13: 832–42.
11. Miyanishi M, Tada K, Koike M, Uchiyama Y, Kitamura T, Nagata S. Identification of Tim4 as a phosphatidylserine receptor. Nature 2007; 450(7168):435–9.
12. Albacker A, Karisola P, Chang J, Umetsu E, Zhou M, Akbari O, Kobayashi N, Baumgarth N, Freeman GJ, Umetsu DT, DeKruyff RH. TIM-4, a receptor for phosphatidylserine, controls adaptive immunity by regulating the removal of antigen-specific T cells. J Immunol 2010;185(11):6839–49.
13. De Souza AJ, Oriss TB, O'Malley K, Ray A, Kane LP. TIM-1 is expressed on in vivo-activated T cells and provides a co-stimulatory signal for T cell activation. Proc Natl Acad Sci U S A 2005;102(47):17113–8.
14. Meyers JH, Chakravarti S, Schlesinger D, Illes Z, Waldner H, Umetsu SE, Kenny J, Zheng XX, Umetsu DT, Dekruyff RH, Strom TB, Kuchroo VK. TIM-4 is the ligand for TIM-1, and the TIM-1-TIM-4 interaction regulates T cell proliferation. Nat Immunol 2005;6(5):455–64.
15. Umetsu SE, Lee WL, McIntire JJ, Downey L, Sanjanwala B, Akbari O, Berry GJ, Nagumo H, Freeman GJ, Umetsu DT, Dekruyff RH. TIM-1 induces T cell activation and inhibits the development of peripheral tolerance. Nat Immunol 2005;6(5):447–54.
16. Rodriguez-Manzanet R, Meyers JH, Balasubramanian S, Slavik J, Kassam N, Dardalhon V, Greenfield EA, Anderson AC, Sobel RA, Hafler DA, Strom TB, Kuchroo VK. TIM-4 expressed on APCs induces T cell expansion and survival. J Immunol 2008;180(7):4706–13.
17. Takada A, Watanabe S, Ito H, Okazaki K, Kida H, Kawaoka Y. Downregulation of beta1 integrins by Ebola virus glycoprotein: Implication for virus entry. Virology 2000;278(1):20–6.
18. Schutters K, Reutelingsperger C. Phosphatidylserine targeting for diagnosis and treatment of human diseases. Apoptosis 2010 Sep;15(9):1072-82.
19. Su W, Lin Y, Kane L. TIM-1 and TIM-3 proteins in immune regulation. Cytokine 2008 Oct;44(1):9-13.
20. Moller-Tank, S, Kondratowicz, Davey A, Rennert D, Maury W. Role of the Phosphatidylserine Receptor TIM-1 in Enveloped-Virus Entry. Journal of Virology 2013; 87(15), 8327-41.
21. Schornberg KL, Shoemaker CJ, Dube D, Abshire MY, Delos SE, Bouton AH, White JM. Alpha5beta1-integrin controls ebolavirus entry by regulating endosomal cathepsins. Proc Natl Acad Sci U S A 2009;106(19):8003–8.
22. Kondratowicz AS, Lennenmann NJ, Sinn PL, Davey RA, Hunt CL, Moller-Tank S, Meyerholz DK, Rennert P, Mullins RF, Brindley M, Sandersfeld LM, Quinn K, Weller M, McCray PB Jr, Chiorini J, Maury W. T-cell immunoglobulin and mucin domain 1 (TIM-1) is a receptor for Zaire Ebolavirus and Lake Victoria Marburgvirus. Proc Nati Acad Sci USA 2011;108(20):8426-31.
23. Sinn PL, Hickey MA, Staber PD, Dylla DE, Jeffers SA, Davidson BL, Sanders DA, McCray PB Jr. Lentivirus vectors pseudotyped with filoviral envelope glycoproteins transduce airway epithelia from the apical surface independently of folate receptor alpha. J Virol. 2003 May;77(10):5902–10.
24. Li M, Ablan SD, Miao C, Zheng YM, Fuller MS, Rennert PD, Maury W, Johnson MC, Liu SL. TIM-family proteins inhibit HIV-1 release. PNAS 2014;111(35)E3699-707.
25. McIntire JJ, Umetsu SE, Macaubas C, Hoyte EG, Cinnioglu C, Cavalli-Sforza LL, Barsh GS, Hallmayer JF, Underhill PA, Risch NJ, Freeman GJ, DeKruyff RH, Umetsu DT. Immunology: Hepatitis A virus link to atopic disease. Nature 2003;425(6958):576.
26. Zhu C, Anderson C, Schubart A, Xiong H, Imitola J, Khoury J, Zheng X, Strom B, Kuchroo V. The Tim-3 ligand galectin-9 negatively regulates T helper type 1 immunity. Nat. Immunol 2005;6: 1245–52.
27. Jones RB, Ndhlovu LC, Barbour JD, Sheth PM, Jha AR, Long BR, Wong JC, Satkunarajah M, Schweneker M, Chapman JM, Gyenes G, Vali B, Hyrcza MD, Yue FY, Kovacs C, Sassi A, Loutfy M, Halpenny R, Persad D, Spotts G, Hecht FM, Chun TW, McCune JM, Kaul R, Rini JM, Nixon DF, Ostrowski MA. Tim-3 expression defines a novel population of dysfunctional T cells with highly elevated frequencies in progressive HIV-1 infection. J Exp Med 2008;205(12):2753-79.
28. Kaplan G, Totsuka A, Thompson P, Akatsuka T, Moritsugu Y, Feinstone SM. Identification of a surface glycoprotein on African green monkey kidney cells as a receptor for hepatitis A virus. EMBO J 1996;15(16):4282–96.
29. Meertens L, Carnec X, Lecoin MP, Ramdasi R, Guivel-Benhassine F, Lew E, Lemke G, Schwartz O, Amara A. The TIM and TAM families of phosphatidylserine receptors mediate dengue virus entry. Cell Host Microbe 2012;12(4):544–57.
30. Santiago C, Ballesteros A, Martinez-Munoz L, Mellado M, Kaplan GG, Freeman GJ, Casasnovas JM. Structures of T cell immunoglobulin mucin protein 4 show a metal-ion- dependent ligand binding site where phosphatidylserine binds. Immunity 2007 Dec;27(6):941–51.
31. Nakayama M, Akiba H, Takeda K, Kojima Y, Hashiguchi M, Azuma M, Yagita H, Okumura K. Tim-3 mediates phagocytosis of apoptotic cells and the cross-presentation. Blood 2009 Apr 16;113(16):3821-30. doi:10.1182/blood-2008-10-185884.
32. Wu Y, Tibrewald N, Birge RB. Phosphatidylserine recognition by phagocytes: a view to a kill. Trends Cell Biol. 2006 Apr;16(4):189–97.
33. Schoenfeld Y, Zandman-Goddard G. HIV and autoimmunity. Autoimmunity Reviews 2002 Dec;1(6):329-37.
34. Dolnik O, Kolesnikova L, Becker S. Filoviruses: Interactions with the host cell. Cell Mol Life Sci 2008 Mar;65(5):756–76.
35. Sanchez A. Analysis of filovirus entry into vero e6 cells, using inhibitors of endocytosis, endosomal acidification, structural integrity, and cathepsin (B and L) activity. J Infect Dis 2007;196(Suppl 2):S251–8.
36. DeKruyff RH, Bu X, Ballesteros A, Santiago C, Chim YL, Lee HH, Karisola P, Pichavant M, Kaplan GG, Umetsu DT, Freeman GJ, Casasnovas JM. T cell/transmembrane, Ig, and mucin-3 allelic variants differentially recognize phosphatidylserine and mediate phagocytosis of apoptotic cells. J Immunol 2010 Feb 15;184(4):1918-30.

# Dr. Titia de Lange

**Dr. de Lange is known for her discovery of anomalous telomeres in tumour cells. Her recent discovery of Shelterins - the mechanistic protein by which mammalian telomeres are protected from deleterious DNA repair and damage responses - earned her a prestigious 2014 Gairdner Award.**

Interview conducted by Imindu Liyanage

***"What I study is telomeres, we don't study genetics, we do genetics and cell biology to understand how telomeres work."***

(**IL** - Imindu Liyanage; **TD** - Dr. Titia de Lange)

**IL:** Hello Professor, thank you meeting me. […] Clearly genetics is among the most transformative fields in science, therefore (as an expert) how have you seen it change in your experience?

**TD:** How has genetics changed?

**IL:** Perhaps we can start with how the *study* of genetics has changed?

**TD:** Well genetics is a tool, you don't study genetics, you use it as a tool, a technique. In the old days, it was 'studied' by Mendel, it was studied to understand how genes are inherited. By and large, what we do now is we use genetics as a technique; so we remove genes from the mouse genome, and see what the effect is. What I study is telomeres, we don't study genetics, we *do* genetics and cell biology to understand how telomeres work.

**IL:** So rather than study genetics, we now use it as a means to understand something else.

**TD:** Yes, yes.

**IL:** That's certainly a new perspective. Now, speaking of your study of telomeres, you are of course among the first to report that tumour cells have shortened telomeres. How did you make such a remarkable discovery?

**TD:** […] I didn't have any ideas, I was just looking. It's important to just look at things. I had cloned telomere DNA, so I was going to look at telomeres, and I just looked at any DNA I could get my hand hands on. I had a set of Wilm's tumour (it's a childhood kidney tumour), and the normal neighboring tissues, and I just looked at the telomeres – it's what I had. And low and behold, they're really short, and so then I got more tumour material and they all seemed to be pretty short. It's important in biology to just look, not always to search for proof of your model, sometimes you just have to look.

**IL:** Would you say that there was something in your training, specifically in your undergraduate training which may have prepared you to make your discovery?

**TD:** When I was an undergraduate, I was so bored by biology. I didn't like it at all because it was not modern. I didn't think they were doing very interesting things. I hadn't met my thesis advisor yet, [but] later I figured out he was doing interesting things. But it was pretty boring; I almost dropped out. Then I met a very inspiring guy - Richard Flavel - who was working on genes, β-globin genes. and he really saved science for me. Because I probably would have stopped. So, it's important to find something that's really interesting, and somebody who's doing

research has to find it inspiring. But you can't go looking for it, you have to to run into it - you have to let things come to you.

***"It's important in biology to just look, not always to search for proof of your model, sometimes you just have to look."***

**IL:** And leading from that professor, do you have any advice for undergraduate students – especially those prospectively going into research?

**TD:** For me, I told students that […] science is how to make money without doing any work, or how to work hard without making any money. That's both true in science. For me, I haven't worked really since I was 23 and had a job in a bar, and yet I'm being paid. But, as a scientist you never get rich and you'll really work hard. You'll spend long hours, but it doesn't feel like work. You [also] don't get an enormous amount of respect. If you want to pick up somebody in a bar and you tell them, "I'm a scientist" - not so much. If you say, "I'm a stockbroker" - [then] people show some interest. So you have to do it because you love it, and not for what you might gain from it.

**IL:** Thank you very for your time professor, and I also wanted to say that I really enjoyed your lecture this morning.

**TD:** Thank you, good luck.

**IL:** Thank you, professor.

# Dr. Napoleone Ferrara

**Dr. Ferrara is known for his discovery of VEGF and its role in blood vessel formation. This eventually led to the development of bevacizumab, the first anti-VEGF therapy for cancer; and ranibizumab, a highly effecitve treatment for wet macular degeneration. His work has earned him a prestigious 2014 Gairdner Award.**

Interview conducted by Charles Lee

***"Yes, at certain point you need to make the difficult realization that what you have may not lead anywhere. This is also another feature that is important to being successful: not only to follow through, but also to understand and learn from mistakes, and to take a different path."***

(**CL** - Charles Lee; **NF** - Dr. Napoleone Ferrara)

**CL:** So you went to medical school and residency in Italy?

**NF:** Not full residency. I finished medical school, and went to the United States to start on research and I actually interrupted my research to start on residency. Then, I decided to go back to research.

**CL:** When you switched over from residency to research, how did you know that you wanted to become a scientist as opposed to a practicing physician?

**NF:** That's a great question, but I didn't know for sure. I only knew that I was really interested in research, and then I actually followed a bit of conventional wisdom that clinical training is very important. So I started residency in the United States, and I spent a year there and that was a very fundamental year for me because I understood exactly what I liked to do and what I didn't like to do. In the end, I went back to research.

**CL:** And why did you decide to go to the US for research?

**NF:** Well my mentor in Italy introduced me to some scientists at the UCSF [University of California, San Francisco], and I saw the opportunity.

**CL:** How did you get into the study of the regulation of angiogenesis and the role it plays in cancer and blindness?

**NF:** My interest really started from really basic science questions - more of a curiosity, actually. In the beginning, I was very interested in endocrinology and the pituitary; and at that time, there was a problem of neovascularization. We needed to be aware that vascularization was a fundamental physiological phenomenon that is not only limited to cancer. Initially, I found that the pituitary cells produce angiogenic factors and that the pituitary gland is highly vascularized; that was the question that I sought at the time. Then I isolated VEGF [vascular endothelial growth factor], and it became clear that its involvement was

much broader; not only in the pituitary, but it was a universal angiogenic factor, produced by cancer cells and many others.

***"But persistence, not to be discouraged by setbacks, is a very critical quality of being a successful scientists"***

**CL:** During your journey of becoming and being a scientist, what important lessons have you learned and kept with?

**NF:** I think if you're a scientist and you want to be successful, you have to be really persistent. You need to also be, of course, very lucky because even if you're very persistent, unless you discover something interesting, you wouldn't be able to fulfill all your aspirations. But persistence, not to be discouraged by setbacks, is a very critical quality of being a successful scientist.

**CL:** Then at what point do you think you should abandon the question you were investigating? When should you give up experiments or projects that may seem unpromising?

**NF:** I think it's very critical to be persistent, but at the same time, not to be stubborn. That is another key quality. You don't want to waste your career chasing something that isn't important. Yes, at a certain point you need to make the difficult realization that what you have may not lead anywhere. This is also another feature that is important to being successful: not only to follow through, but also to understand and learn from mistakes, and to take a different path.

**CL:** When your lab first isolated VEGF in 1989, did you expect VEGF would play such an important role in the human body and the pathogenesis of cancer?

**NF**: Well, it was very early stage. You can give lots of hope, but it was unknown at the time we discovered it, how important it was. It took many years of basic research, fundamental research, basic biology to understand that. But there were some interesting features of VEGF that hinted at the extent to which it was involved in many processes.

**CL:** And you have been in this field for around 30 or 35 years...

**NF:** No, probably not 35 years. Maybe 30 years.

**CL:** But a very long time. How has your perception about the regulation of angiogenesis changed over the course of 30 years and has your initial drive to be in this field changed?

**NF:** I think, of course, we learned a lot over the last few decades. It became very clear that VEGF was a fundamental molecule in angiogenesis. But clearly there are more refined details about angiogenesis, additional molecules that we need to study. So there are stages of refinement in terms of [the] mechanism. The challenge now is to fill up some important details.

**CL:** One final question, many readers of this journal are aspiring scientists. What advice would you give to our readers on becoming successful scientists or excelling in academia in general?

**NF:** Well, I think it's very difficult to give generalized advice because everybody has different stories and interests. One important thing is that you need to really find your interest yourself, and reflect [upon] what you want to do and enjoy doing, almost like a philosopher. You can't just think about how much money you're going to make from your career. For example, I gave up the clinical career when everybody thought that it was a better thing to do. But I enjoy science, and I think I've made a good choice.

**CL:** On behalf of the JULS staff, I would like to thank you for your time and congratulations once again!

JULS
Journal of Undergraduate Life Sciences
University of Toronto

## Call for Submissions

The *University of Toronto Journal of Undergraduate Life Sciences (JULS)* is always looking for submissions that showcase the research achievements of undergraduate life science students. We welcome manuscripts in the form of Research Articles or Reviews. Submissions must come from University of Toronto undergraduate students or undergraduate students outside of U of T who have conducted research for at least three months under the supervision of a faculty member at U of T.

Research articles should present original research and address an area of the life sciences. Mini-reviews should focus on a specific scientific topic of interest or related to the research work of the author. Research articles should be between 2,000-3,000 words and mini-reviews between 1,500-2,000 words. All works must not have been previously submitted or published in another undergraduate journal. The deadline for submissions for each issue will appear on the JULS website at http://juls.sa.utoronto.ca.

## Contact Us

JULS is always looking for contributions from writers, artists, designers, and editors. Please contact JULS at juls@utoronto.ca if you are interested in joining the JULS team, or have any questions regarding any matter pertaining to the journal, or visit our websites: http://juls.sa.utoronto.ca or http://jps.library.utoronto.ca/index.php/juls.

Share your thoughts on this year's issue on our facebook page: https://www.facebook.com/julsuoft.

# DISCOVERY @ utoronto

**Graduate studies in biomedical research: Training leaders of tomorrow**

**www.facmed.utoronto.ca**

cancer

endocrinology

biochemistry

medical imaging

stem cells

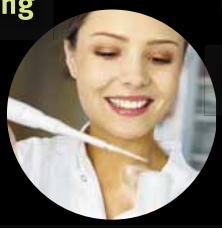

proteomics

structural, molecular & cell biology


neuroscience

reproduction

immunology

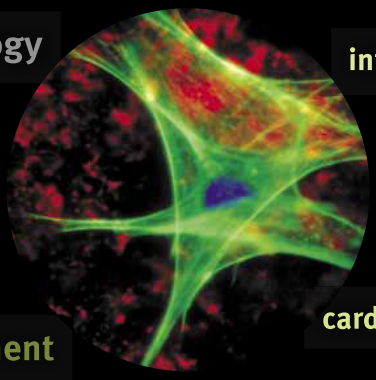

infection & immunity

genetics

nutrition

pharmacology & toxicology

cardiovascular sciences

development

- Eight basic science departments in the Faculty of Medicine
- A community of internationally renowned researchers
- State-of-the-art facilities on campus and at affiliated hospitals and institutes
- Guaranteed financial support

UNIVERSITY OF TORONTO
FACULTY OF MEDICINE